Optimising the gas chromatography – mass spectrometry (GC-MS) analytical protocol for the identification of Martian meteorite organics

Jodie Anna Douglas

Supervised by Dr Lydia Hallis and Prof. Jamie Toney

Submitted in fulfilment of the requirements for the Degree of Master of Research (Earth Science)

College of Science and Engineering

School of Geographical and Earth Sciences

University of Glasgow

November 2025

Abstract

Martian missions and meteorite analyses confirm the presence of indigenous, organic compounds in the planet's atmosphere, sediments and rocks. However, investigations are constrained by the basaltic nature and limited mass of available Martian meteorites. The Mars Sample Return (MSR) mission will enable comprehensive laboratory analyses of Martian material on Earth highlighting the need to optimise methods for detecting trace organics in low-mass, organic-poor igneous materials.

This study aimed to optimise sample preparation, extraction, and GC-MS analytical protocols using basaltic analogues from the Bockfjorden Volcanic Complex (BVC), Svalbard. Scanning Electron Microscopy (SEM) analysis revealed carbonate globules textually and mineralogically similar to those found in Martian meteorite Allan Hills 84001 (~4 Ga), confirming the suitability of BVC rocks as terrestrial analogues.

The findings from this study reveal that ball milling was the most efficient method for producing a more homogenous finer powder, improving extraction reproducibility. Solvent extractions using an Accelerated Solvent Extractor (ASE) yielded total TLE for GC-MS analysis, which successfully identified indigenous organic compounds. A fuller molecular suite required 1.5g of sample, exceeding typical Martian meteorite allocations of ~0.25g. These results emphasise the challenges of detecting organics in low-carbon igneous materials and the need to refine GC-MS protocol for low-mass planetary samples ahead of MSR analyses.

Table of contents

Contents

List of Figures

List of Tables

Acknowledgements

I would firstly like to thank Dr Lydia Hallis for the opportunity to undertake this research Masters. I am extremely grateful for the support and advice given throughout my project. Thank you to my supervisor Professor Jamie Toney without whom my project would not be possible.

Thanks also to the lab technicians Charlotte Slaymaker and Ali Salik for all of your time and knowledge. Charlotte for the support during the arduous hours of sample crushing. Ali for guiding me through the wet laboratory process and GC-MS.

I would like to express gratitude to Áine O'Brien for all your words of wisdom and support to help me stay on track and to Holly Hourston for being in this with me.

Thank you to my friends and family who were my *rock* throughout my research. To my KG girls (Kirst, Mad, Lil, Reg, Freya, Zo) who saw me through the best and the worst of it all. To my family, thank you for always having faith in me and for your endless encouragement.

Author’s Declaration

I declare that, except where explicit reference is made to the contribution of others, that this dissertation is the result of my own work and has not been submitted for any other degree at the University of Glasgow or any other institution. This work was supervised by Dr. Lydia Hallis and Professor Jamie Toney.

Jodie Anna Douglas - 2025

1. Introduction

1.1 Mars

1.1.1. Geological History of Mars

The accretion and differentiation of Mars occurred within tens of millions of years after Solar System formation and prior to the formation of the Earth and the Moon, Mars, the red planet, has been a topic of scientific research for approximately the past 60 years. Much of early Martian history is difficult to constrain due to the lack of surviving surface features but from the geomorphological features, including fluvial valleys and outflow channels remaining, it is speculated that Mars was once a wetter and warmer planet which could have hosted the conditions for life (Ehlmann et al.,2011). Four age groups exist for surface features on Mars; Pre-Noachian, Noachian, Hesperian and Amazonian as outlined in Figure 1.

1.1.1.2 Pre-Noachian

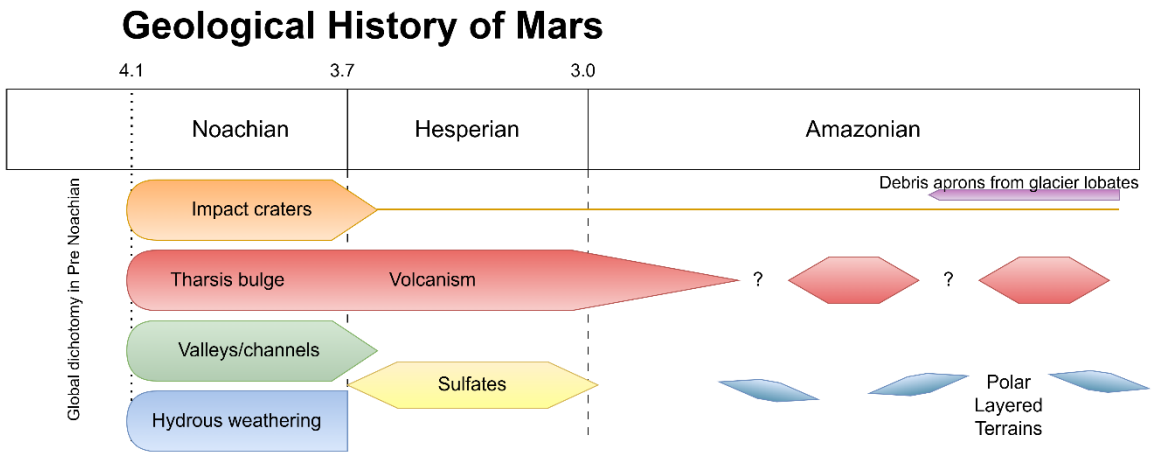

Figure 1- Geological history of Mars outlining timeline and major events. Adapted from Carr and Head 2010.

The pre-Noachian time period spans from the formation of the planet until the formation of Hellas, a 2300 km impact crater in the southern highlands (~4.5-4.1 Ga ago). As there are almost no surviving surfaces from the pre-Noachian, early Mars history is difficult to constrain (Carr and Head, 2010). The pre-Noachian can therefore be characterised by presence of a magnetic field, basin forming impacts and the subsequent global dichotomy formation as a result of this (Carr and Head, 2010). Global dichotomy is thus the earliest geologic event recorded in the geography of the surface providing a bimodal distribution of elevations known as the northern lowlands and southern highlands (Neumann et al., 2004).

1.1.1.3 Noachian

Noachian (~4.1-3.7 Ga ago) hosts evidence of heavy impact bombardment, volcanism, and widespread aqueous alteration within the rocks (Carr and Head, 2010). A magnetic field and denser atmosphere were likely present during this period. Widespread Noachian terrains are host to clay minerals that are believed to have formed by water rock interactions (Ehlmann et al., 2011; Farley et al., 2022).

Hellas Planitia is a ~2,300 km wide impact basin in the southern hemisphere of Mars which defines the base of the Noachian period (Carr and Head, 2010). The smaller impact craters that are visible on the Martian surface appear to postdate the formation of Hellas and thus are implied as at least Noachian in age. Heavy bombardment by comets and asteroids would have triggered hydrothermal activity at site of impact, widespread distribution of ejecta and brecciation of surface materials consequently increasing erosion rates (Carr and Head, 2010).

Geomorphological evidence of valley networks is widespread on the Noachian surface. Imaging from Martian orbiters and data from rovers, including NASA's Perseverance rover reveals the presence of past deltaic environments as well as ancient rivers and lakes suggesting a warmer and wetter time period (Sharma et al., 2023). The aqueous interaction with basalt resulted in widespread phyllosilicates associated with the Noachian surface (Bibring et al., 2006; Ehlmann et al., 2011). Aqueous alteration lessened towards the end of the Noachian suggesting a shift from the warmer, wetter environment to a colder, drier one (Carr and Head, 2010).

The Tharsis bulge had largely accumulated by the end of the Noachian, deforming the Martian lithosphere. Tharsis is an elevated region located in the Western hemisphere of Mars stretching across ~5000 km and ~9 km high (Philips et al., 2001). The release of volatile elements from volcanism within this region would have warmed the atmosphere allowing liquid water to be stable on the surface (Phillips et al., 2001).

Towards the end Noachian, volcanism waned, rate of impacts reduced, and the magnetic field severely weakens (Phillips et al., 2001).

1.1.1.4 Hesperian

The Hesperian period (~3.7-3 Ga ago) is characterised by water-rock interactions, volcanism, and outflow channels (Carr and Head, 2010). A decline in erosion and weathering rates as well as impact cratering occurred in the Hesperian. Aqueous alteration of clays was rare in this time period (Carr and Head, 2010), with sulphate deposits becoming more dominant in the Western hemisphere. Debate centres around the origin of these outflow channels between lava or water but the latter is favoured (Bibring et al., 2006).

1.1.1.5 Amazonian

Amazonian (3.0 Ga-Present) is the longest geological time period for Mars yet experienced the least amount of geomorphological change. This was a dry, oxidising time and thus anhydrous ferric oxides can be traced throughout this period (Bibring et al., 2006). Episodic volcanism occurred at much slower rate than previous periods and was mainly constrained to the Tharsis and Elysium regions (Carr and Head, 2010) This period is characterised by ice, specifically the features preserved by glacial accumulation and movement (Carr and Head, 2010). This is supported by several geomorphic features including recurrent slope lineae, lineated valley fill and concentric crater fill (Carr and Head, 2010), a result of episodic ice melts (Head et al., 2003).

1.1.1.6 Present Day Surface

Present day Mars is a largely hostile dry, cold environment with sub-zero temperatures and a thin CO^2 dominated atmosphere - any water would be in the form of ice or exist below the surface (Wordsworth et al., 2021). However, orbital observations reveal seasonal brine flows in the summer and spring and atmospheric data from SAM indicate seasonal cycles for major gases (Trainer et al., 2019). The Martian upper crust is basaltic with regional varying quantities of plagioclase, pyroxene and olivine associated with different terrains (Ehlmann and Edwards., 2014). Although the present-day Martian surface is highly oxidising, organic matter (including thiophenes and aromatic and aliphatic compounds) was discovered in 3-billion-year-old lacustrine mudstones on the surface of Mars by the Sample Analysis at Mars (SAM) Suite on Curiosity (Eigenbrode et al., 2018). These findings imply that beneath the surface could potentially harbour wider molecular information that has been preserved from the harsh surface conditions (Kminek and Bada, 2006; Eigenbrode et al., 2018).

1.1.2 Martian organics

Organics exist within Martian material; however, the nature and formation of these organics is a topic of debate within the scientific community (McKay et al., 1996; Bada et al., 1998: Steele et al., 2012). These compounds can exist in a variety of different forms - in the sedimentary rocks, basalts, soils and thus within the planets' meteorites. Organic carbon compounds are essential building blocks for life on Earth, therefore, evidence of these compounds on Mars is therefore pivotal to understanding habitability on the planet and aid in interpreting Mars' history (Steele et al., (2016); Chan et al., 2020).

A diverse but low-abundance suite of organic compounds has been identified within Martian materials though both meteoritic and in situ analyses. These organics span from simple volatile species to complex macromolecular carbon. Martian meteorites such as ALH 84001, Nahkla, Tissint, and NWA 7034 contain aliphatic and aromatic hydrocarbons, oxygen and nitrogen bearing organics and refractory macromolecular carbon (MMC) structurally analogues to terrestrial kerogen (Steele et al., 2012; Steele et al., 2018; Sephton et al., 2002; Jaramillo et al., 2019) In situ analyses conducted by Martian missions such as Viking, Curiosity and Perseverance have detected chlorinated hydrocarbons, thiophenes, aromatics and other C-bearing fragments within sedimentary and igneous materials. However, concentrations are generally very comparatively low ranging from parts per billion in surface regolith to tens or hundreds of parts per million (ppm) total organic carbon in some meteorites. These findings show that Mars hosts a chemically varied, indigenous organic suite that has been found associated with mineral matrices and likely influenced by volcanic activity, aqueous alteration and radiation-driven surface chemistry (Steele et al., 2012) Table 1 provides a broad overview of the organics detected from Martian meteorites and missions.

Table 1 - Organics discovered in Martian meteorites (purple) and missions with their relative abundances (References within)

Meteorite / Mission	Organic Molecules Detected	Analytical Method	Approx. Abundance	Key References
ALH 84001	Macromolecular organic carbon (MMC), aromatic associated with carbonyl, carboxyl and carbonate group functionality	Raman spectroscopy, STXM, NanoSIMS, XANES	Trace (<10 ppm C)	Steele et al. (2012); Steele et al., (2022)
Tissint	Aromatic and alkyl-substituted aromatic hydrocarbons, chlorobenzene, thiophenes	TOF-SIMS, NanoSIMS Py-GC-MS	Low (~1–50 ppm C)	Lin et al. (2014), Jaramillo et al., (2019); Steele et al. (2022); Schmitt-Koplin et a., (2023)
Nakhla	Aliphatic and aromatic hydrocarbons; carboxylic acids	Solvent extraction, GC–MS, NanoSIMS, Laser Raman Spec	Trace to low (<10 ppm C)	Sephton et al. (2002); Grady et al. (2004); Gibson et al., (2006)
NWA 7034	Complex aromatic/aliphatic MMC-like organics	Raman, XANES, Pyrolysis–GC–MS, NanoSIMS	Moderate (up to ~200 ppm C)	Steele et al. (2018); Goodwin et al., (2024)
Viking Landers	Chloromethane, dichloromethane (possible indigenous)	GC–MS	Trace (ppb range)	Biemann et al., (2007)
Curiosity Rover (SAM, Gale Crater)	Long chain alkanes, chlorobenzene, chloromethanes, thiophenes, aliphatic fragments	(Pyrolysis–) GC–MS	Low (0.1–5 nmol C/g)	Glavin et al., (2013); Eigenbrode et al. (2018); Freissinet et al. (2025)
Perseverance Rover (SHERLOC, Jezero Crater)	Aromatic organics associated with sulfates and carbonates	Raman + fluorescence spectroscopy	Trace to low (qualitative detection only)	Sharma et al., (2023); Farley et al., (2022)

In recent decades, organic matter (OM) has been confirmed both on Mars (Eigenbrode et al., 2018; Franz et al., 2020) and within Martian meteorites (Sephton et al., 2002; Steele et al., 2012), including sulfur-bearing organics such as thiophenes (Eigenbrode et al., 2018; Steele et al., 2018). The latest rover missions, NASA's Perseverance and ESA's Rosalind Franklin, are equipped with Raman spectrometers and mass spectrometers specifically designed to detect OM (Vago et al., 2017), with Perseverance additionally collecting and caching samples for return to Earth under the Mars Sample Return (MSR) program. As organics in meteorites correlate with those detected in situ, Martian meteorites and their

analogues are critical materials for refining organic extraction and detection techniques ahead of MSR.

Martian meteorites are primarily igneous rocks, representing the only physical samples of Mars currently available for high-resolution laboratory study (Udry et al., 2020). They contain both insoluble organic matter (IOM) and soluble organic matter (SOM), each providing complementary insights into Martian organic chemistry (Sephton, 2002). IOM is typically refractory, aromatic, and kerogen-like, dominated by polycyclic aromatic hydrocarbons (PAHs) closely associated with oxide and silicate minerals, suggesting an abiotic, possibly hydrothermal origin (Steele et al., 2012; Steele et al., 2016). SOM, is composed of extractable aliphatic and aromatic hydrocarbons, amino acids, and heteroatom-bearing species (nitrogen and oxygen), representing the more labile and mobile organic fraction (Sephton et al., 2002; Chan et al., 2020). These soluble organics can be released and concentrated through aqueous alteration, providing key evidence for carbon cycling on Mars (Tutolo et al., 2025).

Analytically, SOM is typically extracted using solvent-based techniques and characterised by gas chromatography–mass spectrometry (GC–MS), liquid chromatography–mass spectrometry (LC–MS), or high-performance liquid chromatography (HPLC) (Sephton et al., 2002; Glavin et al., 2010; Callahan et al., 2013; Chan et al.,2020). These methods enable compound-specific identification of aliphatic chains, aromatic rings, and oxygen- or nitrogen-bearing molecules that may record abiotic synthesis pathways, such as Fischer–Tropsch-type reactions, or secondary alteration processes on Mars (Schulte et al., 2006, Steele et al., 2018; Schmitt-Koplin et al., 2023; Goodwin et al., 2024). Understanding SOM in Martian meteorites is therefore essential to developing and optimising analytical protocols for detecting trace organics in forthcoming Mars Sample Return materials.

The Mars Sample Return (MSR) mission aims to return pristine Martian samples to Earth to enable laboratory analyses of potential biosignatures and organic molecules (Beaty et al., 2019; Grady, 2020); MOMA (Mars Organic Molecule Analyser) will be the main instrument on ExoMars and is equipped with a GC-MS which has already successfully detected a variety of organic molecules at the Svalbard sites (Siljestrom et al., 2014). GC-MS data from Svalbard revealed that hydrothermal CO_2-rich alteration of basaltic rocks can abiotically generate aromatics, long-chain hydrocarbons, carboxylic acids, and amino acids (Siljestrom et al., 2014) which has major implications for future Martian missions. MOMA will

investigate the scientific objective set out by ExoMars to search for signs of past or present life on Mars (Goesmann et al., 2017).

1.1.2.1 Origin of organics on Mars

Organic molecules have been discovered on Mars and within the planets' meteorites, although, there is still debate regarding their origin and whether they are indigenous compounds or exogenous (Steele et al., 2016). Koike et al (2020) discuss the possible methods for carbon delivery; abiotic synthesis, organics delivered to Mars via impact and biotic origin, through the nitrogen-bearing organics found within Noachian carbonates.

A potential abiotic mechanism for indigenous organic molecules on Mars is carbonation and serpentinization reactions from aqueous alternation of mafic igneous minerals by hydrothermal fluids (Steele et al., 2022*).* The organics in ALH 84001 have been used to investigate early Martian environments; the ALH 84001 carbonate globules are speculated to have formed through precipitation from aqueous fluid (18±4ºC) near Mars' surface during the Noachian (Halevy et al., 2011; Koike et al., 2020).

Fischer-Tropsch-type reaction produces straight chain hydrocarbons (normal n-alkanes) from reaction of CO and H^2 on mineral catalyst surface and thus has been considered as a source of organics in the early Solar System due to the presence of n-alkanes in meteorite extracts (Ehrenfreund and Sephton, 2006).

Exogenous carbon may have been delivered by organic-bearing comets, meteorites or interplanetary dust particles which continue to fall on the surface of Mars (Sephton et al., 2014). Carbonaceous chondrites, which exist in the asteroid belt and contain various soluble and insoluble nitrogen bearing organic matter groups, have also been suggested for exogenic organic delivery (Koike et al., 2020). The organic matter may include, but is not limited to, amines, amides and macromolecular carbon up to 100s ppm (Koike et al., 2020).

Although not yet discovered on Mars, biogenic organic matter would be difficult to characterise on the Martian surface today due to the high UV and oxidising nature of the environment. However, it has been debated that a once warmer and wetter Noachian Mars

may have harboured the necessary ingredients for life with evidence of delta lake deposits on the Martian surface (Carr and Head, 2010; Koike et al., 2020; Gupta et al.,2021).

Liquid water is an essential ingredient for life on Earth, so the clear evidence that water once existed on Mars has deeper implications for organics on the red planet. Carbon and nitrogen reactions are fundamental ingredients to life and so their detection on the Martian surface is an incredibly important find (Koike et al., 2020). Organics on the present-day Martian surface are difficult to define due to the atmospheres oxidising nature – They may also be destroyed or altered at the surface due to this radiation. Therefore, digging beneath the surface may be the key in finding Martian biosignatures (Eigenbrode et al., 2018; Baqué et al., 2022).

Carbonates on Mars provide key evidence for past interactions between the atmosphere, hydrosphere, and basaltic crust (Morris et al., 2010; Ehlmann et al., 2011; Mahaffy et al., 2012; Bridges et al., 2019). Early Mars (Noachian) had extensive volcanic activity, thought to have released significant amounts of CO_2 into the atmosphere, estimated between 0.1 and 10 bar (Lammer et al., 2013), creating conditions under which aqueous alteration is predicted to have produced sedimentary carbonates. Although much of this CO_2 (up to 3 bar) was later lost to space, aqueous alteration reactions would have converted some atmospheric CO_2 into carbonate minerals, partially sequestering carbon from the atmosphere. Carbonates have been identified both remotely and in situ by Martian orbiters and rovers as well as within Martian meteorites and typically occur in association with dominantly iron (Fe), but also magnesium (Mg)- Calcium (Ca)– and manganese (Mn) phases. Magnesium carbonate was detected in bedrock within the Nili Fossae region by orbital spectroscopy (Ehlmann et al., 2011), in the soil by the Phoenix Lander at its landing site, in the Comanche carbonate investigated by the Spirit Rover (Morris et al., 2010) and within drill samples taken by Curiosity at Gale Crater (Tutolo et al., 2025). Nahkla, Lafayette, EETA 79001 and ALH 84001 have all been found to contain some association with carbonate (McKay et al., 1998; Treiman et al., 2002; Steele et al., 2007 Niles et al., 2013)

Martian carbonate compositions and their co-location with primary basaltic minerals (olivine and pyroxene) imply a formation of aqueous alteration of basalt which in turn indicates that the main mode of carbonate mineral formation on Mars is possibly hydrothermal replacement of basaltic minerals (Tutolo et al., 2025). These observations

imply that carbonate formation on Mars reflects dynamic water-rock interactions within the basaltic crust and offers a valuable record of the planet's early carbon cycle and thus habitability potential of early Mars (Bridges et al., 2019; Hickman-Lewis et al., 2022).

1.1.2.2 Martian meteorites

The majority of Martian meteorites are mafic to ultramafic igneous rocks, formed from magmas that erupted at or near the Martian surface (Herd et al., 2024). Martian meteorites were originally split into three separate groups based on petrological similarity of the meteorites: Shergotty, Nahkla and Chassigny therefore becoming Shergottites, Nahklites, Chassignittes or 'SNC's. Not all Martian meteorites fall within this traditional understanding such as ALH 84001, an orthopyroxenite, and NWA 7034, a basaltic breccia (Figure 2).

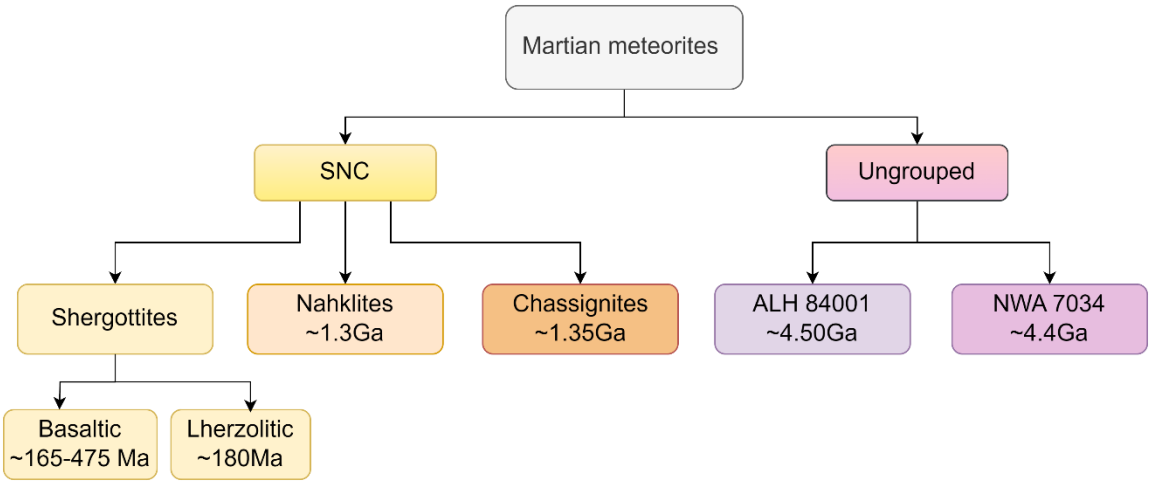

Figure 2 - Martian meteorite classifications and their associated formation ages (Nyquist et al., 2001, Santos et al., 2015 and references therein).

The SNC meteorites exhibit a wide range of mineralogical and chemical compositions with distinct isotopic and noble gas signatures that link them to Mars. Their relatively geologically young crystallisation age (less than 1.4 billion years) indicate that Mars experienced prolonged igneous and volcanic activity well into the Amazonian period (Nyquist et al., 2001; Borg & Drake, 2005).

Shergottites account for over 80% of the Martian meteorites; they are predominantly mid- to late Amazonian in age (crystallisation ages of < 716 Ma) and are a suite of tholeiitic igneous rocks (Udry et al., 2020, Herd et al., 2024). The nakhlites are clinoproxenites from shallow intrusive bodies and chassignites are olivine-rich cumulates (Treiman, 2005). Our

understanding of Mars from the meteorite data is, other than ALH 84001 and NWA 7034, centred and therefore biased towards the Amazonian (Udry et al., 2020).

The only sample suite available for studying Martian materials is in the form of Martian meteorites of which only ~272 meteorite samples are currently available to understand the entirety of the red planet. These samples provide invaluable insights into Mars' geochemistry and history, yet they represent a limited and potentially biased record of the planet's surface evolution. The majority of these, excluding polymict breccia NWA 7034 and orthopyroxenite ALH 84001, are Amazonian-age igneous rocks. Making them unrepresentative of much of Mars's crustal history (Udry et al., 2020). Remote sensing records of Mars indicate that approximately 75% of the surface of Mars is Hesperian to Noachian (>~3.4 Ga) and only 25% is Amazonian in age (Herd et al., 2024). This discrepancy highlights the need for Mars Sample Return mission that can provide geologically diverse material from older terrains (Udry et al., 2020; Farley et al., 2022).

1.1.2.3 Organics in Martian meteorites

Carbon is present in primitive meteorites as organic matter and includes compound classes of low molecular weight; aliphatic and aromatic hydrocarbons, amino acids, nucleic acid bases, carboxylic acid, phosphonic acids, sulfonic acids, sugar-related compounds (Sephton et al., 2002). The aromatic network is the major component to the organic matter found within the meteorites (Sephton, 2012). Martian meteorites contain indigenous insoluble and soluble (macromolecular) organics, including aliphatic and aromatic hydrocarbons, hetereoatom-bearing species (N, O, S compounds), and kerogen like carbon (Sephton et al., 2002; Glavin et al., 2010; Steele et al., 2016 Chan et al., 2020). Solvent soluble organic material (SOM) can be sub-divided into labile (macromolecules and amino acids affected by heat/water) and volatile organics (Chan et al., 2020). Insoluble organic material (IOM) refers to refractory macromolecular material unaffected by heat and water (Sephton et al., 2013). The focus for this project is on extracting and investigating the SOM material through solvent extractions and gas chromatography – mass spectrometry.

Abiotic reduced macromolecular carbon (MMC) inclusions in magmatic minerals have been detected in Martian meteorites (Steele et al., 2012). The organic material is dominantly polycyclic aromatic hydrocarbons (PAH) which are reactants in amino acid synthesis (Steele et al., 2012). The MMC is closely associated with the mineral structure which is important as it firstly implies an indigenous origin and secondly confirms that this

MMC crystallised from the host magma (Steele et al., 2012). As MMC is found associated with an igneous component, it has been argued that this organic matter is a result of hydrothermal processes as part of an abiotic organic synthesis like serpentinization (Steele et al., 2021).

Mars Sample Return mission will provide samples with a background context with extremely minimal contamination (Grady, 2020). Thus, it is crucial that a method for organic extraction from Martian material is optimised ahead of sample return. Martian meteorite material is dominantly basaltic and the MSR samples are likely to be similar in rock type; therefore, understanding how to identify organic material and subsequently extract and analyse these organics from igneous samples is extremely important.

1.1.3 Martian Missions

Several missions over the past ~50 years have endeavoured to uncover more about our neighbour planet, Mars. Orbiters, landers and rovers have revealed crucial information regarding the planet's history (Biemann, 2007; Carr and Head, 2010; Farley et al., 2020). Mission aims often involve an astrobiological aspect in order to understand habitability on the red planet. Below outline some of the key findings from previous missions which are relevant to this project.

1.1.3.1 Viking

The Viking projects first launch in 1975 marked the beginning of the (in-situ) search for signs of life on the red planet (Biemann, 2007). Viking 1 and Viking 2 consisted of an orbiter and lander respectively to carry out 13 scientific investigations regarding the surface and the atmosphere (Soffen & Synder, 1976). Viking 1 landed on Chryse Planitia (22°N, 312°E) chosen as it appeared close to the end of multiple ancient large channel systems associated with fluvial and aeolian processes, Viking 2 landed at Utopia Planitia (48°N, 134°E), an impact basin chosen due to evidence of periglacial features (Soffen & Synder, 1976). The orbiter took multiple images of the surface which enhanced the understanding of the wider geology of the area (Synder & Evans, 1981). In-situ experiments were conducted by the landers in search of organic material within the Martian regolith and determine whether the synthesis of this material was abiotic or biotic. These experiments were aided by a GC-MS with a 12-200 Dalton mass range and a ppb detection limit (Anderson et al., 1972). The results from both rovers reported chlorinated

hydrocarbons at 0.04-40 ppb however, this was originally attributed to terrestrial contamination deeming the results inconclusive. Conversely, these findings have since been revised by numerous studies (Navarro-Gonzalez et al., 2010; Guzman et al., 2018) This mission revealed important information about the Mars surface, climate and atmosphere; the UV radiation from the sun paired with the extremely dry regolith at the surface would create a hostile environment for any living organism (Soffen & Snyder, 1976).

1.1.3.2 Spirit and Opportunity (MER)

Mars Exploration Rover (MER) mission by NASA involved two Mars rovers, Spirit and Opportunity which both landed by January 2004 to explore separate areas of Mars with onboard laboratories. The rovers purpose was to provide wider context and ground-truth orbiter observations in terms of geology and previous aqueous history (D'Uston, 2011). Spirit explored Gusev Crater to discover the intricacies of Columbia Hills in attempt to characterise Early Mars. The Comanche outcrops at Columbia Hills were discovered to host carbonate with Mg-Fe rich compositions (Morris et al., 2010), similar to the globules found in ALH 84001, which has been attributed to possible hydrothermal origin and thus evidence of previous habitable conditions (Ruff and Farmer, 2016). This analogy was aided by studying analogue material from Svalbard where similar carbonates are formed through hydrothermal origins.

Opportunity explored Meridiani Planum near the equator of Mars which hosts various geologic units from Early Noachian to Late Amazonian (Hynek and Di Achille, 2017). Here, the rover observed numerous features such as trough cross laminations that would suggest near surface flowing water (Squyres et al., 2006). Spectrometry on board also discovered hematite and layered deposits of sulphate again supporting the case for aqueous processes on the surface and within the groundwater table (Squyres et al., 2006).

1.1.3.3 Phoenix

After successfully landing on Mars in 2008, the Phoenix lander began its 3-month investigation. The key goals of the Phoenix lander were to assess local habitability and gather information about the history of water in the Martian arctic. The lander would analyse soil samples using its robotic arm to dig and collect samples for further analysis using its onboard wet chemistry laboratory. The major find for this mission was the

presence of water-ice and perchlorates at the Martian surface and methane in the atmosphere (Hecht et al., 2009).

1.1.3.4 Curiosity

Curiosity was launched in 2011 as part of the Mars Science Laboratory mission and set out to uncover if Mars ever hosted the right environmental conditions to support life (Grotzinger et al., 2012) Gale crater was the chosen area for this mission, a ~154 km impact crater, chosen due to the strong evidence of water being previously present in this impact area with observations implying a previously habitable fluvio-lacustrine environment (Jones, 2018).

Curiosity is equipped with the SAM (Sample Analysis on Mars) suite which contains a quadrupole mass spectrometer (QMS), a gas chromatograph (GC) and a Tuneable Laser Spectrometer (TLS). These instrumentations allow the rover to measure the chemical composition of the major atmospheric species (Trainer et al., 2019).

Organic molecules were discovered by the Mars Science Laboratory (MSL) on board Curiosity Rover at the Sheepbed Mudstone at Gale Crater using GC-MS and EGA (evolved gas analysis) (Freissinet et al., 2015). The Sheepbed Mudstone was interpreted to have formed in a lacustrine environment around 3.6-3.1 Ga ago (Summons et al., 2011) and contained ~20% of smectite in the samples that were drilled. On Earth, smectite aids in protecting organic compounds (Freissinet et al., 2015) and so detection at or below the Martian surface could imply preservation potential.

Further organic material was discovered in the ~3 Ga year old mudstones within the Murray formation at Gale Crater. Refractory organic material was found within Martian mudstones around the ancient lake environment although, it is still unclear whether the source is biological, geological or meteoric in origin (Eigenbrode et al., 2018). Within the Yellowknife Bay area of Gale Crater, GC-MS analyses of a drilled mudstone known as Cumberland have identified dichlorinated alkanes, chlorobenzenes, benzoic acid thiophenes, and other sulphur-containing organic compounds of Martian origin (Freissinet et al., 2025)

1.1.3.5 Perseverance and Mars Sample Return (MSR)

The Perseverance Rover landed in 2021 with astrobiology focussed mission goals. The chosen location to help answer these questions is Jezero crater, a 45km diameter paleolake system hosting delta deposits hypothesised to be from the early Noachian through to the Hesperian, with possible biosignatures (Hickman-Lewis et al., 2022). Another interesting feature surrounding this site is basin fill from the mid to late Noachian containing Mg- rich carbonate and olivine (Goudge et al., 2015). Carbonate minerals have been detected in this area believed to have formed in this previous fluvial/lacustrine environment through hydrothermal alternation (Gupta et al., 2021) Surrounding rocks in the Nili Fossae region appear to have similar composition therefore implying a similar formation mechanism (Tarnas et al., 2021). Igneous rocks that have experienced interactions with liquid water have been discovered at the floor of Jezero crater which has important implications for ancient habitability of Mars (Farley et al., 2022)

Perseverance is currently caching rock core and regolith samples in collaboration with the Mars Sample Return mission; a collaborative event with NASA and the European Space Agency (ESA). MSRs main job is to return the samples, collected by Perseverance, back to Earth, which is expected around 2033. An extensive team of landers, orbiters and rockets will collaborate on the mission of returning samples (Beaty et al., 2019).

Returned Martian samples will allow for further analysis on Earth based labs without the limitations of size and weight constraints present during in-situ analysis (Grady, 2020; Farley et al., 2022). Returning pristine samples for which we will have wider stratigraphic and geologic context which is lacking from meteorite samples and is integral for investigating the red planet (Grady, 2020). We will not know the wider context of Mars' geological history and associated astrobiological queries until we can perform ex-situ analysis on indigenous Martian rocks with state-of-the-art equipment within Earth based laboratories (Beaty et al., 2019; Farley et al., 2022). It is thus imperative that an optimised protocol for organic extraction and subsequent GC-MS analysis is established prior to sample return.

1.1.3.6 Knowledge and understanding gained from Martian missions

Decades of Martian exploration by orbiters, landers and rovers have yielded critical insights in to the red planet's geological, climatic and astrobiological history. These

discoveries have transformed scientific perspectives of Mars and provided an essential foundation for future research projects, including this one.

The Viking mission began the search for in-situ organic detection revealing that the harsh UV radiation, extreme dryness and oxidising conditions create a hostile surface environment preventing organic preservation (Soffen & Synder, 1976). The robotic exploration of Mars has also aided in confirming that Mars was once hosted a thicker atmosphere with an aqueous environment and thus increasing the potential for habitability (Wordsworth, 2016). The Mars Exploration Rover mission revealed that Mg-Fe rich carbonates, hematite and sulphate deposits could indicate hydrothermal aqueous processes similar to those features observed in ALH 84001 and Svalbard analogues (Morris et al., 2010) The Phoenix lander confirmed water ice at the Martian poles as well as percholates (Hecht et al., 2009). The SAM suite onboard the Curiosity rover detected organic molecules in ancient mudstones and demonstrated the importance of smectite in shielding organics from radiation and oxidation (Freissinet et al., 2015; Eigenbrode et al., 2018). Perseverance and the MSR mission show that Mars' surface and sub-surface have recorded water-rock interactions, redox chemistry and meteoritic input over billions of years (Hickman-Lewis et al., 2022).

Previous in-situ GC-MS analyses have had varying success levels due to the harsh Martian surface conditions which again reinforces the importance of returning contextualised bore samples to Earth for ex-situ analysis to overcome payload limitations. It is therefore crucial to establish an optimised GC-MS analytical protocol for ex-situ analysis in Earth based labs ahead of the Mars Sample Return mission (Grady, 2020). Refining the protocol will allow us to overall help to address fundamental questions surrounding habitability, prebiotic chemistry and potential biosignatures on Mars.

1.1.4 ALH 84001

ALH 84001 from Allan Hills, Antarctica, is the oldest Martian meteorite discovered with a crystallisation age of ~4.09 Ga which provides insight into early Mars (Lapen et al., 2010). This meteorite sparked controversy when McKay et al. (1996) declared that there was evidence of ancient extra-terrestrial life due to the present of polycyclic aromatic hydrocarbon (PAH) within the meteorites carbonate globules. Further inspection disproved this theory when Anders (1996) debated this theory to prove that these PAHs were likely formed by Fischer-Tropsch reactions making them abiotic in origin, this was also

supported by further studies (Clemett et al., 1998; Zolotov and Shock, 2000). This controversy helped to widened the discussion and subsequent investigation into astrobiological research.

1.1.4.1 Geology

ALH 84001 originated from a basaltic magma within Mars and was a cumulate of igneous rock, orthopyroxene, chromite and olivine (Mittlefehldt, 1994; Treiman, 2021). The meteorite is an orthopyroxenite; a coarse-grained igneous rock that is rich in pyroxene with grain size up to 3.5mm (Udry et al., 2020). Isotope data reveals a crystallisation age of ~4.09 ± 0.3 Ga, around the time of heavy bombardment and just prior to the cessation of the global magnetic field (Lapen et al., 2010). ALH 84001 has a long and complex history of deformation and shock metamorphism (Treiman, 1998) complicating geological interpretations. ALH 84001 and the Nakhlites carbon may have been preserved due to a pre-ejection burial depth shielding the material from the UV exposure and oxidising agent (McKay et al., 2010). The carbonate globules within this meteorite have been a key focus for astrobiology. There is also evidence for nitrogen-bearing organic compounds within this meteorite, discovered using X-ray Absorption Near Edge Structure (XANES) analyses, (Koike et al. 2020) suggesting that the surface of early Mars (Noachian) at the time of carbonate formation must have been a less oxidising environment than what we see today (Koike et al., 2020).

1.1.4.2 Carbonates

The carbonates present in ALH 84001 have been intensively studied and are the only carbonates we are aware of that have experienced an early Martian environment (Treiman et al., 2002). As a result of this, the atmospheric compositions and associated compounds from the Noachian-Amazonian can be deduced (Treiman et al., 2002) to reveal a more habitable environment in the Noachian (Treiman et al., 2002). Fe-Mg zoned carbonates can be found as hemispherical to spherical globules and are commonly concentrically zoned with calcite centres and magnesite-magnetite rims (Vago et al., 2017; Treiman, 2021).

The rims of the carbonate globules are associated with magnetite and pyrrhotite (Treiman, 2021). Formation of the magnetite has been attributed to shock metamorphism from Fe-rich carbonates (Treiman, 2003). Isotopic compositions of strontium within the carbonate show that these compounds are mainly derived from phyllosilicates dating back more than

~4.2 Ga ago when aqueous alteration occurred at a low temperature in crustal rocks (Beard et al., 2013).

Carbonates present in ALH 84001 have been dated between 3.9-4 Ga (Borg et al., 1999). They were precipitated from near-surface aqueous fluids (Gibson et al., 2001) at a precipitation temperature of 18 ± 4 °C with neutral water and CO_2 derived from Mars' ancient atmosphere (Havely et al., 2011). Thus proving fluid movement in water reservoirs within the Martian crust during the Noachian (Gibson et al., 2001). This aqueous environment in the early Mars' epoch is consistent with perhaps a previously warmer Mars or equally a hydrothermal heat source (Havely et al., 2011).

1.1.4.3 Organics

The organic carbon in this meteorite is closely associated with the carbonates and located with the magnetites (Steele et al., 2020). Organic matter can be attributed to serpentinization (when water alters the mafic basalts crystal structure of the mineral) and carbonation (chemical reaction forming carbonates from the CO_2 in aqueous fluids on early Mars) reactions (Steele et al., 2022). Serpentinization produces H which is then able to reduce aqueous CO_2 to organics such as methane and CO. Carbon monoxide and hydrogen can also react via Fischer-Tropsch-type (FFT) reactions to produce organic molecules such as alkanes and Ni-bearing organics (Schulte et al., 2006).

The organic matter was able to survive in the fluids trapped within carbonates stored within the Martian surface, shielding it from Mars' harsh UV radiation (Koike et al., 2020). Investigation into the lack of nitrate signatures within ALH 84001 infer that 4Ga when near-surface fluid was flowing on Mars, the surface environment was less oxidising, at least in this case (Melwani Daswani et al., 2016; Koike et al., 2020). Therefore, ALH 84001s host rock must have been stored within the Martian surface shielding it from billions of years' worth of radiation (Koike et al., 2020).

Within this orthopyroxene cumulate, parts per million amounts of polycyclic aromatic hydrocarbons (PAH) are found associated with carbonate globules (Bada et al, 1998). The formation of these compounds is associated with FTT reactions catalysed by the magnetite in this case (Treiman, 2003). As the PAH is associated with the mineral phases, this would suggest an indigenous origin (Steele et al., 2016).

1.2 Svalbard: A terrestrial analogue for ALH 8001

1.2.1 AMASE

The Arctic Mars Analogue Svalbard Expedition (AMASE) is a collaborative project with NASA and ESA which has occurred annually from 2003-2011 to test Martian analogue sites on Svalbard, specifically to test Mars mission field instruments for their robustness on Martian-like conditions future missions (Mahaffy et al., 2010). The Bockfjorden Volcanic Complex (BVC) was discovered in AMASE 2009 and set as a target for instrument testing on Martian analogue material for AMASE 2010 (Steele et al., 2011). The geomorphology and geology of the BVC closely resembles the volcano-permafrost-ice interactions on Mars (Treiman et al., 2002; Steele et al., 2007; Steele et al., 2011). The main goals for the project included testing robustness of the field instruments in rugged, Martian-like terrain, investigate Martian analogue settings for biosignatures and define a protocol for reduction of contamination (Steele et al., 2011).

BVC volcanics, particularly Sverrefjelle exhibit hydrothermal alteration as pillow lavas and palagonite, a result of lava and hydrothermal interaction during eruption (Treiman et al., 2002). This feature can be traced through many of the volcanoes within the BVC (Amundsen et al., 1987). Clay minerals and microscopic carbonate spherules are also found associated with hydrothermal alteration, most likely derived from CO_2-rich hydrothermal fluids carrying and subsequently depositing carbonate material (Mojzsis et al, 1999; Treiman et al., 2002). The carbonate minerals are concentrically zoned with Fe-rich cores and Mg-rich rims (Treiman et al., 2002) and can be found within xenoliths and their host basalts. These spherules display a similar texture and composition to the abiogenic carbonate deposits within the Martian meteorite ALH 84001 (Steele et al., 2007).

The magnesium-rich carbonate found in the BVC has been attributed to hydrothermal fluid precipitation because of volcanic activity (Treiman et al., 2002; Steele et al., 2007) Thus, by analogy, it could be hypothesised that the carbonate globules in ALH 84001 were also a result of primary deposition from hydrothermal activity (Steele et al., 2016). An early Martian environment may have had water in ice form periodically heated and made fluid from potential impacts or volcanic activity (Treiman et al., 2002). The eruption setting of the BVC volcanoes being subglacial also supports this area as a representative proxy of

early Mars during active volcanism as the direct eruption into the ice means it would have melted and thus enabled hydrothermal systems (Stern et al., 2013). Understanding the origin of organics within the carbonates structures present in Svalbard rocks is crucial in deducing atmosphere-hydrosphere interactions on Mars (Shaheen et al., 2014).

Table 2 - Different types of carbonates found within the BVC adapted from Blake et al., 2011

BVC Carbonate Cements (Blake et al., 2011).	
Type 1	Mg-Fe-rich carbonate in sub mm globules found within the basalts and the ultramafic xenoliths (Amundsen, 2011).
Type 2	1-3cm coatings of carbonate cement. Found on the walls of volcanic pipes.
Type 3	Pipes or vents filled with breccia where the fragments of breccia are cemented by carbonate. These fragments are known to contain carbonate globules

Samples collected during the AMASE11 mission were used to test out equipment (MOMA) created for organic analysis on Mars ahead of the proposed ExoMars mission (Siljestrom et al., 2014). Further research investigating Martian analogues can be found in the Appendix (Section A.1).

1.2.2 Geological History of Svalbard

Svalbard is an archipelago composed of nine islands lying between Norway and the North Pole within the Arctic Ocean. It lies at the northwest corner of the Eurasian plate and is separated from Greenland by the North Atlantic mid-ocean ridge (Elvevold et al., 2007). Glacial ice conceals over half of Svalbard which has been massively shaped by glaciation to provide it with an array of features such as fjords and mountains (Elvevold et al., 2007).

The basement rocks are known as the Hecla Hoek succession from the Precambrian - Silurian era which consist of amphibolites and felsic gneisses which were altered during the Caledonian Orogeny ~400-450Myr (Amundsen et al.,, 1987). During the Devonian, mud, sand, and gravel were deposited as Svalbard was under water as part of a shallow ocean. Limestone successions followed during the Carboniferous and Permian (Amundsen et al., 1987). During the transition period of Cretaceous to Tertiary, the Eurasian plate and the North American plate started to drift apart pushing Greenland's continental plate against Svalbard, which ultimately created a mountain range known as the Tertiary fold and thrust belt (Elvevold et al., 2007). The Cretaceous interrupted Svalbard's stability with a period of volcanic activity and faulting with intrusions in fractures and bedding. Sandstone and shale successions are apparent from the Mesozoic and Tertiary (Amundsen et al., 1987). Plate movement from the end Mesozoic- early Tertiary created a new mountain belt in Western Spitsbergen and was synchronous with the North Atlantic and Arctic Ocean formation, which formed by seafloor spreading (~60-40Ma) (Elvevold et al., 2007).

Bockfjord as an area shows evidence of crustal uplift as well as thinning of the mantle lithosphere and associated volcanism mainly from the Neogene (Banks et al., 1999). Volcanism occurred near Bockfjord during the Pleistocene, roughly 1Ma, and created the Bockfjorden Volcanic Complex (Treiman, 2012) with volcanoes Sverrefjelle and Sigurdfjellet protruding in the landscape today (Elvevold et al., 2007). These features lie on the Breibogen-Bockfjorden N-S fault system which is shared with hot springs with Jotun to the north and Troll to the South (Banks et al., 1999) evidently implying a high surface heat flow (Skjelkvåle et al., 1989).

1.2.3 Eruption history of the BVC

Spitsenberg, the largest island within Svalbard at 40,000km^2, lies near the Bockfjorden and Woodfjorden fjords and is host to the Bockfjord Volcanic Complex (BVC). Samples from two of the volcanoes within this complex are analysed for this project; Sverrefjelle(t) and Sigurdfjelle are subglacial Quaternary-age volcanoes composed of dominantly primitive alkali basaltic material which is rich in mantle peridotite xenoliths (Treiman, 2012). The volcanism which formed these structures can be attributed to reactivation of Devonian fractures which display a N-S trend and are host to an array of features including hot springs (Amundsen et al., 1987). The volcanoes lie near the Breibogen-Bockjfjorden regional deep fault which developed from Caledonian tectonism (Figure 3).

The reactivation of this fault resulted in the Quaternary volcanism which shifted from South to North, consistent with the opening direction of the Norwegian-Greenland basin (Sushchevskaya et al., 2008). The Quaternary volcanism occurred during glacial periods approximately 1-2Myr according to Ar-Ar dating (Treiman et al., 2012) and is thought to have erupted into thick ice caps (Stern et al., 2013).

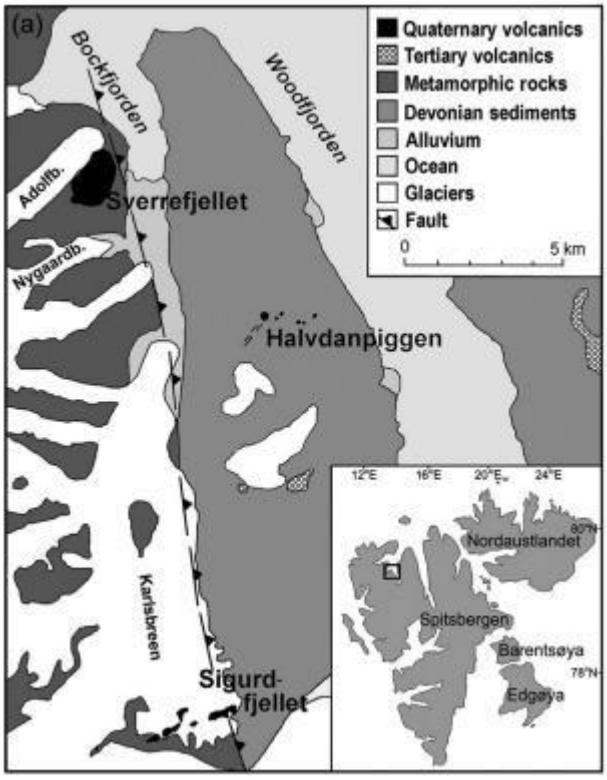

Figure 3 - Simplified geological map of the BVC area (from Treiman, 2012) outlining the Quaternary volcanic sample sites lying near the fault system with Sverrefjelle to the North and Sigurdfjelle to the South

1.2.3.1 Age

Geochemical analysis on these volcanoes reveals a similarity to hawaiite composition. The mantle xenoliths allow the conclusion that the magmas that fed these structures quickly rose from mantle depths (Sushchevskaya et al., 2008). Both volcanoes host a range of upper mantle and lower crustal xenoliths (Skjelkvale et al., 1989). The dominant xenoliths are Cr-diopside lherzolite and represent mantle wall-rock. Mantle xenoliths, crustal xenoliths, secondary minerals, and low-temperature alterations are common throughout both BVC volcanoes suggesting a similar eruption age (Amundsen et al., 1987). Ar-Ar and K-Ar dating reveals the ages of these volcanoes at ~1Ma with the upper limits reaching 2Ma suggesting they have experienced many glaciation events (Treiman, 2012).

1.2.3.2 Sverrefjelle

Sverrefjelle is an alkali olivine basaltic 506m high stratovolcano largely composed of pyroclastic frost-weathered material (Skjelkvåle et al., 1987). There is evidence of the products of this volcanism interacting with glacial ice which would suggest ongoing volcanism during glaciation. Sparse arrangements of pillow lavas at various heights suggest that water or ice was present during lava extrusion (1987). Mantle and crustal xenoliths are most abundant within these pillow lavas at this location displaying an angular – subangular shape at the base of the exposure and more rounded xenoliths in the dyke structures present (Treiman, 2012). Sverrefjellet contains the highest amount of ultramafic xenoliths of any volcanic complex in the world in areas for as much as 50% the outcrop volume (Blake et al., 2011).

1.2.3.3 Sigurdfjelle

Sigurdfjelle is composed of pyroclastics and small explosion vents exhibiting similarities to a diatreme-like vent. Pahoehoe flows rest unconformably on Devonian sandstone and appear to intrude it at some localities (Skjelkvåle et al., 1989). Layered pyroclastic material is rich in mantle and crustal xenoliths dominantly found in the cores of volcanic bombs and breccia (Skjelkvåle et al., 1989). This edifice can be deduced to have formed around the same time as Sverrefjellet based on geomorphological interpretations and geochemical similarities; both primitive and xenolith rich which suggests intraplate volcanism (Skjelkvåle et al., 1989).

1.2.4 BVC vs ALH 84001

Table 3 - Comparison of ALH 84001 and BVC carbonate globules outlining the key similarities and differences outlined from the literature (Treiman et al., 2002; Steele et al., 2011; Steele et al 2016).

A comparison of ALH 84001 and BVC carbonate globules	
Similarities	**Differences**
Size: 10-250μm diameter Shape: ellipsoidal to disc Zoning (optical and chemical): Ca, Fe rich cores to Fe, Mg rich rims. Carbonate layers. Both carbonate minerals are scattered non-homogeneously throughout the rock Organic compounds formed through abiotic processes Olivine dissolution Formation in a hydrothermal environment (?)	Void space: BVC carbonates appear to grow in void space whereas ALH 84001 has no void space History: ALH 84001 has a complex geological history spanning 4 Ga with multiple deformation events including heavy bombardment. BVC less complex, BVC volcanism dated to 1 Ma Clay: Saponite clay appears in and around some globules in BVC rocks but not ALH 84001

There are several variabilities between the carbonate globules present in ALH84001 and BVC rocks but with valid cause. Clay does not appear in all BVC samples, it also postdates carbonates in some areas and is not always associated with carbonates (Treiman et al., 2002; Steele et al., 2011). The BVC samples have pristine silicate glasses, and the clay appears in fractures and void space and is therefore clays are not alterations of silicate glass. Reasoning for the lack of void space in ALH 84001 can be attributed to the long history of deformation of this meteorite. Evidence of shock is apparent in the carbonates and shock feldspathic glass can be observed filling void space. Therefore, void space in ALH84001 was either crushed or filled with shock melts (Treiman et al., 2002). Although there are some notable differences between the ALH84001 and BVC carbonates, this does not necessarily imply different geological formation settings (Steele et al., 2007).

1.3 Extra-terrestrial organics

The study of soluble organic material (SOM) in Martian meteorites is central to understanding the potential for abiotic organic synthesis and prebiotic chemistry on Mars. Over the past 3 decades, GC-MS has been a principal technique used to extract and characterise soluble organics from Martian meteorites, providing molecular level insights into their composition, origin, and preservation (Sephton et al., 2002; Siljeström et al., 2014 Eigenbrode et al., 2018; Guzman et al., 2018; Simkus et al., 2019; Freissinet et al., 2025). Early investigations of ALH 84001 revealed PAHs and other aromatic species associated with carbonate and magnetite assemblages interpreted as possible products of low-temperature aqueous alteration (McKay et al., 1996). Py-GC-MS analyses of the nakhlites and shergottites (e.g Tissint) expanded the known organic inventory to include aliphatic hydrocarbons, alkylbenzenes, carboxylic acids and heteroatom-bearing (N and O) molecules (Jaramillo et al., 2019; Schmitt-Kopplin et al., 2023). These studies show that Martian SOM is chemically diverse but extremely low in abundance, typically occurring in concentrations of a few to tens of micrograms of carbon per gram of rock, much of it likely formed through abiotic water-rock interactions such as serpentinisation or CO_2 reduction reactions (Koike et al., 2020; Steele et al., 2022; Schmitt-Koplin et al., 2023 Sharma et al., 2023)

1.3.1 In-situ GC-MS analysis on Mars

1.3.1.1 Viking Landers 1 and 2

NASA's Viking landers detected organic compounds on Mars using GC-MS paired with Thermal Volatilisation (TV-GC-MS) with MS scan range from m/z 12 to 220 (Biemann, 2007). The GC-MS heated soil samples to 200, 300 and 500 °C to investigate the surface regolith for any potential signs of life (ten Kate, 2010).

Chloromethane and dichloromethane were found and were initially interpreted as terrestrial contamination, however, a reassessment of this data, through the use of a Martian analogue from the Atacama Desert, revealed that this detection was a result of indigenous organics on Mars reacting to perchlorate (Navarro-González et al., 2010). Chlorobenzene was also detected and dismissed as a contaminant; however, the Curiosity rover also discovered this compound implying an indigenous origin (Heinz and Schulze-Makuch, 2020).

1.3.1.2 Curiosity

SAM on board the Curiosity rover has the primary focus of searching for organic molecules in situ, on the Martian surface using pyrolysis-GC-MS analysis (Mahaffy, 2007). SAM uses wet chemistry (derivatisation and thermochemolysis) to help analyse less volatile organics by dissolving the organics prior to pyrolysis to make them more volatile. The derivatisation agent used is N-methyl-N-tert-butyldimethylsilyl-trifluoroacetamide [MTBSTFA] in dimethylformamide [DMF] generally referred to together as MTBSTFA. The thermochemolysis reagent is tetramethyl ammonium hydroxide in methanol (TMAH) which helps to free fatty acids in macromolecules (Williams et al., 2019).

Eigenbrode et al., (2018) detected and analysed in-situ organic matter on the Martian surface using the SAM suite. The organic matter was discovered at Gale Crater, in ancient lake mudstones at the base of the Murray formation dating back ~3.5Ga (Noachian). The mudstones are dominantly basaltic mineral with a mix of phyllosilicates, sulphate and iron oxide. Thiophenes were detected in the Mojave and Confidence Hills, within the Murray formation at Mount Sharp. This detection has important implications as this indicates that this organic matter was aided in preservation by sulfurization (Eigenbrode et al., 2018).

Long-chain alkanes (decane, undecane and dodecane) were discovered by the SAM suite in the Cumberland drilled mudstone within Yellowknife Bay at Gale Crater at the tens of pmol level using GC-MS (Freissinet et al., 2025). The mudstone contained smectite clay and Fe- and Mg-sulfates which helped preserve the organic molecules over geological time (Freissinet et al., 2025). The detection of organic molecules at different temperatures (e.g. chlorobenzene, thiophenes, alkanes) suggests that multiple organic sources and preservation systems may exist within the Cumberland sample (Freissinet et al., 2025). The detection of the long chain alkanes has important implications about Mars' habitability as it suggests that some areas on Mars have organic molecules which are better preserved despite the planets oxidizing surface conditions (Freissinet et al., 2025). The origin of these alkanes is uncertain; however, laboratory studies imply they could be a result of the reduction of straight-chain carboxylic acids such as undecanoic, dodecanoic and tridecanoic acids. These compounds can form through abiotic or biotic processes therefore making their presence on Mars especially significant in the search for potential biosignatures (Freissinet et al., 2025).

1.3.1.3 ExoMars

The ExoMars mission, if successful, will launch the Rosalind Franklin rover, which is equipped with the MOMA (Mars Organic Molecule Analyser) Instrument. MOMA is designed to search for astrobiological signatures and address key questions about the potential for life on Mars by analysing organic compounds (Goesmann et al., 2017). A key feature of the mission is the rover's drill which can collect samples up to 2 metres below the Martian surface, allowing for a more detailed investigation of Martian sediments which may have been shielded from the harsh surface radiation Pavlov et al., 2012).

The primary goal of MOMA is to characterise the range of organic materials present in these sediments (Goesmann et al., 2017). MOMA is a mass spectrometer-based instrument designed for in situ analysis on Mars. It features four individual column modules, each targeting a specific group of chemical compounds. These include volatile organics (with 1-25 carbon atoms), organic enantiomers, derivatisation products and inorganic volatiles (Goesmann et al., 2017)

The GC-MS component of MOMA will offer two types of sample analysis: pyrolysis and wet chemistry. These methods will enable the identification of volatile compounds, polar compounds and macromolecules, providing valuable insights into the chemical makeup and history of Mars (Goesmann et al., 2017).

to answer key questions relating to life on the red planet by searching for astrobiological signatures. This will be benefited using a drill which will collect samples up to 2m below the Martian surface to analyse a wide range of organic compounds (Goesmann et al., 2017). The overarching goal of MOMA is to characterise the range of organic material in Martian sediments (Goesmann et al., 2017; Vago et al., 2017). MOMA is a mass spectrometer-based instrument build for in-situ analysis on Mars which will acquire drill samples up to 2m below the Martian surface. The MOMA GC-MS contains 4 individual column modules to each target a different specific group of chemical compounds such as volatile organics (1-25C atoms), organic enantiomers, derivatisation products and inorganic volatiles (Siljeström et al., 2014; Goesmann et al., 2017). The GC-MS will offer two types of sample analysis including in order to target volatile compounds, polar compounds or macromolecules (Goesmann et al., 2017)

1.3.2 Ex-situ GC-MS analysis of extra-terrestrial material on Earth

Meteorites are subject to a range of different processes to extract organic content. GC-MS is a tried and tested method of successful organic detection for extra-terrestrial material. (Sephton et al., 2002, Steele et al., 2007, Jaramillo et al., 2019, O'Brien, 2022). This section will outline some of the previous studies conducted on extraterrestrial material using GC-MS, including both Martian meteorites and carbonaceous chondrites (Murchison and Winchcombe). Carbonaceous chondrites hold abundant, diverse soluble organic (amino acids, carboxylic acids, PAH's) and are amongst the richest extraterrestrial organic reservoirs known (De Gregorio & Engrand, 2024). Martian meteorites instead typically show substantially lower organic concentrations and typically host more refractory or localised organics, for example within carbonate globules, shock glass, veins (Steele et al., 2016)

1.3.2.1 Tissint

Tissint is an olivine-phyritic shergottite with magnesium rich olivine megacrysts, the cores of the megacrysts have uniform Mg and exhibit Fe zoning with enrichment towards the rims (Liu et al., 2016). The matrix is dominantly composed of pyroxene and maskelynite and shows some minor chromite, pyrrhotite and phosphates (Liu et al., 2016). Tissint is known for its lack of contamination and was analysed using py-GC-MS to show that aromatic and alkyl-substituted aromatic hydrocarbons benzene, toluene, xylene, styrene, and naphthalene were found at low abundance within the meteorite, chlorobenzene and thiophenes were also detected which is consistent with in-situ discoveries at Gale Crater (Eigenbrode et al., 2018; Jaramillo et al., 2019). The composition of organics within Tissint is similar to that found in other picritic (and also basaltic) Martian meteorites such as Elephant Moraine 79001 (hereby known as EET A79001) and Nakhla implying a similar origin (Rochette et al., 2005). Studies have suggested a Martian fluid source for the organic carbon in Tissint (Steele et al., 2012; Steele et al., 2016).

1.3.2.2 Nakhla and EET A79001

Sephton et al., 2002 analysed Nakhla and EET A79001 using pyrolysis- gas chromatography – mass spectrometry to detect high molecular weight organic matter within these Martian meteorites. This organic matter was very similar to that found in carbonaceous chondrites (2002) including PAHs, aliphatic hydrocarbons and amino acids (Glavin et al., 1999). The high molecular weight organic matter in these respective meteorites was very similar (Sephton et al., 2002). Within the cracks of Nakhla, clay

phases (serpentine) and secondary Martian carbonate can be found, providing major insight into Mars' water-crust interactions (Bridges and Schwenzer, 2012; Hicks et al., 2014); an impact induced CO_2-rich hydrothermal fluid precipitated Fe-rich carbonate within brittle fractures; and the subsurface fluid which formed phyllosilicates may have potentially provided habitable temperatures and nutrients necessary for life (Bridges & Schwenzer, 2012).

1.3.2.3 Murchison

Murchison is a widely studied CM meteorite which has been found to contain over 70 extra-terrestrial amino acids as well as carboxylic acids, alcohols, aliphatic and aromatic hydrocarbons (Ehrenfreund and Sephton, 2006). GC-MS detected abiotic, indigenous amino acids in the carbonaceous chondrite (CM2) Murchison proven by the racemic mixtures and structural diversity (Sephton, 2013). Dicarboxylic acids (Lawless et al., 1974) and alcohols (Jungclaus et al., 1976) were also identified in Murchison using GC-MS proving its varied range.

Martins et al., 2008 searched for nucleobases in the Murchison meteorite using GC-MS and discovered that dicarboxylic acids were the most abundant class of compounds detected (Martins et al., 2008). As a result, it could be hypothesised that life on earth and perhaps other rocky bodies may have been delivered by an exogenous source such as carbonaceous meteorites which held the ingredients for life (Martins et al., 2008).

1.3.2.4 Winchcombe

Winchcombe fell in Gloucestershire in February 2021 and was rapidly recovered by the University of Glasgow's Planetary Science team, UK Fireball Alliance, citizen scientists and the UK planetary science community after tracking the fall making this the most accurately recorded carbonaceous chondrite to date (King et al., 2022). It has since been classified as a chondritic meteorite as part of the CM group (a group based on similarity to chondrite Mighei), this group is known for its diverse range of abiotic organic chemistry (Sephton et al., 2023). Around ~10mg of this meteoritic material was subject to analysis using py-GC-MS (Sephton et al., 2023). The chromatogram from Winchcombe revealed aromatic and polycyclic aromatic hydrocarbons along with their derivatives which have undergone substitution and alkylation. It also displayed aromatic compounds containing functional groups incorporating oxygen and sulphur (Sephton et al., 2023). This meteorite contains abundant hydrated silicate minerals formed through fluid-rock interactions, as

well as carbon- and nitrogen- bearing organic matter including soluble amino acids (King et al., 2022)

1.3.3 Other techniques for extra-terrestrial organic extraction

1.3.3.1 GC-IRMS: Murchison

Gas chromatography isotope-ratio mass spectrometry (GC-IRMS) has previously been used to identify compounds evolved from the carbonaceous chondrites Murchison and Orgeuil by hydrous pyrolysis, although the sample size required was too large (>100mg) to be feasible (Sephton et al., 1998, Sephton et al., 1999). Sephton et al., 2001 combined pyrolysis with GC-IRMS and scaled down the sample size required (1-2mg) to successfully achieve the same results. This technique allows for examination of the finer details of the macromolecular material including the isotopic and structural make-up. It produces carbon isotope measurements with a very small solvent extracted sample required (Sephton et al., 2000). GC-IRMS is also useful in identifying a terrestrial signature from an extraterrestrial signature through deuterium/hydrogen (D/H ratios) of an organic molecule although this is limited due to large sample requirement as a result of low organics in these rocks (Callahan et al., 2013).

1.3.3.2 LC-MS: Roberts Massif (RBT) 04262, Lafayette, BVC

Liquid chromatography-mass spectrometry (LC-MS) paired with time-of-flight mass spectrometer has been used to identify amino acids in Roberts Massif (RBT) 04262, a Martian meteorite. Although >20 amino acids were identified by this technique paired with carbon isotope measurements (Callahan et al., 2013), it is still difficult to confirm whether these amino acids are entirely terrestrial or extra-terrestrial, but a Martian origin cannot be ruled out (Callahan et al., 2013). This data offers important insights for sample analysis ahead of MSR where terrestrial contamination should be at an absolute minimum.

O'Brien, 2022 used a non-targeted LC-MS approach in order to investigate organic matter in Lafayette and also Martian analogues (JSC-1, BVC rocks). A range of organic material including fatty acids were detected in Lafayette and JSC-1 (O'Brien, 2022). Through this technique, interesting contaminants were also identified in Lafeyette which could be traced back to field in Indiana within a specific time period verified by further analysis of the metabolomics also highlighting of the importance of documented curation practices ahead of MSR (O'Brien et al., 2022).

Further techniques for extra-terrestrial organic extraction are outlined in the Appendix, Section A.2

1.4 Aims and Objectives

1.4.1 Aim

The aim of this project is to determine the most efficient and effective method of extracting and identifying organic compounds in basaltic Martian analogue rocks through GC-MS analysis. Optimising this protocol will be beneficial for analysing Martian meteorite material and returned Martian samples.

1.4.2 Objectives

1. Optimise organic solvent extractions from BVC Martian analogue samples both containing similar abundance and type of organic material to Martian meteorites.
   Determine the minimal sample mass viable for this analysis.
2. Identify individual organic compounds present in each extraction, along with abundance, via gas-chromatography mass-spectrometry (GC-MS). Use this dataset to determine the optimal protocol for organic extraction and analysis via GC-MS.

   Multiple experiments will trial different methods of sample preparation, organic extraction and analysis as outlined in Figure 4.

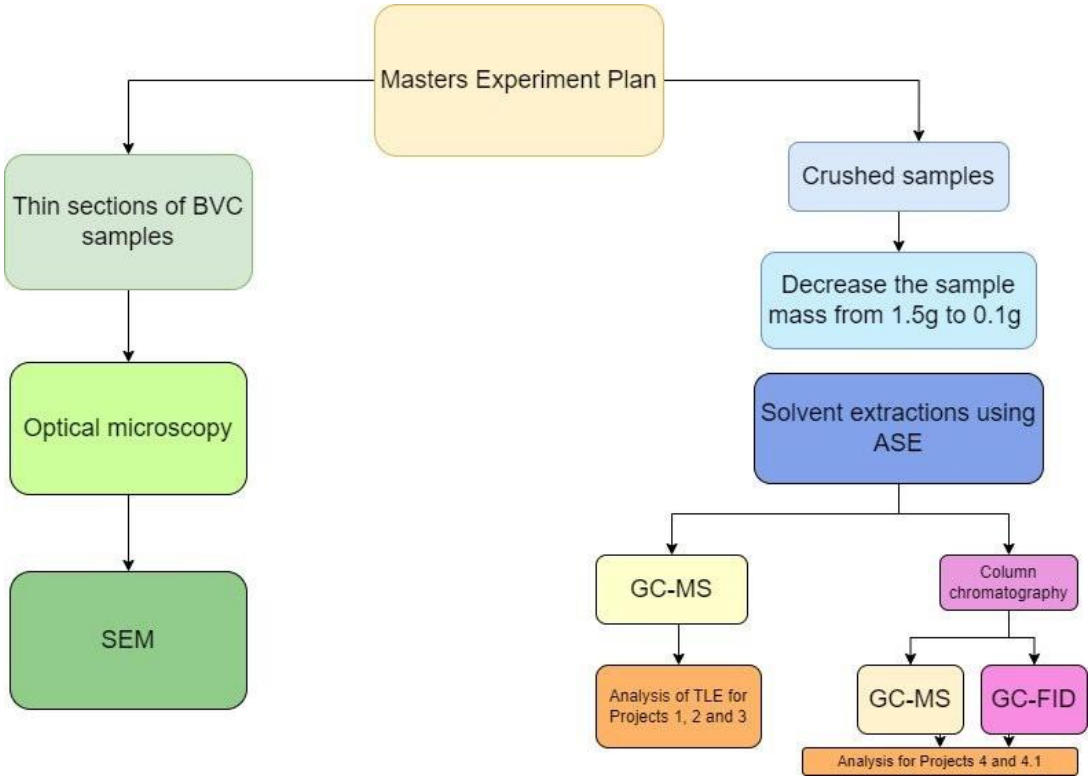

Figure 4 - Masters experiment plan outlining the mineralogical and chemical analysis

1.4.3 Rationale

The importance of the project lies in the preparation of an optimised and tested protocol ahead of the Mars Sample Return mission. Currently, the only material available for study from Mars is in the form of Martian meteorites. NASA's Mars Sample Return (MSR) however will, if successful, provide samples from Mars for analysis in laboratories on Earth. Therefore, it is imperative that organic extraction and GC-MS analytical protocol is optimised to utilise the small volume of material distributed for scientific investigation. Martian analogue material allows for representative testing on bulk material in order to identify the most effective, efficient and practical methods of Martian meteorite organic analyses. Analogues are the closest representation available to test out potentially destructive processes on samples and to understand how this affects the organics within the sample. The analogues used for this study are basaltic rocks which dominate the red planet and yet are not often studied for their organic content.

2. Methods

The methods explored for this project strived to identify the optimal process for organic extraction. The experiment plan flowchart can be found in section 2.2 (Figure 7). Each experiment was adjusted accordingly based on the results of previous experiments. The standard operating procedures (SOP) for the ASE, GC-MS and GC-FID were created by Professor Jamie Toney for the BECS lab and utilised for this project (Appendix, Section B)

2.1 Samples

The samples chosen for this project include combusted sand, JSC-1A Martian Soil Simulant (JSC), Sigurdfjelle and Sverrefjelle from the BVC, Svalbard (Figure 5).

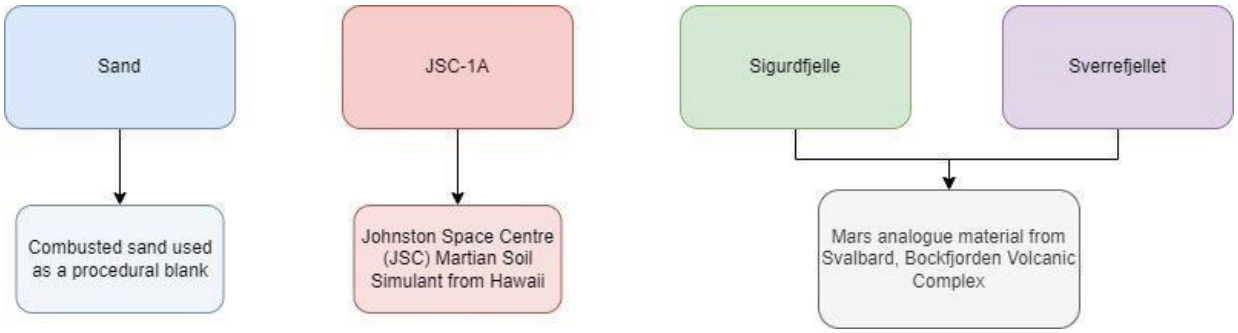

Figure 5 -- Samples chosen for this project and their source

Combusted sand was chosen as a procedural blank / control and was exposed to the same experimental procedure as the other samples for a better representation of any contamination that may be present. JSC was chosen as it is a Martian soil simulant and thus is closest to the material previously examined in situ by past missions. The BVC rocks samples were selected due to their abundance of carbonate globules similar to those discovered in ALH 84001.

2.1.1 Combusted sand

Combusted sand was used as a procedural blank in order to trace any contamination that may come from different areas of the laboratory. The sand was bought in bulk from Fisher Scientific, extra pure, SLR, low iron 40-100 mesh. It was then combusted to 450 degrees Celsius for 8 hours overnight prior to becoming a procedural blank, therefore treated as a sample throughout each experiment.

2.1.2 JSC-1

Martian soil simulants are material which closely resemble Martian regolith in terms of mineralogy, chemistry and geotechnicality (Clark et al., 2021). JSC Mars-1 is a Martian soil simulant developed by NASA Johnston Space Centre for scientific research and education purposes. The material is dominantly palagonic tephra from the Pleistocene cinder cone Pu'u Nene, found between Mauna Loa and Mauna Kea on the latter's south flank on the island of Hawaii, USA (Allen et al., 1998). Palagonitic tephra forms as a result of basalt melt and water interacting which then accumulated on the cinder cone flanks. The simulant is composed of the <1mm fragment of volcanic ash of hawaiite composition particles (glassy and crystalline) and was altered at low temperatures (Allen et al., 1998). Comparison of the chemical composition of JSC Mars-1 and the regolith at Viking and Pathfinders landing sites reveals striking similarities. The material also shares similar spectral properties to that of the tephra analysed on board by the Viking landers, Mars and X-Ray Spectrometry (Bonin, 2012). The similarity of the Hawaiian palagonitic tephra to the regolith found on Mars proves that this is an accurate Martian soil simulant. As well as being a spectral simulant, this material also has a similar chemical composition to the regolith analysed at the Viking and Pathfinder landing sites (Table 4) (Allen et al., 1998). Previous mineralogy work conducted by Allen et al., (1998) confirms that the JSC is a mixture of ash particles which are finely crystalline and glassy of hawaiite composition.

Figure 6 -Map outlining the location of Pu'u Nene (red star) on Hawaii within the flanks of Mauna Kea and Mauna Loa (blue markers).

The crystalline grains are dominantly Ca-feldspar and titanium-magnetite with no signs of phyllosilicates within the sample. Anorthite and olivine were also identified in this sample as well as traces of hematite and pyroxene (augite) (Allen et al., 1998).

The average particle size for JSC particles is around 295µm (Alexiadis et al., 2017) and was therefore already fine enough to be run on the ASE. However, the sample was taken

through the full crushing process to ensure representative results based on the complete method.

Table 4 - Wt% oxides of JSC-1A adapted from Manufacturers data, Goulas et al., 2017 and Allen et al., 1998.

Chemical compound	**Martian Regolith Simulant (Manufacturer data)**	**Martian Regolith (Goulas et al., 2017)**	**JSC Mars-1 (Allen et al., 1998) (Oxide wt %)**
Silicon dioxide (SiO_2)	34.5-44	43-44	43.5
Titanium dioxide (Ti_{O2})	3-4	0.56-1.1	3.8
Aluminium oxide (Al_2O_3)	7-7.5	7-7.5	23.3
Ferric oxide (Fe_2O_3)	9-12	16.5-18.5	
Iron oxide (FeO)	2.5-3.5	N.D	15.6
Magnesium oxide (MgO)	2.5-3.5	6-7	3.4
Calcium oxide (CaO)	5-6	5.6-5.9	6.2
Sodium oxide (Na_2O)	2-2.5	2.1	2.4
Potassium oxide (K_2O)	0.5-0.6	0.15-0.3	0.6
Manganese oxide (MnO)	0.2-0.3	N.A	
Diphosphorus pentoxide (P_2O_5)	0.7-0.9	N.A	0.9

JSC-1 has been studied for organic content previously using HPLC (Garry et al., 2006), LCMS, and HyPy GC-MS, (O'Brien, 2022).

2.1.3 BVC Samples

Sigurdfjelle and Sverrefjelle are igneous basalt samples from Svalbard which are analogues for Martian meteorites, hosting carbonate globules similar to ALH 84001 (Further information in Section 1.1.4). Both volcanic samples were in the form of igneous hand specimens (~6-10cm) stored originally in polyethylene plastic bags due to the nature of the collection. The first stage in the crushing process was to break the rock using a sterilised hammer to uncover a 'fresh', less weathered surface that would be more representative for analysis. BVC samples were kindly provided by Dr. Andrew Steele from the Carnegie Institute.

2.2 Experiment Plan

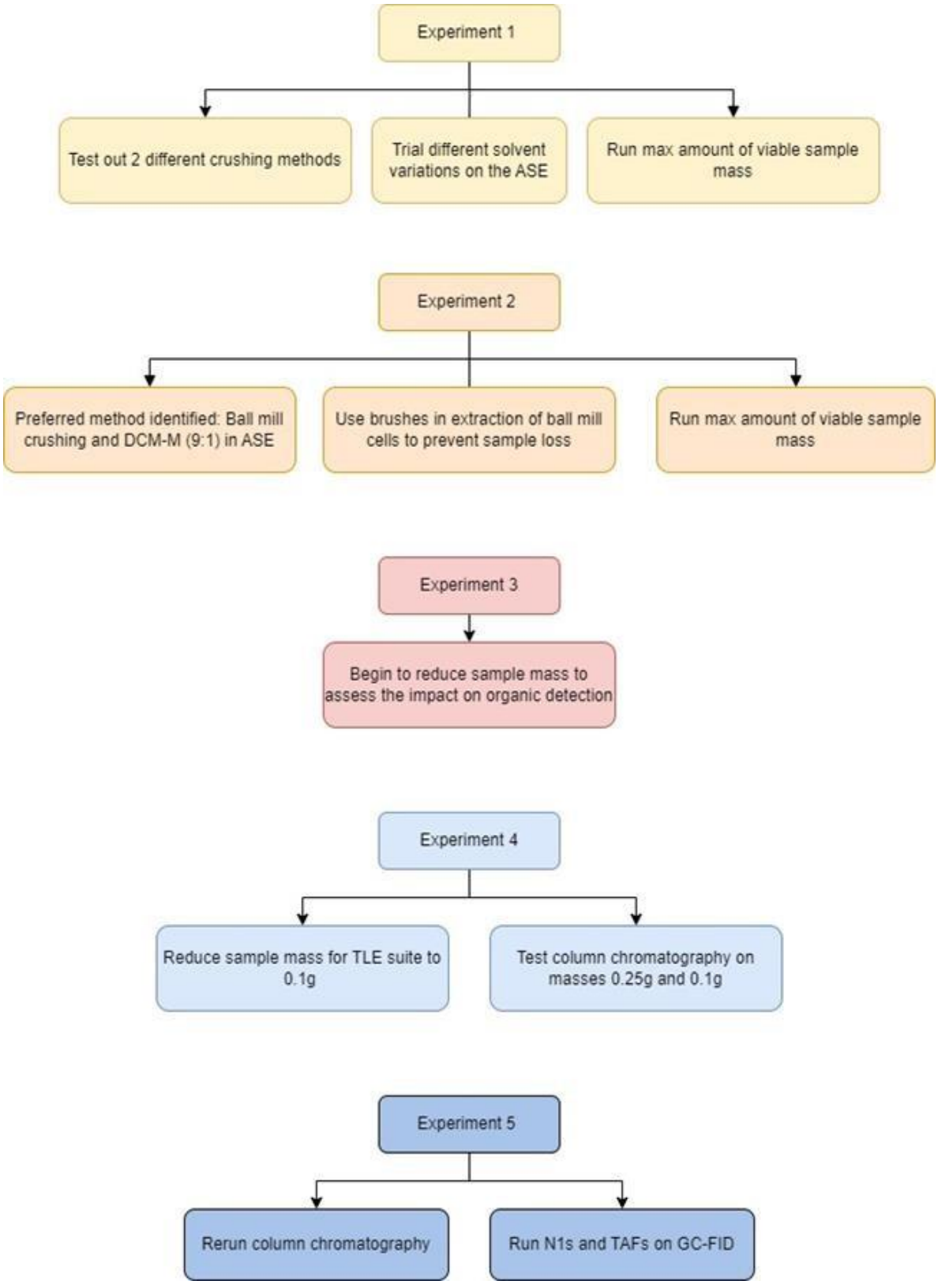

Figure 7 - Flow diagram outlining the overall procedures taken between experiments

Method	Description
1	Crushed by ball mill. Extracted with DCM-M (9:1)
2	Crushed by mortar and pestle. Extracted with DCM-M (9:1)
3	Crushed by ball mill. Extracted with Hexane-Acetone (2:1)
4	Crushed by mortar and pestle. Extracted with Hexane-Acetone (2:1)

Table 5 - Various methods trialled during Experiment 1

2.3 Equipment

2.3.1 Accelerated Solvent Extraction (ASE 350)

A Dionex accelerated solvent extractor (ASE) 350 was utilised to extract organics from the samples. Nitrogen supply ensures that an inert atmosphere is created, and the sample is heated to 120ºC with preferred solvent flushed through the cells to be collected in assigned vials. This piece of equipment was chosen as it is more time efficient, solvent efficient, reliable, and reproducible than alternative solvent extraction methods as expanded in Appendix Section B.2 (ThermoFischer Scientific, 2013). Samples from 1-100g can be extracted using this system and uses between 50-90% less solvent than other methods (ThermoFischer Scientific, 2016). The method chosen for this instrument is shown in Section 2.5.1 (Table 7).

2.3.2 GC-MS

The Agilent GC-MS (5977A MSD/7890B GC System) was utilised for this project. This specific system gives host to the industry's highest signal to noise ratio and lowest instrument detection limit (University of Glasgow, 2013). It is equipped with MassHunter Quantitative and Qualitative Analysis Software as well as the NIST Mass Spectral Library 2014. The GC-MS is hybrid analytical machine made up of a gas chromatograph and a mass spectrometer. The two instruments work together to identify substances within a sample to very small amounts with the GC separating compounds and the MS detecting them.

GC vaporises the sample, separating volatile components in the sample. Inert carrier gas (helium) transfers this through a capillary column where the phase separation into various components occurs. MS helps to fragment and identify the compounds based on mass; It ionizes chemical compounds to generate charged molecules and measuring their mass to-to-charge ratios (m/z). Each compound from the sample elutes from the column at a

specific time based on polarity and boiling point, the time it elutes is known as its retention time. Some molecules have the same retention time and co-elute and sometimes molecules can have the same mass spectrum (similar pattern of ionized fragments in a MS). Using the GC and the MS in conjunction reduces this opportunity for error.

2.3.4 GC-FID

The GC in this case is attached to a flame ionisation detector which measures analytes within a gas flow. The FID detects ions which form during the combustion of organic compounds in hydrogen flame and thus informs how much carbon is in a sample (Wang and Pare, 1997). The pre-set method used is outlined in Appendix B (subsection B.3.2).

2.3.5 SEM

Scanning Electron Microscopy (SEM) uses electrons to form an image. The interaction with the electron beam with atoms at various depths within the sample produces an image. Secondary electrons (SE), backscattered electrons (BSE), x-rays and light, absorbed current and transmitted electrons. SE provide information about the surface regions whilst BSE is useful for looking deeper into the sample, BSE are beam electrons that are reflected from the sample by elastic scattering. SEM produces high quality, detailed magnified images of sample to reveal information about the sample's properties such as topography, microstructures, and composition. Energy Dispersive Spectroscopy (EDS) analyses the elemental composition sample by measuring the unique X-ray released as the sample interacts with the electron beam. SEM-EDS was utilised for this project to understand the bulk mineralogy of the sample and to identify carbonate globules and their associated minerals using EDS within the BVC samples.

SEM was carried out at the GEMS (Geoanalytical Electron Microscopy & Spectroscopy Centre) facility within the School of Geographical and Earth Sciences at the University of Glasgow (henceforth UofG). The Carl Zeiss Sigma Variable Pressure Field-Emission Analytical SEM was equipped with an Oxford Instruments X-Max EDS SDD and the AZtec/INCA software package - the INCA analysis software was used for quantitative analysis. Samples were carbon coated to 20nm. Scan size was 1024 pixels per frame, dwell time was 30s, working distance was 8.5mm operating at 20 kV.

A thin section from each BVC sample was examined using these techniques to create large area maps, secondary electron and backscatter electron images and false colour images of

each sample. False colour images were created by assigning each element a colour, these were then layered to highlight the minerology of the sample at both large and small scale (Table 6).

Table 6 - Outlining colours assigned to minerals and elements for the false coloured EDS maps – a) Colour scheme chosen for minerals within the SEM images b) False coloured EDS maps key outlining which elements have been assigned

Mineral	Colour
Olivine	Light green
Pyroxene	Dark green
Feldspar	Blue
Oxides	Bright red
Sulphides	Yellow

Element	Colour
Si	Dark blue
Fe	Red (bright)
Mg	Green (bright)
Ca	Pink
Al	White
S	Yellow
K	Cyan
Ti	Pink (never in same image as Ca)
Cr	Orange

2.4 Bulk rock crushing

The initial stage was to crush each bulk rock sample into a fine enough powder (<0.5mm) in order to run them on the ASE. Two established crushing methods were initially tested for each sample: Ball mill and agate mortar and pestle. All crushing took place within the BECS lab at UofG.

Both methods were trialled in order to draw comparison for the more efficient technique in terms of sample loss and time. It would also test which method (if any) was responsible for any sort of contamination on the samples.

Sterilized glass beakers and vials were used for the weighing and storage of samples. The samples were weighed out before and after crushing using the analytical balance (HR100A;102g/0.1mg) for each method in order to trace sample loss.

For experiment 1, ~3 grams of each sample was crushed for each method. A large batch of material was crushed so that we could trial a series of different methods for the initial experiment. Appropriate PPE was worn for each experiment to reduce contamination risks; Lab coat, face mask, powder-free nitrile gloves and goggles and ear protective equipment, where necessary. All surfaces were sterilised with acetone:methanol (1:1) and lined with aluminium foil for each sample. All glassware was combusted overnight to ~450 degrees for 8 hours prior to use. Stainless steel equipment was rinsed with methanol:ethanol (1:1) and dried in an oven (~40 degrees) for 5-10mins prior to use.

Powder free nitrile gloves were worn and changed per sample (and where necessary) to minimise contamination. All equipment was sterilised in-between sample crushing and extraction. The crushed samples were stored in pre-combusted glassware, labelled accordingly and kept within an airtight box pending solvent extraction.

2.4.1 Ball mill

The ball mill is located within the Bio-Earth BECS (Biomarkers for Environmental and Climate Science) lab at UofG. 50ml volume stainless steel grinding jars were used. Frequency and shakes per second (s/1) were controlled accordingly for each sample dependent on hardness of the sample. The aim was to ensure samples were <0.5mm as recommended by the method optimisation for ASE protocol (ThermoFischer, 2013). BVC samples were taken from the core of the rock –a sterilised hammer allowed access to a fresh surface in attempt to avoid analysing weathered material.

16 ml vials were pre-weighed and the material from the ball mill was collected here to obtain the initial starting weight of the sample. This process was aided using a glass funnel to minimise sample loss from the ball mill holder to the vial. The ball mill holders and ball itself were scraped of material using a stainless steel spatula and tweezers. Particular care was taken when extracting the sample from the ball of the ball mill holder as this shape was difficult to extract efficiently. After extraction the ball mill cells were rinsed with water, wiped with fibreless tissue (Kimtech) and then rinsed with acetone:methanol and left in the oven (~60degrees) until dry.

Figure 8 - Image of the set up required for ball mill crushing (ball mill not pictured)

2.4.3 Agate mortar and pestle

Agate is a strong, durable material for crushing with a variety of benefits for homogenising material. It is chemically inert and therefore does not react with the majority of chemicals, it has a low level of contamination in comparison to other materials (i.e ceramic) and is easy to clean due to the lack of porosity thus limiting cross contamination between samples. However, agate cannot be heated to high temperatures as part of the cleaning procedure and so the solvent cleaning procedure must be rigorous (Simkus et al., 2019).

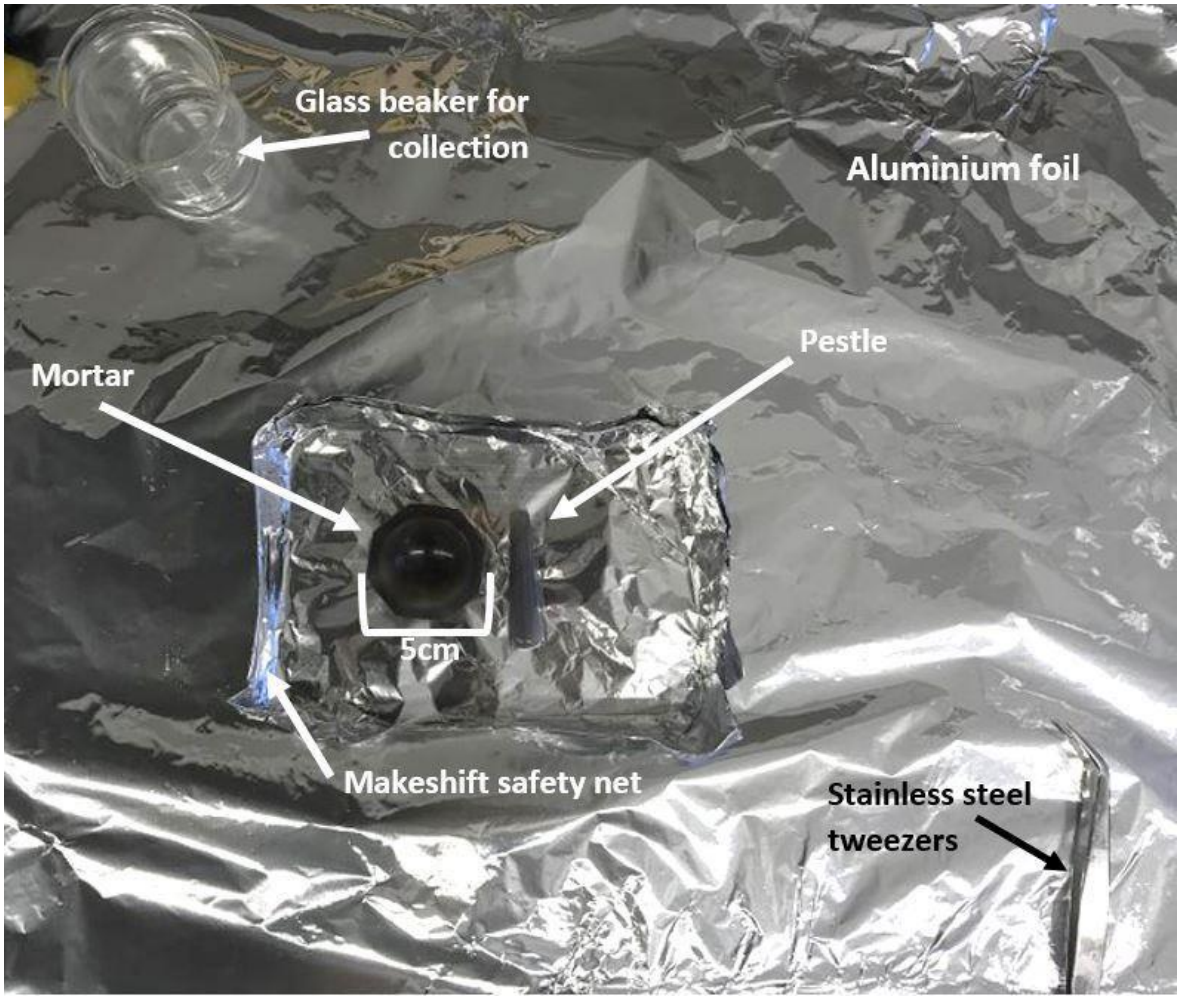

Figure 9 - Equipment and set up for agate mortar and pestle crushing

The agate mortar is approximately 5cm in size. This small size allowed for minimal amounts of material to be crushed at a time in an attempt to reduce sample loss and allow for a more consistent grain size. The set up included a makeshift tin foil tray in order to catch any grains that might escape the mortar. This equipment was rinsed with dionised water, wiped with Kimtech wipes and rinsed with solvent (50:50 acetone:MeOH) and dried in between samples to mitigate contamination.

~3g of each sample was crushed by ball mill and by mortar and pestle respectively. The sand and JSC required less grinding than the coarser Sigurdfjelle and Sverrefjelle samples. The sand and JSC were already fine enough to be run on the ASE but were crushed for consistency and repeatability of the experiment. It was also important to note the sample loss of this material for this method.

For the Svalbard samples, due to the nature of the rock, approximately 3.5g of loose unconsolidated material was weighed out in a beaker to be crushed by mortar and pestle.

When in the beaker, the weathering rim material was easy to spot and would be preferentially taken out of the sample batch using sterile tweezers. The sample was added in small batches appropriate for the size of the mortar and carefully crushed into a homogenous powder <0.5mm as per the ASE requirements. It took approximately 5 hours to crush 3g of BVC material. The samples were crushed until a homogenous powder was created and then was transferred into a reweighed glass beaker to record the weight of the final sample. This was then transferred into a combusted 8mL vial using a sterilised glass funnel and capped and labelled ahead of further analysis.

2.5 Solvent Extraction

Solvent extractions were performed as part of the sample preparation for the GC-MS. Solvent soluble organic matter was extracted from JSC, Sigurdfjelle and Sverrefjelle using various solvent combinations including hexane: acetone (2:1) and dichloromethane: methanol (9:1) in conjunction with Dionex ASE 350 Accelerated Solvent Extractor (ASE). These solvents were chosen as they have high polarities and therefor extract a wide range of polarities from the samples. As there was uncertainty as to what kind of compounds would exist within these samples, we trialled a range of solvents to extract the most organic material.

Hexane-Acetone (2:1) is an effective solvent Hexane is a non-polar organic solvent and therefore dissolves non-polar compounds, acetone has a higher polarity and therefore hex-ace (2:1) allows a range of polarities of compounds to be extracted (O'Brien, 2022; King et al., 2022)

DCM-M (9:1) (dichloromethane-methanol) is a common technique for extracting organics compounds (Jenniskens et al., 2012; Sephton, 2012; Pizzarello et al., 2013). It is a polar, aprotic solvent which dissolves polar and non-polar compounds and therefore extracts a wide range of different compounds. The boiling point for this solvent is low which is beneficial for evaporating and collecting solutes.

2.5.1 Accelerated Solvent Extractor (ASE)

Solvent extractions were all performed on the ASE 350 (Figure 10). The ASE works by combining high temperatures and pressures with organic solvents. Extraction cells loaded with sample are firstly heated in an oven to a pre-set temperature for a fixed amount of

time. Extraction cycles are also programmed prior to use as part of the chosen method - the pre-set methods used for the ASE are outlined in Table 11.

Once the number of cycles is complete, the cell is flushed and purged with nitrogen. The ASE makes solvent extractions more time and energy efficient, reduces the amount of solvent required for extraction and also improves the yield of the extraction (Buch et al., 2006). The solvent is flushed through each ASE cell and collected in the corresponding vial lined up below (Figure 10). These are then evaporated using Turbovap and the Sample Concentrator (Appendix Section B.1). Once they are dried up, they are weighed to record the TLE mass.

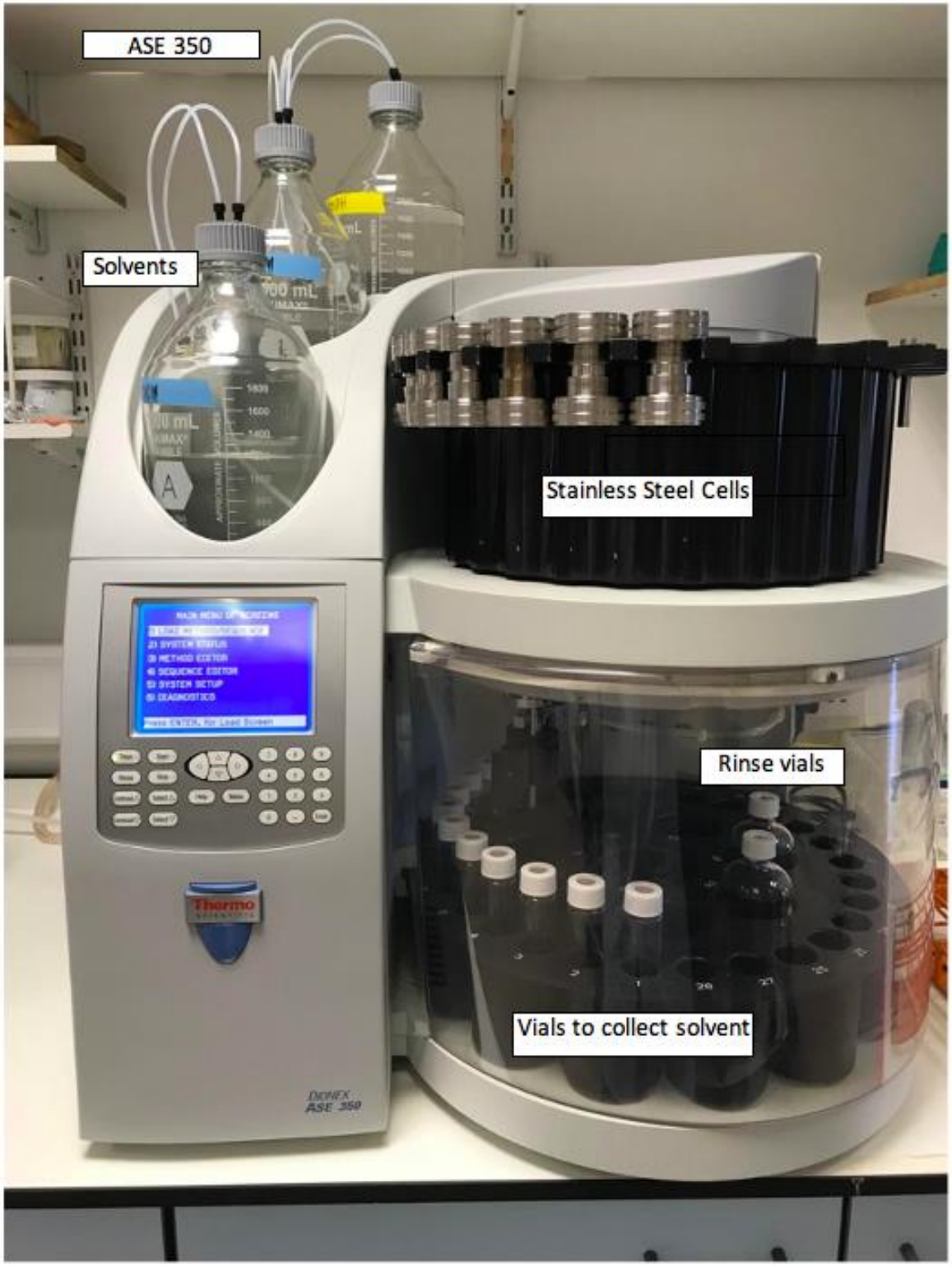

Figure 10 - Dionex 350 Accelerated Solvent Extraction loaded with samples and labelled accordingly within BECS Lab

Figure 11- ASE vials labelled with BECS IDs after solvent extraction prior to evaporation stored within the fume hood

Table 7 - ASE pre-set methods for both solvent systems

ASE Method for Hex:Ace			
Temperature	120 C	**Heat**	6 mins
Static time	5 mins	**Cycles**	2
Rinse Volume	60%	**Purge**	60s
Solvent A	2 Hexane		
Solvent B	1 Acetone		

ASE Method for DCM:M			
Temperature	120 C	**Heat**	6 mins
Static time	5 mins	**Cycles**	2
Rinse Volume	60%	**Purge**	100s
Solvent A	5 MeC12		
Solvent B	4 MeC12		
Solvent C	1 Methanol		

2.5.2 Column Chromatography

Column chromatography (also known as adsorption column chromatography) is a separation method used to separate and isolate a singular component from a mixture. This method can be an important process prior to GC-MS analysis as the MS does not allow for the discrimination between isomers and thus separating via chromatography post derivatisation could allow homochirality to be measured (Chou et al., 2021).

Full details of the standard operating procedure (set out by Prof. Jamie Toney) followed for column chromatography in this project is outlined in Appendix (Section B.3) and the set-up is shown in Figure 12.

Column chromatography starts with a sample mix put through columns packed with solid adsorbents and substances can be separated depending on the different absorptions of the compounds to the absorbent. The adsorbents are polar; therefore, the more polar compounds are absorbed quicker, and the non-polar compounds elute first. The compounds move through the columns are different rates and thus are separated (and collected) into different fractions. Although, this also depends on the solvent used and its polarity and so a specific order of certain solvents is used to ensure for systematic elution of compounds. This method is useful as it allows very small sample volumes to be separated and allows for the analytes of interest to be isolated and concentrated prior to GC-MS analysis. This step can be beneficial for the GC-MS as it improves the sensitivity of the analysis.

Figure 12- Image depicting labelled equipment and set up required for column chromatography within fume hood

2.6 Sample Preparation

2.6.1 Standard preparation

Using standards is important in GC-MS analysis as they are used for calibration and ensure that results of the MS and thus the samples are valid. Three concentrations of standards are prepared for processing on the GC-MS; 2.5, 5 and 10µg/ml. Standards are custom-made prepared by LGC Solutions in a UKAS and ISO17025 accredited laboratory and then diluted in house in the BECS lab using hexane (Table 8). Figure 13 is the expected chromatogram for these standards and used as a basis for calibration. The standard is made of 11 compounds of mostly different chain length n-alkanes to allow multipoint calibration.

Table 8- Standard concentration table (stock refers to the alkane standard from LGC Solutions)

Standard preparation table	
10µg/mL concentration	30µL stock
5µg/mL concentration	30µL stock and 30µL hexane
2.5µg/mL concentration	25µL and 75µL hexane

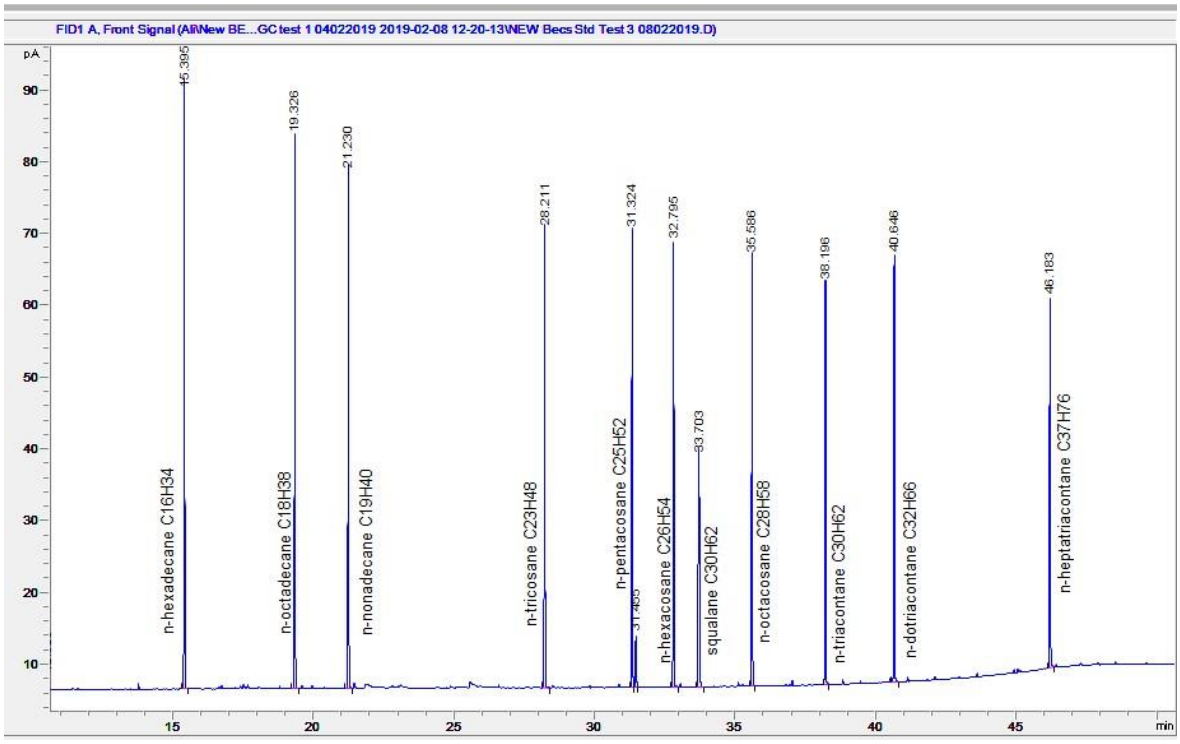

Figure 13- Typical chromatogram for the GC Standard n-alkanes

2.6.2 Sample preparation for GC-MS

After the ASE 350 extracts the samples into 60mL vials, the TLE is concentrated by evaporation of the solvent using heat and nitrogen flow, in 60mL vials and then transferred into 8mL vials. The vials are weighed before and after and sum TLE is recorded. In order to prepare the samples for GC-MS, the 8mL vials were flushed three times with DCM using a sterilised syringe; ~75µL was flushed around the vials sides to collect all possible organic material until evaporation to 50µL for Experiments 1-3 or ~50µL flushed to collect 20µL for Experiments 4 and 5.

The syringe was sterilised in between each sample by having 3x8mL vials of DCM: The first is rinse one, discard, rinse two, discard and the third is clean DCM for transfer into sample. This solvent was then transferred into a 200µL insert within a spring loaded 2mL GC vial and immediately capped and stored in the refrigerator prior to analysis.

Sample preparation for GC-FID can be found in the Appendix B (Section B.3.1)

2.7 GC-MS

The Mass Spectrometer uses two main libraries during qualitative analysis, in order to determine the compound within the analyte. NIST MS 2014 and Agilent MassHunter Quantitative Analysis software libraries are compared in order to assign a name to a compound based on the retention time and mass spectra within a probability percentage. Instrument detection limit (IDL) of the GC-MS is 1000fg however it also depends on the analyte.

Analytes were injected (1µL) and separated on a HPI-MS column (60mx250µmx0.25µm) using He carrier gas at 1.2mL/min. Oven temp was programmed from 60°C (2mins) to 120°C at 30°C/min, then to 310°C at 5°C/min (held 33mins). The specifications for the column within the GC are stated in Figure 14.

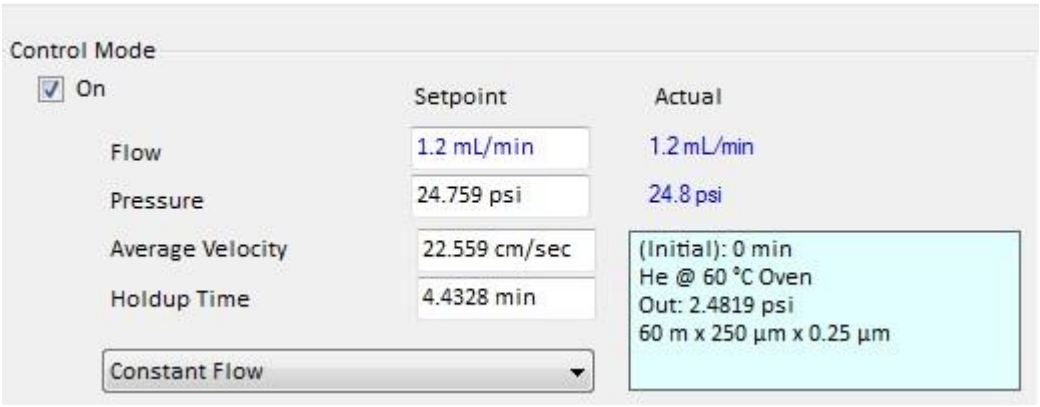

Figure 14- Specifications for the column within the GC

Prior to the sample being mass analysed, it must be ionized in the ion source for which we use electron ionization (EI). This is the most common and well-established method of ionization. Post ionization, the analytes enter the mass analyser which in this case is the Single Quadruple. The mass to charge ratio (m/z) is the mass of an ion (Daltons) divided by the number of charges on the ion.

2.7.1 Calibration Curves

The first stage in GC-MS data processing is creating calibration curves using custom made standards prepared by LGC Solutions in a UKAS and ISO17025 accredited laboratory. The standard is made with 10 compounds (different chain length n alkanes) to allow for multipoint calibration and the concentration of compounds in the standard is constant. Calibration curves are determined by running 3 different concentrations of the standard achieved by dilution of the standard with hexane. These dilutions are created and stored in the lab prior to analysis. 10µg/mL, 5.0µg/mL and 2.5µg/mL of the standard are run on the GC. Three different known compounds are selected from multiple points along the retention time (C16, C23, C28) and the peak areas for each concentration for each of these n-alkanes are recorded. An example of this recorded information can be observed in Table 9. N-alkanes are chosen as the known compound due to the nature of the standard used, the mass spectra for alkanes are also easy to identify as it has a definitive pattern as shown in Figure 13.

Table 9 - Peak areas of chosen alkanes at different concentrations for calibration curve graphs taken from experiment 1

Compound	C16
Concentration µg/mL	Peak Area
2.5	809046
5.0	1775548
10.0	3842220

Compound	C23
Concentration µg/mL	Peak Area
2.5	683202
5.0	1754655
10.0	3536242

Compound	C28
Concentration µg/mL	Peak Area
2.5	478656
5.0	1557608
10.0	3706643

Once the peak area for each alkane at each concentration is identified and in table format, the peak area is plotted against the concentration to give a scatter graph. A line of best fit and equation of the line will provide necessary information for calibration and reveals the R^2 value. An R^2 of >0.9 indicates a statistically dependable result, providing confidence in the standard and subsequent calibration.

The calibration curve is plotted with a line of best fit, thus providing the equation of the line. The equation of the line can be solved allowing us to determine the concentration of each compound in a sample in µg/ml.

The concentration is then normalized according to;

$$C_n = \frac{C_d V}{m}$$

Where Cn is the normalised, Cd is the detected concentration (µg/ml), V is the volume (ml) and m is the mass (g).

The signal to noise ratio (SNR) is given for each of the peaks within the sample. The signal refers to the intensity of the peaks in response to the analyte within the MS. The noise is the random fluctuations within the baseline of the chromatogram. It a vital parameter used to determine the reliability of the peak detected within the chromatogram. The SNR allows

for quantification of the separation between the true signal of the peaks and the background noise of the baseline. SNR should be higher than 5 (5:1 ratio) in order to have confidence within the result (Salik, 2023 (in discussion)).

2.7.2 Analysis

The GC output provides a chromatograph and a peak table or integration peak list. The output chromatograph is a Total Ion Count (TIC) chromatogram; a plot of the ion signal function of the mass-to-charge ratio. The chromatogram represents the chemical compounds in the sample over time and is a function of the intensity (peak area) against the retention time. Each peak has a mass spectrum assigned to it, which reveals information about the structure of the molecules and mass to charge ratio of the compounds within the sample.

A high peak area is indicative of a higher concentration of the compound, but this can be measured and quantified in order to determine the relative concentration of the compound within a sample (Figure 15).

The GC system is connected to the MS which holds two separate libraries for qualitative analysis: the NIST (National Institute of Standards and Technology, 2014) library and the Agilent MassHunter Qualitative Analysis.

From the MS of each sample, peaks are revealed at certain retention times which indicate a specific compound. These peaks can be measured and analysed qualitatively and quantitively. The retention time (R.T) can reveal the identity of a known peak/compound, allowing for qualitative analysis. The peak area is directly proportional to the concentration of the peak/compound present in the sample allowing for quantitative analysis. This is the area between the peak signal and the baseline, calculated by integrating the peak (Figure 15)

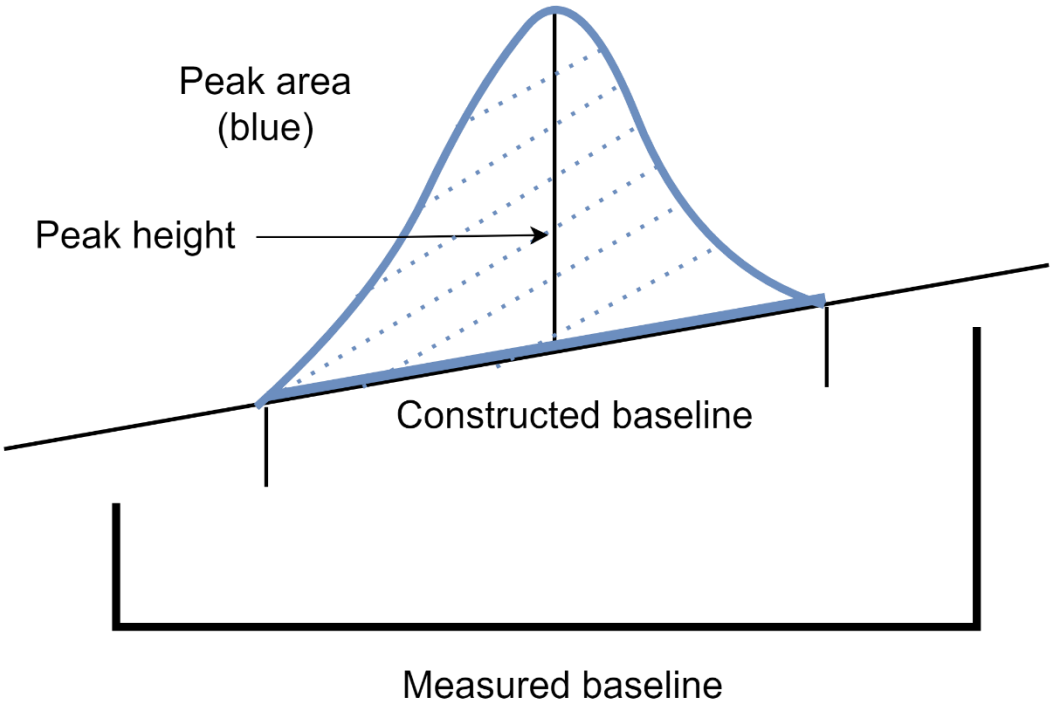

Figure 15- How to measure a peak within a spectra for GC-MS analysis. Blue dots and lines represent the space which is the peak area.

The analysis of the results is aided by the two mass spec libraries which aid in identifying a compound from a peak in the chromatogram. Each peak within a chromatogram has its own unique MS signature. The signature can often help identify the basic organic compound, but the libraries provide greater insight into the compound revealing the name, formula, mass, structure and also a variety of synonyms and other isomers.

2.8 GC-FID

The GC-FID used is part of the Biomarkers for Environmental and Climate Science (BECS) lab within the school of GES, it is an Agilent GC-FID (7890B GC System). The GC in this case is attached to a flame ionisation detector which measures analytes within a gas flow. The FID detects ions which form during the combustion of organic compounds in hydrogen flame.

The GC-MS and GC-FID both begin their analysis similarly by separating the sample through the GC which uses an inert carrier gas as the mobile phase. The carrier gas moves through columns where the sample is physically separated depending on compounds characteristics. The columns are stored within a temperature-controlled oven with controlled gas flow. After the gases have undergone this separation, the detector outputs the proportional concentration of the compound as a signal.

The key difference between GC-MS and GC-FID is in the analysis. MS is advantageous for qualitative analysis (when the compounds within the sample are unknown) and GC-FID can accurately quantify many components. Table 10 compares the GC-MS and GC-FID in terms of analytical quality, sensitivity and S/N ratio.

Table 10 - Comparison of GC-MS and GC-FID features

Feature	GC-MS	GC-FID
Analytical quality	Structural identification and quantification	Quantitative only
Sensitivity	Extremely high (pg-fg range) for a broad range	High (ng range) best for hydrocarbons
Signal-to-noise ratio	Moderate to high depending on scan mode	Very high with low noise
Best use	Trace detection, complex mixtures, molecular ID	Quantifying hydrocarbons, routine analysis

3. Results

Sample blank

The same blank or BLK is combusted sand from the BECS lab which is introduced at the ASE cell preparation stage. It is continued throughout the preparation and into the analysis in order to identify any contamination and subsequently track it. It helps to highlight a 'true' detection within the samples. Any compounds that were detected in the sample blanks or procedural blanks were deemed contamination to be certain about our detections. This project could be analysed differently, by subtracting the blanks from the sample to quantify the 'real' amount of a compound within. However, if this compound is present in the blank at any capacity, then it has come from an external source and is not a true detection since this blank was combusted to begin with. By considering all compounds within the blanks as contamination, it validates our results.

Normalised masses

The results are all calibrated according to various concentrations of standard which calibrate the results and allow us to calculate the concentration of the compounds within a sample. These results are then normalised based on the starting mass of the sample and the volume that they were run on the GC-MS.

This is measured as µg/g and gives us how much compound we have in µg for every g of sample, also known as parts per million (ppm).
The background ions were chosen and removed from each experiment so any peaks that we detected are a positive/real detection. This is also supported by the signal to noise ratio (SNR) which is provided with each detection - if this number >5 then we can be confident in the detection.

In terms of errors, we used the standards that were run in different concentrations (10µg/mL, 5µg/mL and 2.5µg/mL) and took the peak area of 3 peaks within these (C16, C23 and C30) to create a relative standard deviation across the peaks for each concentration which provided the % error.

3.1 Imaging

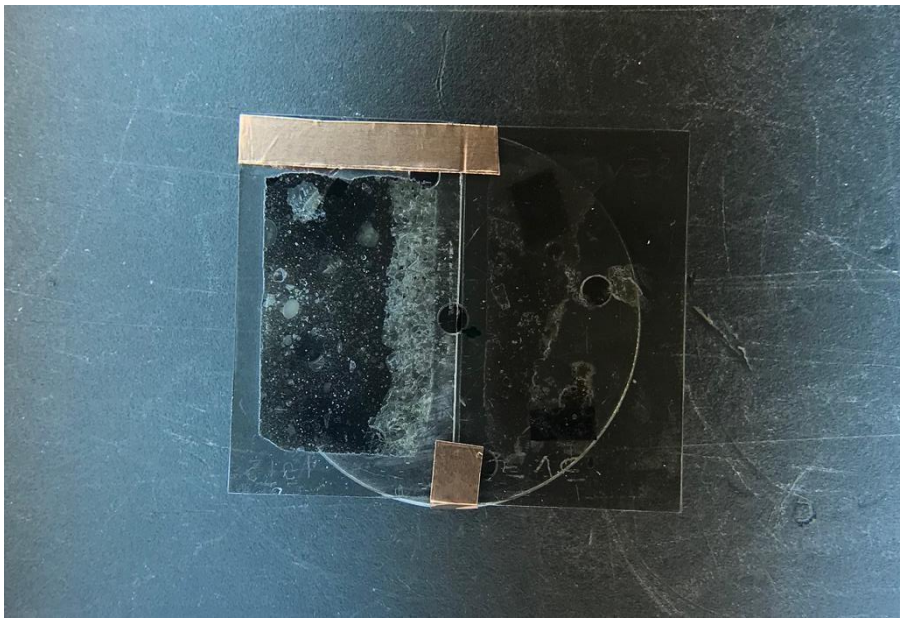

Figure 16 – Scan depicting the carbon coated thin sections of Sigurdfjelle (left) and Sverrefjelle (right). Each thin section is approx. 24 x 46 mm. Copper table prevents charging.

Figure 16 depicts the carbon coated thin sections of our BVC samples. On the left is the thin section of Sigurdfjelle and the right is Sverrefjelle. The thin section for Sverrefjelle was unfortunately slightly broken. Mineralogically it was clear that these basalts were rich in olivine, pyroxene and volcanic glass.

3.1.1 SEM

Scanning electron microscopy (SEM) was carried out within GEMS in the School of Geographical and Earth Sciences (GES) at the University of Glasgow.
SEM imaging revealed the presence of carbonate and magnesium oxide globules 50-100μm in diameter within Sigurdfjelle (Figure 17). The globules were found at grain boundaries, often surrounded by phyllosilicate and had distinctive concentric zoning. The globules were concentrically and mineralogically zoned with the inner part of the globule dominantly magnesium carbonate, and towards the outer rim, iron magnesium carbonate.

Within Sigurdfjelle, there was also minor chromite, spinel, phosphate and iron-nickel metal (molybdenum). Apatite was found at a few microns in size implies that the parent melt must have contained volatile elements (F, Cl, OH). The thin section of Sverrefjelle was unfortunately partially broken. The carbonate globules were not as evident within this

section as in BSE it appeared they had undergone some sort of dissolution, but the shape of the previous globules were still apparent.

Figure 17 is from Sigurdfjelle and shows the carbonate globule within a mafic area with the key feature surrounded by pyroxene and olivine grains, as expected from this basalt.

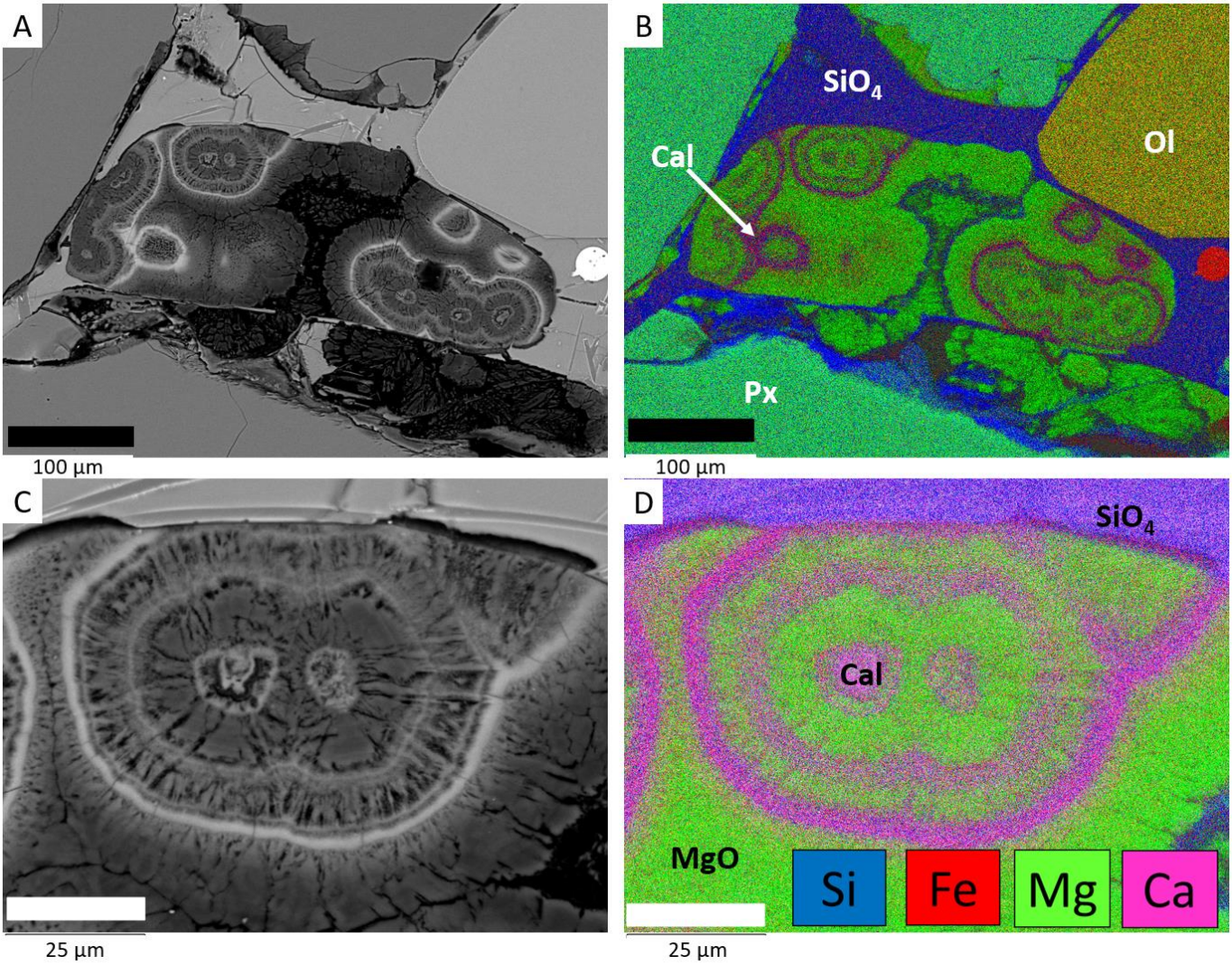

Figure 17- SEM images of carbonate globules within BVC volcano Sigurdfjelle. A – Backscatter Electron (BSE) image of carbonate globule. B – False colour Energy Dispersive X-ray Spectroscopy (EDS) image showing calcite (Cal) and magnesium oxide (MgO) within the globules, surrounded by phyllosilicate (SiO_4) in the space between olivine (Ol) and pyroxene (Px) phenocrysts. C – BSE image of close-up carbonate globule magnified from A. D – EDS false colour image showing calcite (Cal), magnesium oxide (MgO) and phyllosilicate (SiO_4) within the globule

3.1.2 Large Area Maps

Large area maps were produced to get a large area image at a high resolution to get an overall understanding of the samples we were working with. A vertical rectangular area was chosen at random for bulk composition created by mosaicking numerous fields of view together (Figure 18).

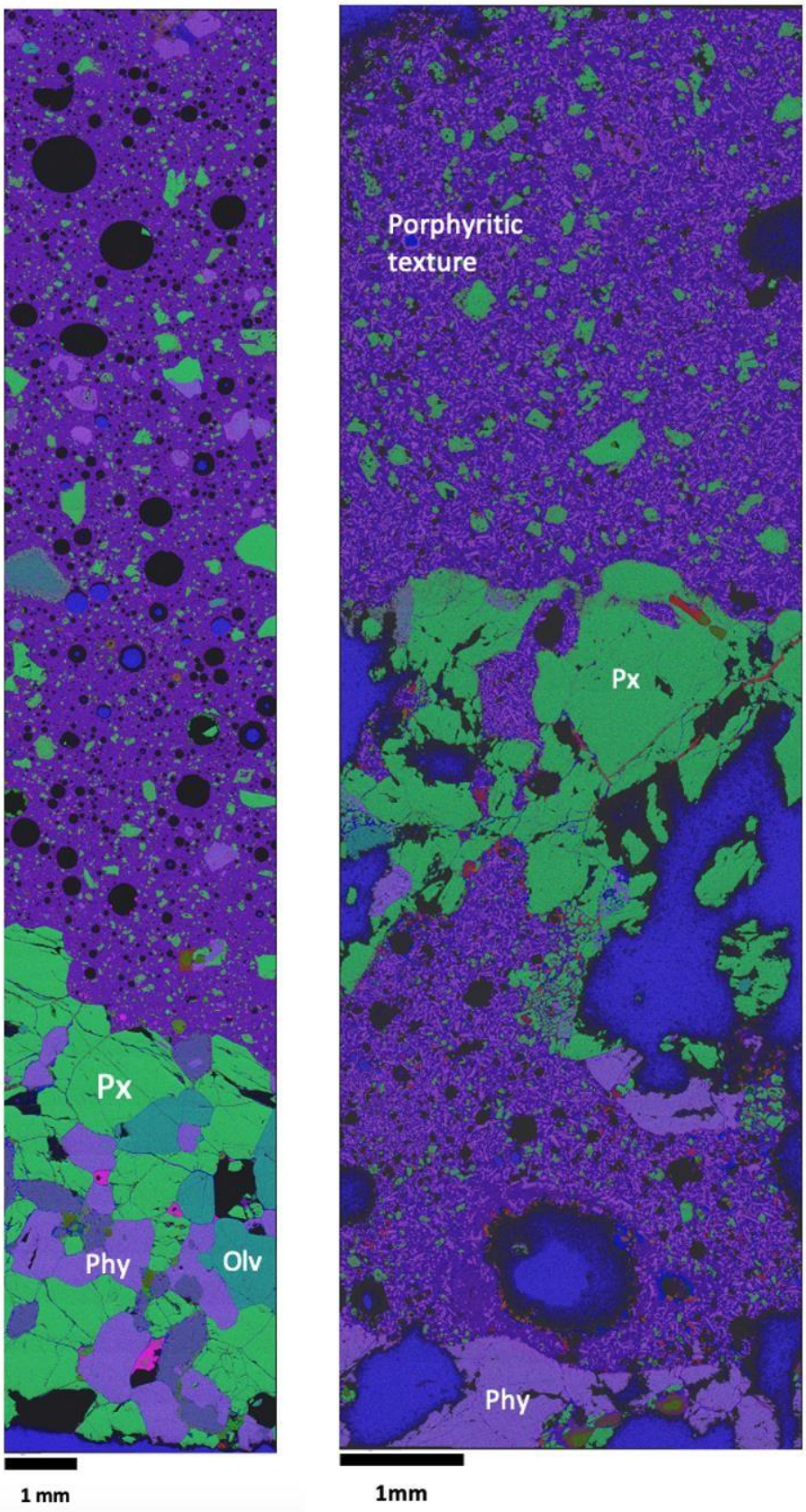

Figure 18- EDS Montage Large Area Maps of Sigurdfjelle (left) and Sverrefjelle (right). The carbonate globules in Sigurdfjelle were found in the bottom left area with the larger grain size amongst the grain boundaries and phyllosilicate.

3.2 Optimising sample preparation and solvent extraction

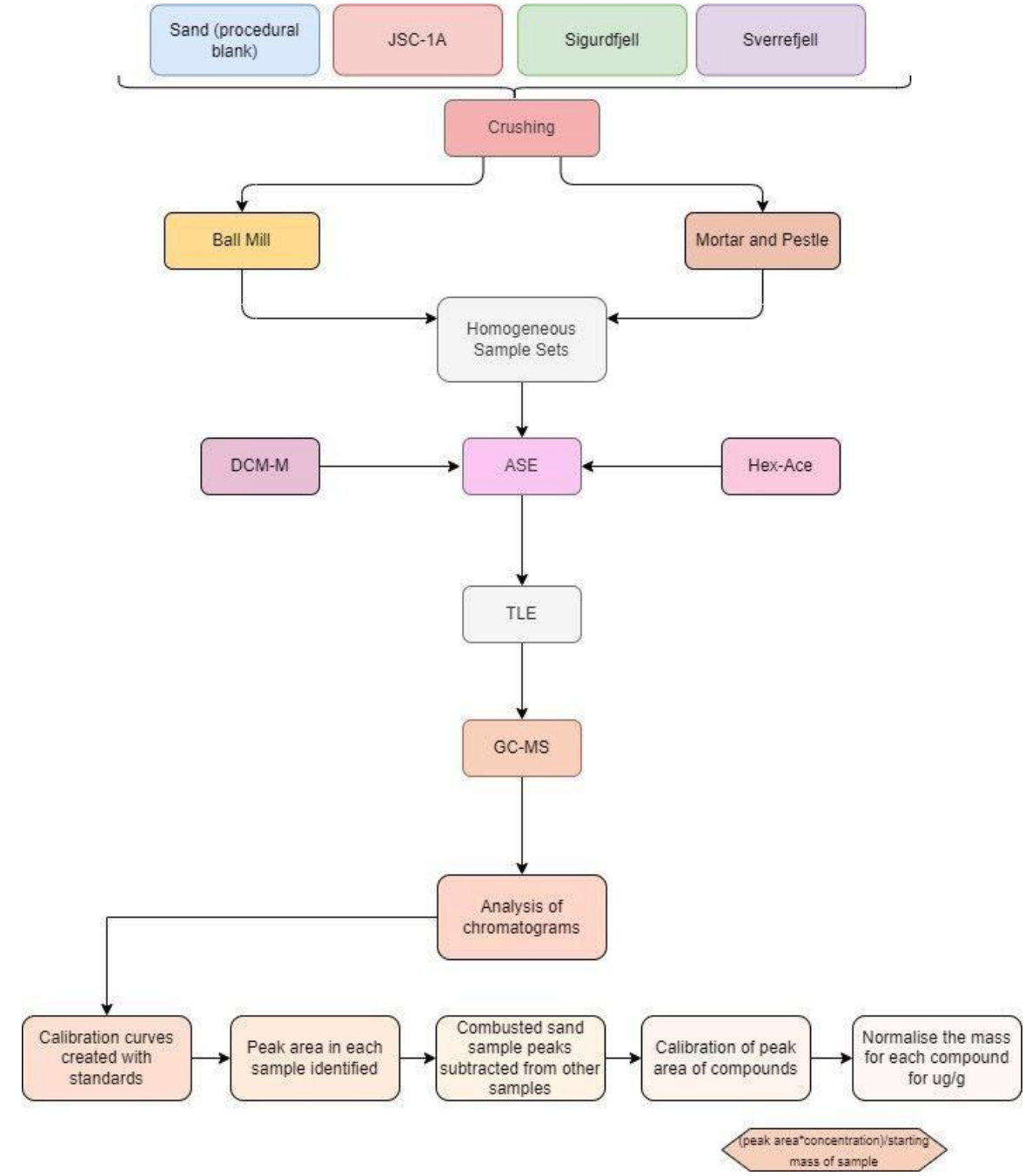

Figure 19- Experiment 1 flowchart

The flow chart diagram (Figure 19) shows the overall method for each sample and the subsequent analysis performed on the GC-MS output. This initial experiment aimed to determine the most effective and efficient sample preparation method for GC-MS analysis, comparing different sample crushing techniques (ball mill vs mortar and pestle) and solvent extraction systems (DCM-M vs Hex-Ace) for obtaining the Total Lipid Extract (TLE).

3.2.1 Crushing

Initially, two variations of crushing methods (ball mill and mortar and pestle) were trialled in order to assess factors such as efficiency in terms of sample loss and time as well as contamination risk. The samples were weighed before and after using an analytical balance.

Sample crushing and subsequent removal from the ball mill holders takes approximately 45 minutes total whereas hand crushing took approximately 5 hours for Martian analogue basaltic material due to the hard nature of the sample

Table 11 - Sample loss according to equipment used; a) ball mill crushing b) mortar and pestle crushing c) percentage loss of sample between crushing techniques

a) Ball mill crushing			
Sample	**Initial wt (g)**	**Final wt (g)**	**Total loss**
Sand	3.1619	3.1348	0.0271
JSC	3.1213	3.0619	0.0594
Sigi	3.0817	2.9983	0.0834
Sverre	3.0735	3.0154	0.0581

b) Mortar and pestle crushing			
Sample	**Initial wt (g)**	**Final wt (g)**	**Total loss**
Sand	3.4197	3.2774	0.1423
JSC	3.4605	3.4017	0.0588
Sigi	3.4105	2.7558	0.6537
Sverre	3.4006	2.5938	0.8068

c) Percentage loss of samples by crushing method		
Sample	**Ball Mill (%)**	**Mortar and Pestle (%)**
Sand	0.86	4.16
JSC	1.9	1.69
Sigi	2.7	19
Sverre	1.89	23.7

Ball mill

The procedural blank (sand) had the least sample loss at 27.1mg and Sigurdfjelle had the highest sample loss from this method at 83.4mg. The interior of the ball mill was scraped with the spatula for around 45 minutes per full holder, including the ball. Although there

were extensive efforts to extract all of the material, it was evident that some sample was still present in the ball mill holder and on the ball evidenced by the residue left behind.

Mortar and pestle

The highest loss for this method occurred when crushing Sverre. The lowest loss for this method was JSC due to the nature of the material not consisting of any individual grains. The nature of the BVC specimen was loose within the weathered outer rim and so this could be easily weighed out to ~3g in a sterilised beaker prior to the crushing to record a before and after weight.

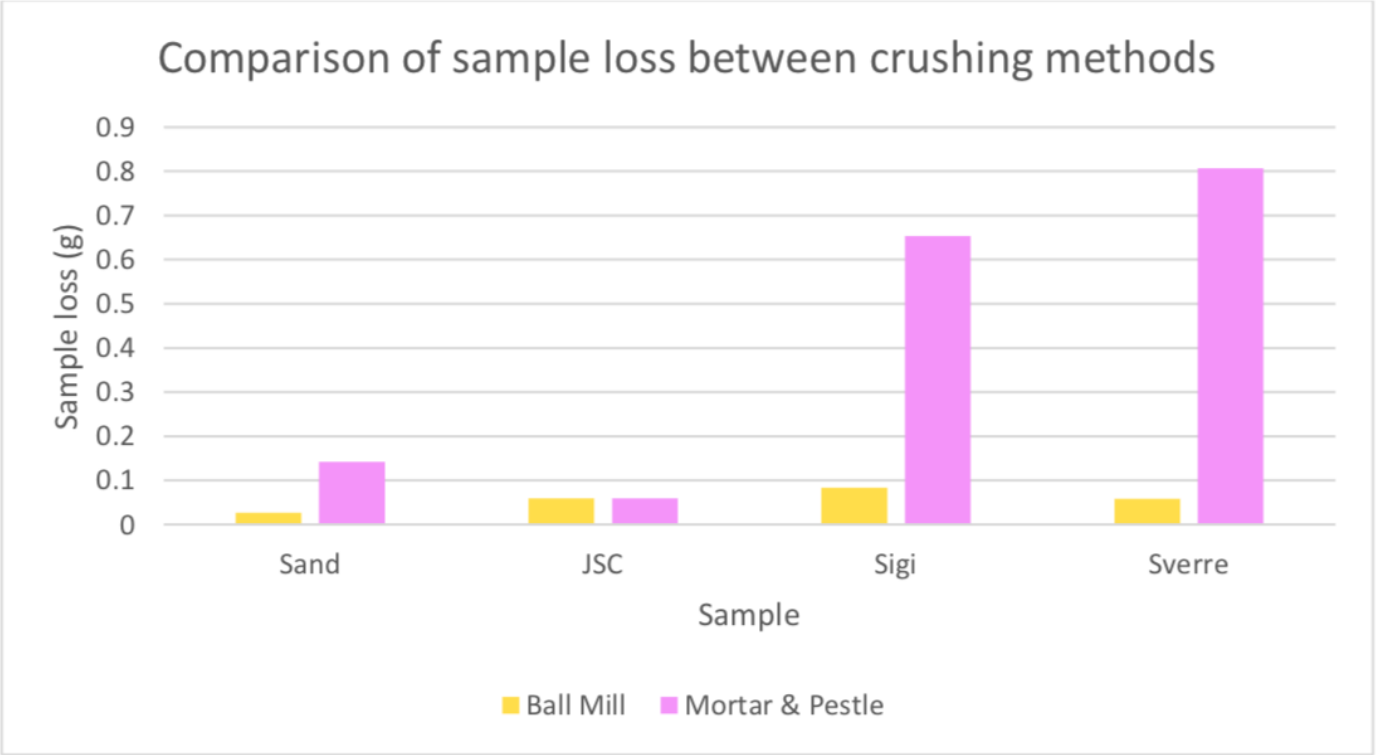

Figure 20 - Graph comparing the sample loss between the separate crushing methods

3.2.2 Solvent Extractions

Two separate organic solvent systems were trialled for this experiment using the ASE; Hexane:Acetone (2:1) and Dichloromethane:Methanol (9:1) (Method in Appendix Section 2 (Table 2)

After the solvent extractions the weight of the total lipid extract (TLE) for each sample could be recorded to give an indication of the amount of organics present in the sample. It can also be used to find the percentage of organic content within each individual sample.

$$Organic\ content = \left(\frac{TLE}{Initial\ sample\ mass}\right) * 100$$

The TLE recorded was very low in mass as demonstrated by table 8 and therefore TLE was run directly on the GC-MS for further analysis. Generally, higher % of organics were present in DCM-M extracted samples than Hexane-Acetone.

Table 12- Experiment 1 Sum TLE and % of organics within the samples at different crushing methods and solvents. BM = ball mill DCM =Dichloromethane-methanol (9:1) HEXACE = Hexane-Acetone (2:1)

Sample_Method_Solvent	Sum TLE (mg)	% of organics
Sand_BM_DCM	0.2	0.01%
Sand_HC_DCM	0.4	0.03%
Sand_BM_HEXACE	0.5	0.03%
Sand_HC_HEXACE	0	0.00%
JSC_BM_DCM	0.6	0.04%
JCS_HC_DCM	0.8	0.05%
JSC_BM_HEXACE	0.7	0.04%
JSC_HC_HEXACE	0.6	0.03%
Sigi_BM_DCM	1.7	0.12%
Sigi_HC_DCM	0.4	0.03%
Sigi_BM_HEXACE	0.3	0.02%
Sigi_HC_HEXACE	0.4	0.03%
Sverre_BM_DCM	0.4	0.03%
Sverre_HC_DCM	0.9	0.07%
Sverre_BM_HEXACE	0.4	0.02%
Sverre_HC_HEXACE	0.3	0.02%

3.2.3 GC-MS

Alkanes

Alkane detections especially appear to be unaffected by the solvent systems and continue a similar distribution across the four separate methods. Within this alkane distribution across all the methods, Sigi contains the highest ppm of C18 and C19 alkanes. A wide variety of alkanes (C17-C24) could be detected in the samples JSC, Sigi and Sverre. C20 and C22 could be found at small concentrations (<0.021ppm) in the procedural blank when using method 1 and 2 and were therefore deemed to be contaminants. C22 and C21 could be detected in the procedural blank when using methods 3 and 4 and therefore had to be ruled as contamination. The SNR for C22 was also <5 for 50% of the samples within this experiment and therefore not valued as a true detection.
C17, C18, C19 and C20 were on average the most abundant alkanes for all methods, in particular C18 and C19.

Esters

Esters are organic compounds formed by the reaction between an alcohol and an organic acid. TXIB ester is the synonym for 2,2,4-Trimethyl-1,3-pentanediol diisobutyrate, a diester from the family of Isooctanes. This compound was detected in all the DCM-M extracted samples. For the hex-ace extraction, it was detected in samples JSC, Sigi and Sverre but not the procedural blank (sand).

Hexanedioic acid, bis(2-ethylhexyl) ester is also known as DOA ester and was found in relatively low concentrations (<0.5) for both extraction methods. DOA ester is a diester and was found in low concentrations in the procedural blank of Method 1 (0.0190ppm).

1,4-Benzenedicarboxylic acid, bis(2-ethylhexyl) ester or Kodaflex DOTP is a primary plasticiser used in polyvinyl chloride (PVC) plastics and cable materials. Often compared to diisooctyl phthalate (DOP), this was detected in all 4 samples (Lyche, 2017). 1,4-Benzenedicarboxylic acid, bis(2-ethylhexyl) ester was detected in the procedural blank for Method 1 and therefore confirmed as contamination.

Others

4,4-Dimethyl-2-phenyl-5, 6-dihydro-4H-1,3-oxazine is an oxazine, a type of heterocyclic compound with a ring structure of oxygen and nitrogen atoms. A phenyl group is attached to the oxazine in this case with 2 methyl groups attached to the carbon atoms within the ring structure.

3.2.4 Summary

- TLE results (Table 12) were higher on average when using DCM-M vs Hex-Ace.
- DCM-M solvent extraction and GC-MS analysis revealed the presence of a range of organic compounds within our igneous samples.
- The compounds detected which were not detected in the sample or procedural blanks are limited to C17, C18, C19, C24 alkanes, 4,4-Dimethyl-2-phenyl-5, 6dihydro-4H-1,3-oxazine. The other compounds could be found at low concentrations within the procedural blanks.

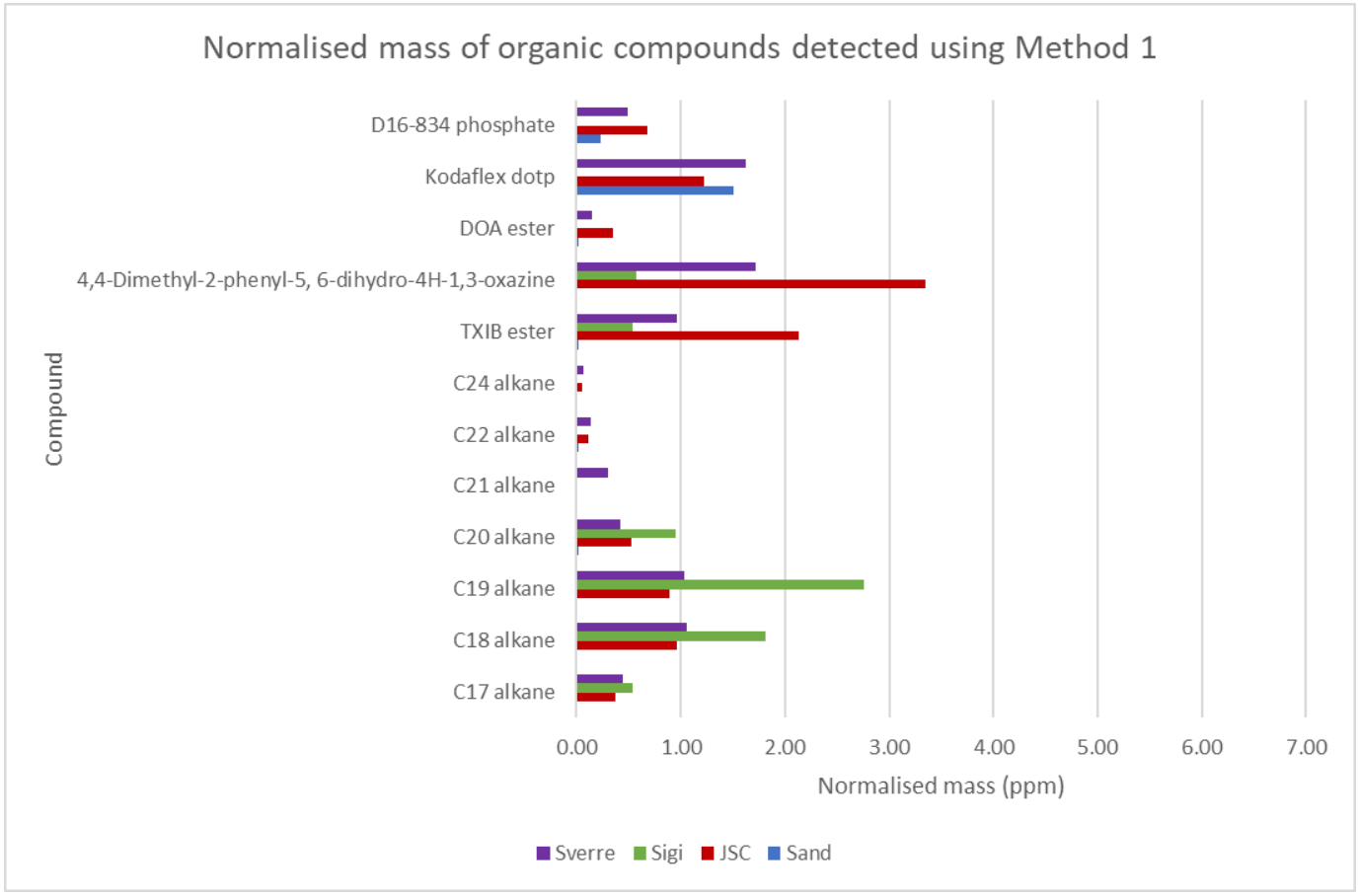
Normalised mass of organic compounds detected using Method 1
D16-834 phosphate
Kodaflex dotp
DOA ester
4,4-Dimethyl-2-phenyl-5, 6-dihydro-4H-1,3-oxazine
TXIB ester
C24 alkane
C22 alkane
C21 alkane
C20 alkane
C19 alkane
C18 alkane
C17 alkane
Compound
0.00
1.00
2.00
3.00
4.00
5.00
6.00
7.00
Normalised mass (ppm)
Sverre
Sigi
JSC
Sand

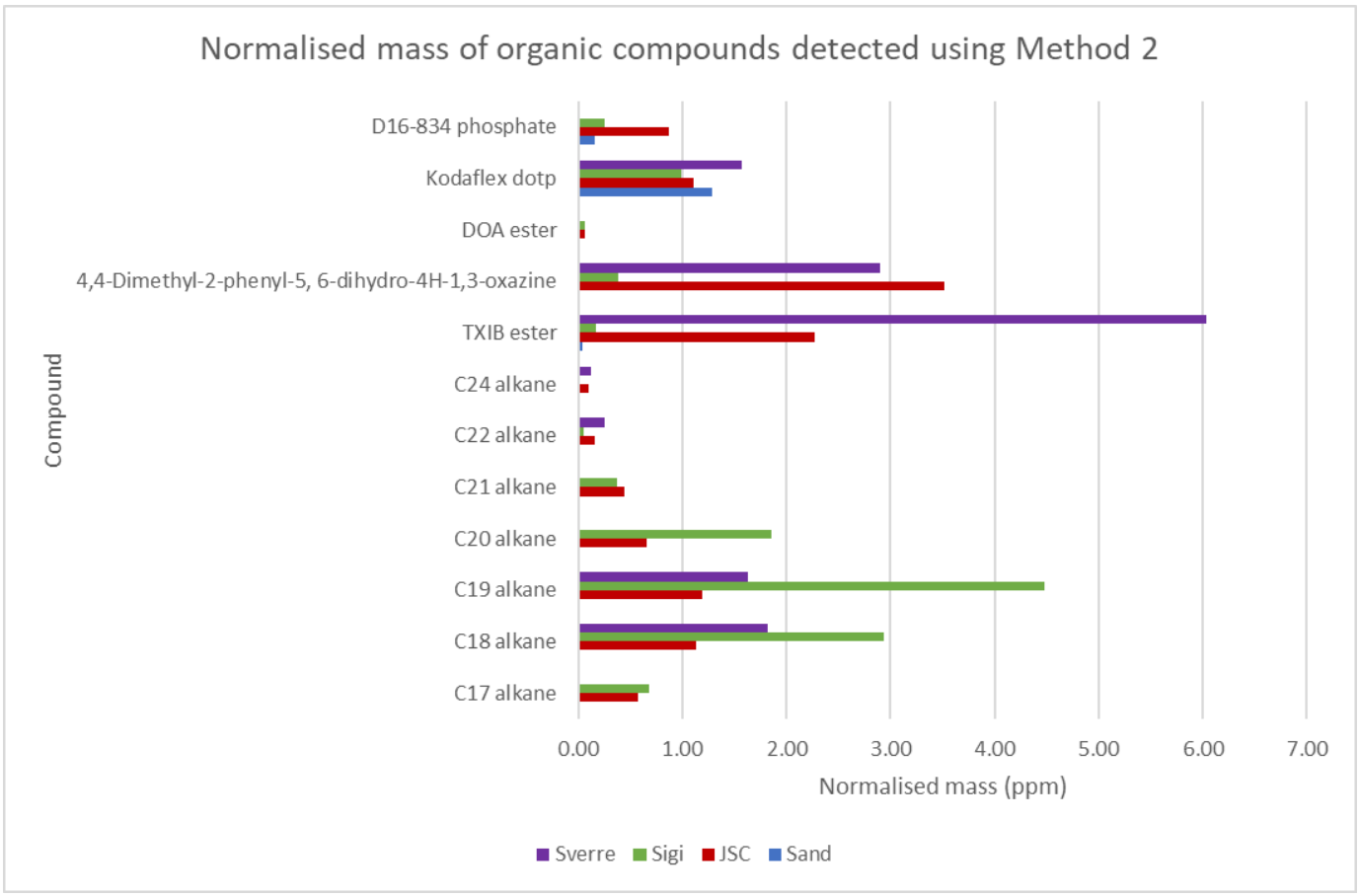
Normalised mass of organic compounds detected using Method 2
D16-834 phosphate
Kodaflex dotp
DOA ester
4,4-Dimethyl-2-phenyl-5, 6-dihydro-4H-1,3-oxazine
TXIB ester
C24 alkane
C22 alkane
C21 alkane
C20 alkane
C19 alkane
C18 alkane
C17 alkane
Compound
0.00
1.00
2.00
3.00
4.00
5.00
6.00
7.00
Normalised mass (ppm)
Sverre
Sigi
JSC
Sand

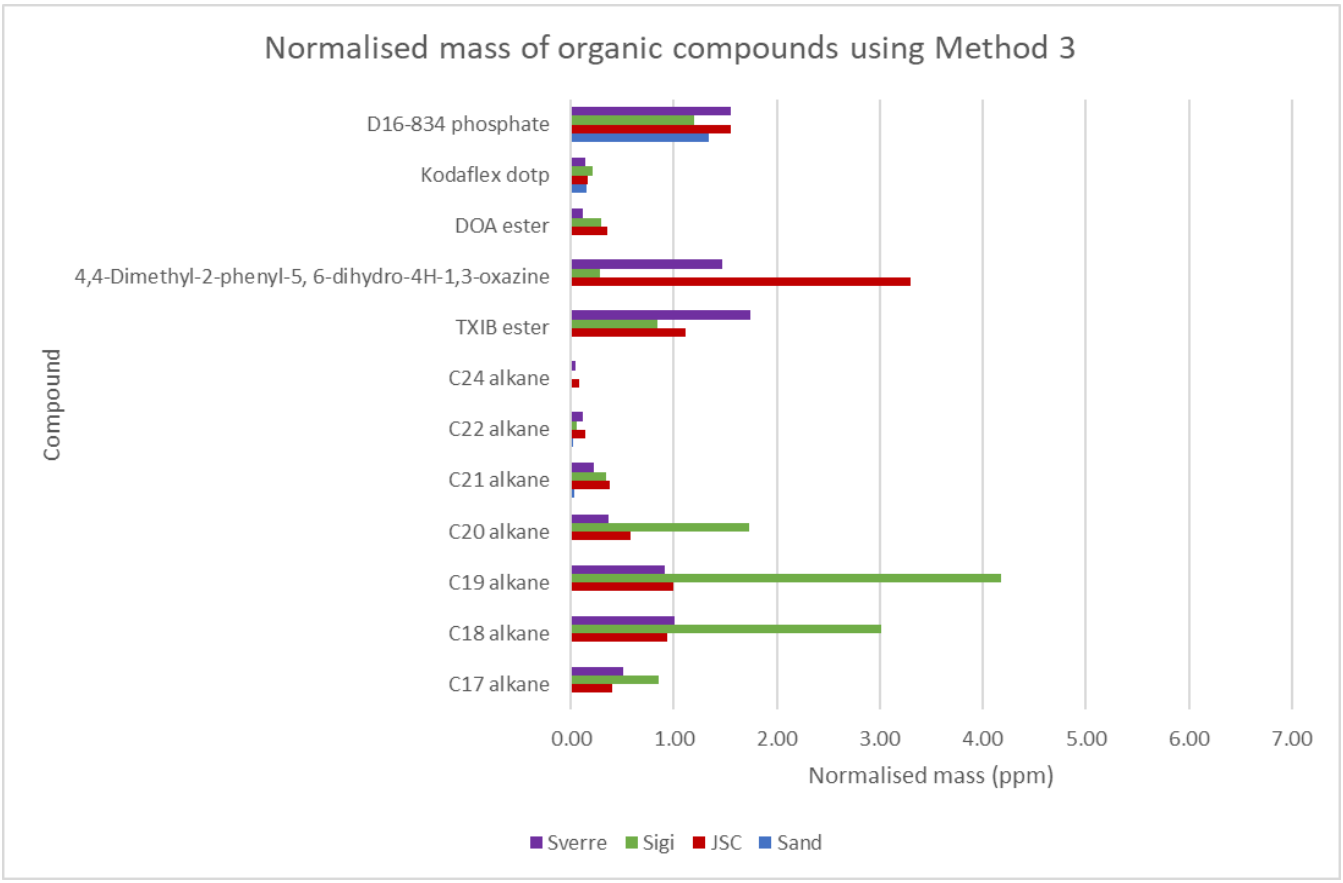

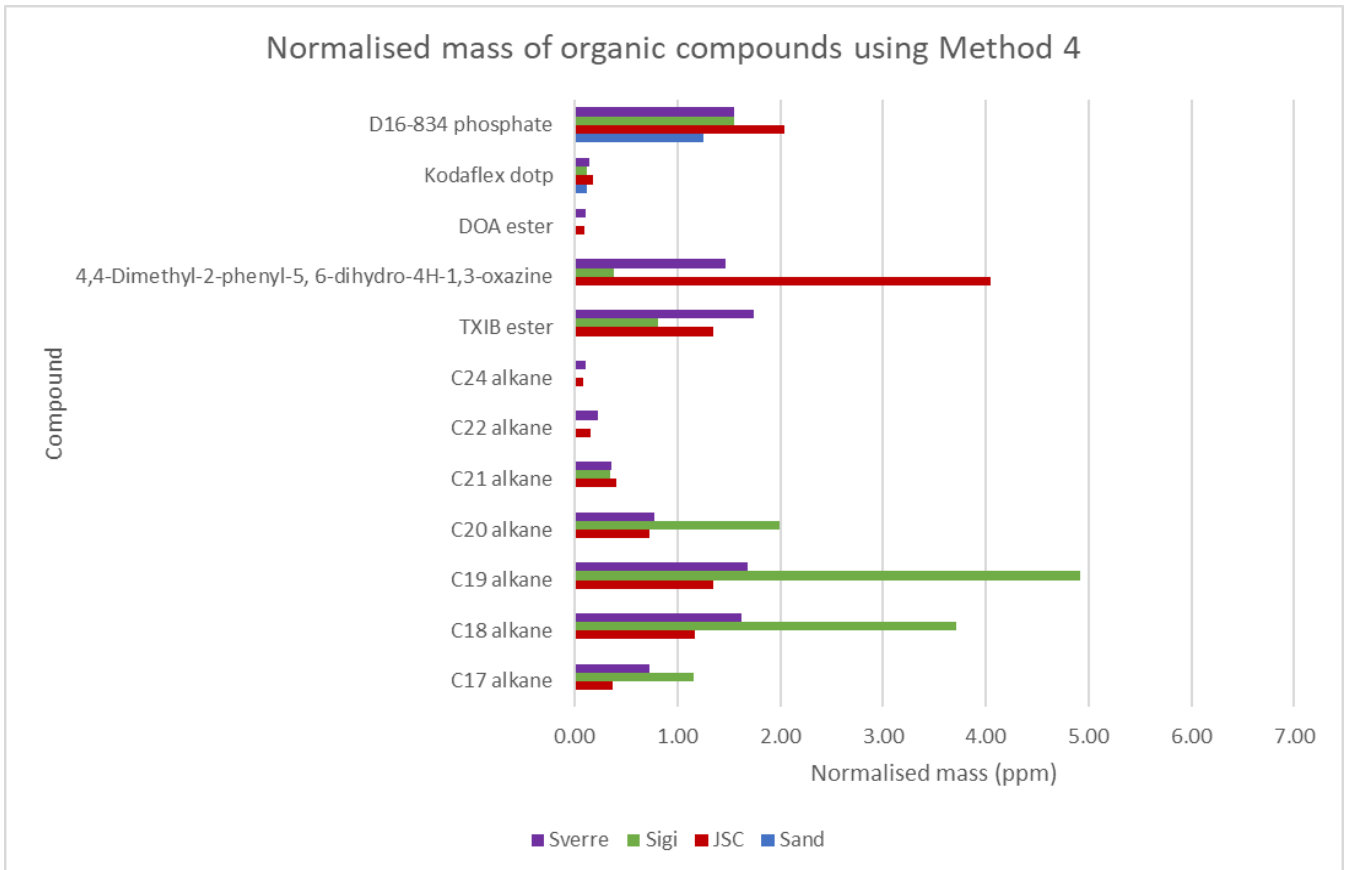

Figure 21 - Experiment 1 graphs visualising the normalised mass of organic compounds using the different methods. The full suite of organics that were consistent throughout the 4 methods (including contaminants) were included for this data set for overall evaluation

3.3 Reducing sample loss during crushing

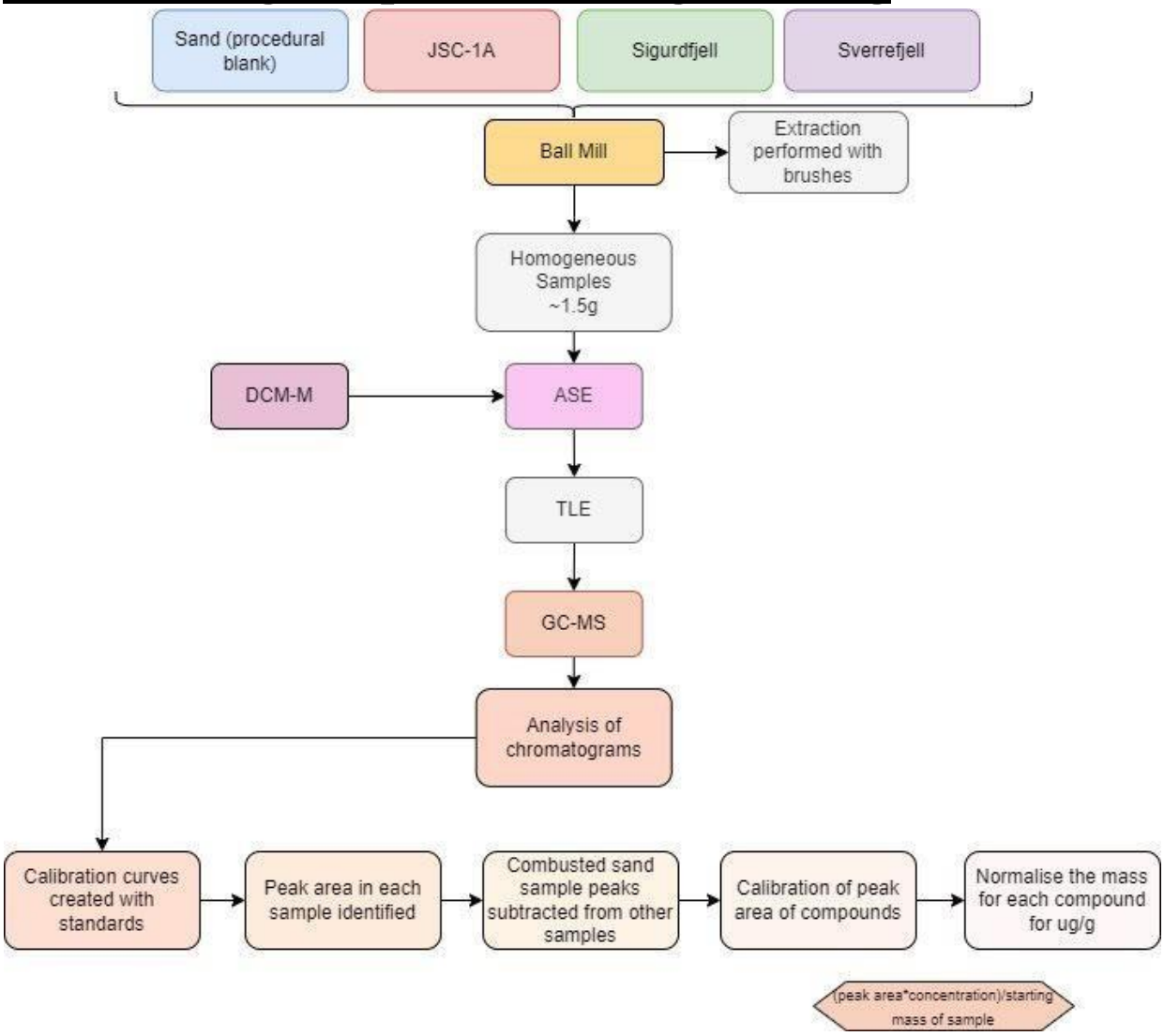

Figure 22 - Flowchart outlining the process for Experiment 2

The aim of this second experiment was to reduce the sample loss from the ball mill by using brushes hoping to extract more sample residue from the holders. The preferred techniques from Experiment 1 were conducted for this experiment for consistency and to support previous results. Thus, the ball mill was used as the crushing technique, DCM-M (9:1) used for the solvent extraction and GC-MS for qualitative analysis.

3.3.1 Crushing

Standard nylon acrylic paint brushes were utilised for the extraction procedure as well as the stainless-steel equipment. Each sample had a separate brush in order to reduce cross contamination. The results for the sample loss and % loss are shown in table 13. From the percentage loss it can be concluded that the introduction of nylon brushes to the extraction procedure for the ball mill holders increases the sample loss substantially compared to the extraction using only stainless-steel equipment (table 14).

After the crushing, samples were stored in labelled glass vials secured with aluminium foil which were then capped and kept in a seal-tight box in a secure location until solvent extractions.

Table 13 -Sample loss as a result of the crushing process for Experiment 2

Sample	Total Loss (g)	% Loss
Sand	0.0195	1.2956
JSC	0.0578	3.835
Sigi	0.0365	2.424
Sverre	0.0426	2.778

Table 14 - Comparison of percentage loss of samples between crushing process for Experiment 1 and Experiment 2

Sample	Without brushes (% Loss)	With brushes (% Loss)	% Difference
Sand	0.857	1.2956	51.1785 increase
JSC	1.90	3.835	101.842 increase
Sigi	2.706	2.424	10.4% decrease
Sverre	1.889	2.778	47.0619 increase

3.3.2 Solvent Extractions

The ASE was again utilised for organic solvent extraction using the method outlined in 4.4.3 for DCM-M. 1 sample blank and 4 samples, each at 1.5g sample mass were run for TLE. The TLE was weighed in order to provide an indication of the % of organics in the sample. The sample blank (introduced at the solvent extraction preparation phase) has a positive TLE measurement which could indicate laboratory contamination as a result of poor cleaning practice and or human error. Any compounds present in the sample blank and our samples are treated as contaminants.

Table 15- - Experiment 2 Sum TLE of samples including % of organics

Experiment 2 Sum TLE		
Sample	Sum TLE (mg)	% organics
BLK	0.3	N/A
Sand	0	0
JSC	0.4	0.0267
Sigi	0	0
Sverre	0.5	0.0333

3.3.3 GC-MS

Alkanes

C17, C19, C20 and C22 were detected in experiment 2. This range of alkanes differs to those previously detected using the same sample mass and also the concentration is lower. Perhaps as a result of inhomogeneity in the samples. The alkanes follow similar trends for each chain length; JSC hosts the smallest amount, Sigurdfjelle slightly higher and Sverrefjellet with the highest concentration. C22 is classed as contamination as it is only detected in the procedural blank.

Benzenes

A variety of benzenes were detected from this experiment. All varieties of benzenes present were detected in the sample blank. The benzenes are all attached to a certain group where the benzene serves the core structure with an alkyl group attached serving as the functional group. 10 benzene groups were detected in the procedural blank. Benzene, (1-ethynonyl) and Benzene, (1-methyldecyl) could both be recorded in all 4 samples. The normalised mass of benzene in our samples never surpassed 0.7ppm for this experiment.

Phosphate

Two different phosphate groups were detected in this experiment. D16-834 phosphate (synonym for Tris(2,4-di-tert-butylphenyl)phosphate) was detected in the procedural blank. 2-Propanol, 1-chloro-, phosphate (3:1) was only detected in the BVC samples around 0.8ppm.

Other compounds

Dodecanoic acid, 1-methylethyl ester also known as Isopropyl dodecanoate or isopropyl laurate is a fatty acid ester obtained by the formal condensation of caboxy group of

dodecanoic acid with propan-2-ol, a metabolite found in human saliva (de Lacy Costello et al., 2014).

Octanal, 2-(phenylmethylene)-, is formed through aldehyde condensation. The functional group is an aldehyde group which is attached to the second carbon in the octanal chain. 13-Docosenamide (Z) or erucamide is a primary fatty amide from the formal condensation of the carboxy group of 13-docosenoic acid with ammonia (Tamilmani et al., 2018).

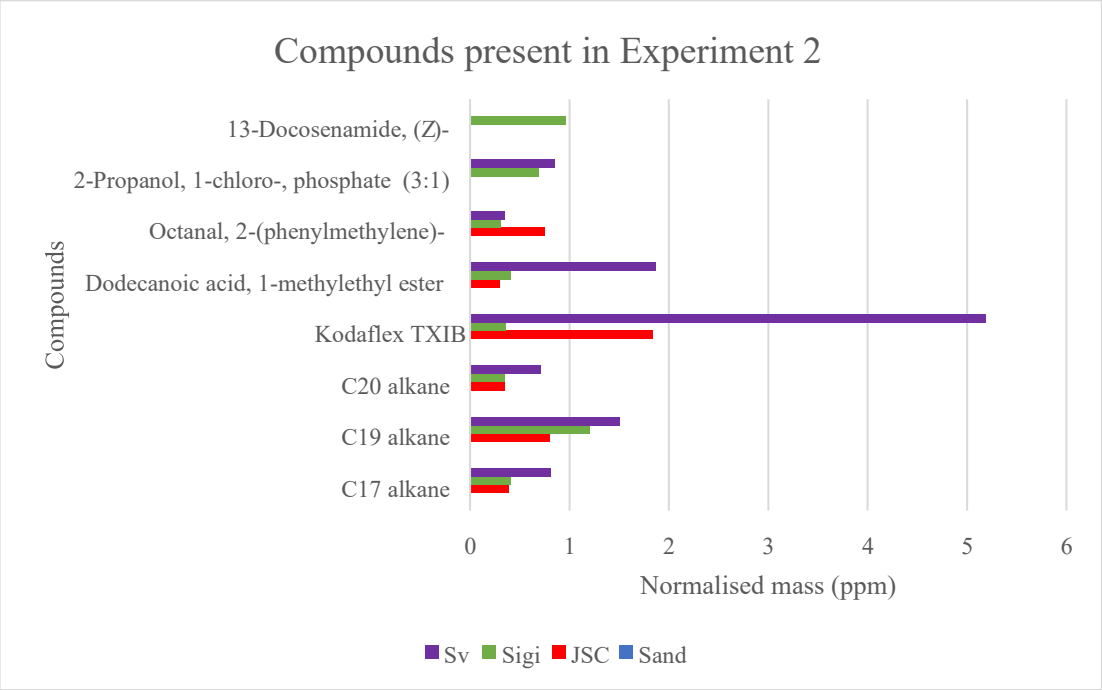

Figure 23- Compounds present in experiment 2 excluding those detected in procedural blank (sand)

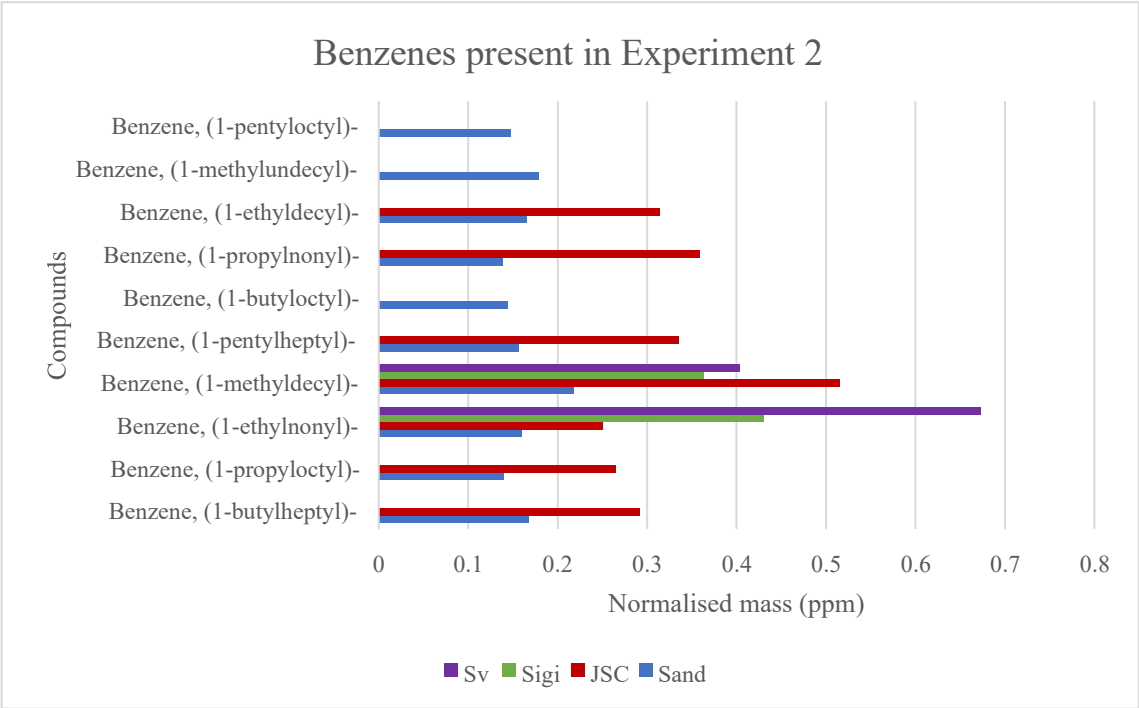

Figure 24- Benzene groups present in experiment 2. All detected in the procedural blank (sand)

3.3.4 Summary

This experiment aimed to reduce the sample loss from the crushing process by using brushes to aid in the extraction of material.

- An array of benzenes were present in the sample blank, procedural blank and JSC. Benzene, (1ethylnonyl)-and Benzene, (1-methyldecyl)- were detected in all four samples.
- Kodaflex TXIB was detected in JSC, Sigi and Sverre with significantly higher concentrations in Sverre at 5.18ppm.
- The samples (JSC, Sigi and Sverre) follow a similar trend for each chain length, particularly within the alkane group; with a gradual increase of normalised mass from JSC to Sverre.
- C22 was present only in the Sand sample.

Table 16 -Compounds detected in Experiment 2 with their respective retention times (R.T). Compounds detected in any blanks were deemed contamination and are highlighted in red.

Experiment 2 Compounds	
Compound	**R.T. (mins)**
Kodaflex TXIB	19.44
Dodecanoic acid, 1-methylethyl ester	20.03
Benzene, (1-butylheptyl)-	20.327
Benzene, (1-propyloctyl)-	20.561
Benzene, (1-ethylnonyl)-	21.03
Benzene, (1-methyldecyl)-	21.802
C17 alkane	21.89
Benzene, (1-pentylheptyl)-	22.319
Octanal, 2-(phenylmethylene)-	22.423
Benzene, (1-butyloctyl)-	22.43
Benzene, (1-propylnonyl)-	22.685
2-Propanol, 1-chloro-, phosphate (3:1)	23.092
Benzene, (1-ethyldecyl)-	23.167
Benzene, (1-methylundecyl)-	23.947
Benzene, (1-pentyloctyl)-	24.36
Benzene, (1-butylnonyl)-	24.505
1,2-Benzenedicarboxylic acid, bis(2-methylpropyl) ester	24.602
Benzene, (1-propyldecyl)-	24.767
Benzene, (1-ethylundecyl)-	25.264
C19 alkane	25.995
Benzene, (1-methyldodecyl)-	26.022
Dibutyl phthalate:	26.422
C20 alkane	27.975
4,4-Dimethyl-2-phenyl-5, 6-dihydro-4H-1,3-oxazine	28.38
C21 alkane	29.773
C22 alkane	31.556
Phthalic acid, di(2-propylpentyl) ester	36.696
13-Docosenamide, (Z)-	40.109
D16-834 phosphate (Tris(2,4-di-tert-butylphenyl) phosphate)	56.3

3.4 Determining GC-MS detection limits with decreasing sample mass

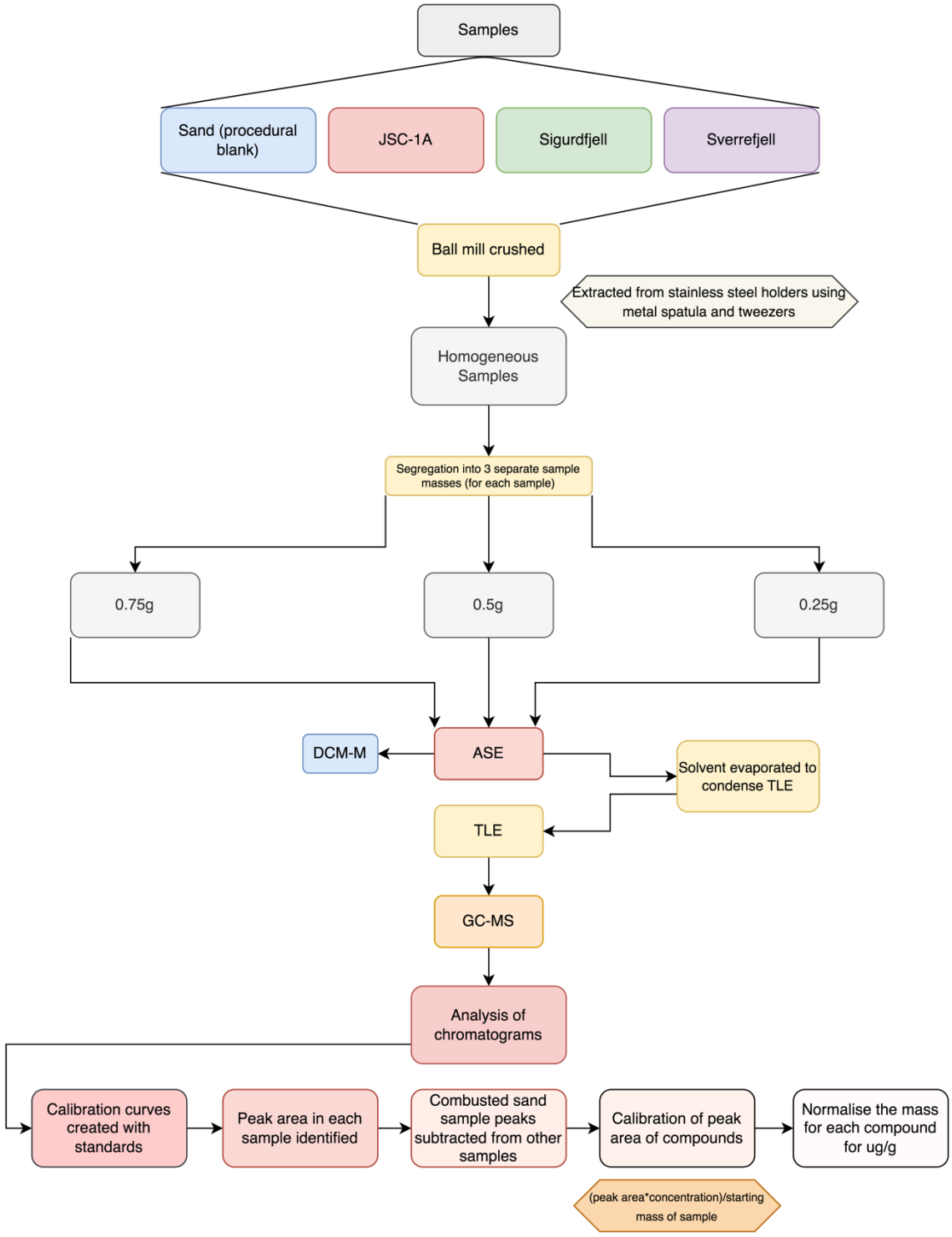

Figure 25 - Flowchart outlining the process for Experiment 3

The aim of the third experiment was to reduce the sample size incrementally in order to understand the detection limits of organic compounds on the GC-MS. It is important to understand the lowest mass possible that will still successfully detect the full range of

organic compounds due to the limited sample size available for processing Martian material.

3.4.1 Crushing

Approximately 2.5g of each sample was crushed using the ball mill for this experiment. 1.5g was required for this experiment however, at the time of crushing, another experiment had been considered which would require a further 1g. The crushing process was aided by stainless steel spatula and tweezers to assist in mobilising the sample out of the ball mill holders and into the glass vials for storage pending ASE use. The samples were stored in combusted glass vials capped with aluminium foil and then secured with screw-top caps to ensure no spillage.

Table 17 - Experiment 3 sample loss from crushing procedure

Experiment 3 ball mill crushing (loss)		
Sample	**Total loss (g)**	**% Loss**
Sand	0.0463	1.8073
JSC	0.0335	1.3116
Sigi	0.0339	1.3259
Sverre	0.0466	1.7978

From table 17, it is clear that the sample loss is consistently lower than 0.05g. The average loss was 0.040075g for this experiment. The % loss was constantly below 1.9%. The samples were split incrementally into 0.75, 0.5 and 0.25g fractions during ASE preparation. The sample was poured from the vial into the ASE cells one fraction at a time and were measured as such. Each sample met the fraction masses exactly within 0.01g fluctuation.

3.4.2 Solvent Extractions

There were 14 samples in total which included each sample at each selected mass (0.75, 0.5 and 0.25g) and a sample blank of unprocessed combusted sand at the start and end of the cycle both introduced at the solvent extraction phase named BLK1 and BLK2. Two sample blanks were chosen due to the large number of samples being processed; it also was to aid in tracing contamination throughout the experiment.

The same method was used on the ASE with DCM-M (9:1). Sample preparation for GC-MS was also kept consistent with previous experiments and so the samples were run in 50µL (or 0.05mL) DCM-M.

Table 18 outlines the sum TLE and % of organics in each sample. There is an obvious outlier in this data with Sigi_0.25 with 53.5% organics. This is likely due to human error and or contamination. Contamination can be supported by the 2mg increase of TLE from BLK1 to BLK 2. Out with this figure and the sample blanks, the average for sum TLE within the range of samples is 0.000436g or 0.436mg and the range 0.5mg.

Table 18 -Experiment 3 Sum TLE outlining the % of organics within each sample

Experiment 3 Sum TLE		
Sample	**Sum TLE (mg)**	**% organics**
BLK1	0.4	N/A
Sand_0.75	0.2	0.03
JSC_0.75	0.6	0.08
Sigi_0.75	0.2	0.03
Sverre_0.75	0.6	0.08
Sand_0.5	0.3	0.06
JSC_0.5	0.6	0.12
Sigi_0.5	0.4	0.08
Sverre_0.5	0.6	0.12
Sand_0.25	0.6	0.24
JSC__0.25	0.6	0.24
Sigi_0.25	133.3	53.3
Sverre_0.25	0.1	0.04
BLK2	2.4	N/A

3.4.3 GC-MS

Alkanes

The procedural blank (sand) does not detect any of the alkanes implying a true result within the samples. There are variations between the chain length of alkanes detected throughout the sample masses visualised in Figure 26 and Table 19.

Table 19 -Alkanes detected in each sample at different masses

Sample mass (g)	Alkanes detected
0.75	JSC: C17-C20 Sigi: C16-C20 Sverre: C17-C18
0.5	JSC: C16-C20 Sigi: C16-C20 Sverre: C16-C20
0.25	JSC: C17, C19 Sigi: C17-C20 Sverre: C17-C20

The detections for this experiment were all relatively low compared to previous experiments, which was expected due to the large reduction in the sample mass, however, the ability to detect alkanes at such low masses is important for future missions.

For 0.5g and 0.25g sample masses, Sigi had the highest ppm of alkanes from C17-C20.

The normalised mass for C19 within the samples was on average very similar for 0.5g and 0.25g sample batch, both at around 0.17ppm. Interestingly, C19 was highest within Sigi at 0.25g sample batch compared to 0.5g and 0.75g.

It was surprising that the same alkanes were not detected in the same samples throughout the masses, for instance C16 only being detected in 0.5g of sample and not 0.75g. At 0.5g, alkanes C16 through to C20 could be detected.

Other compounds

The compounds that were not present in the sample blanks or procedural blank were limited to Octanal, 2-(phenylmethylene)-, Benzene (1-pentyheptyl) and Benzene (1methyldecyl). Both benzenes were attached to an alkyl group and are synthetic compounds.

Octanal, 2-(phenylmethylene) is present in 0.5g of JSC at 0.124ppm.

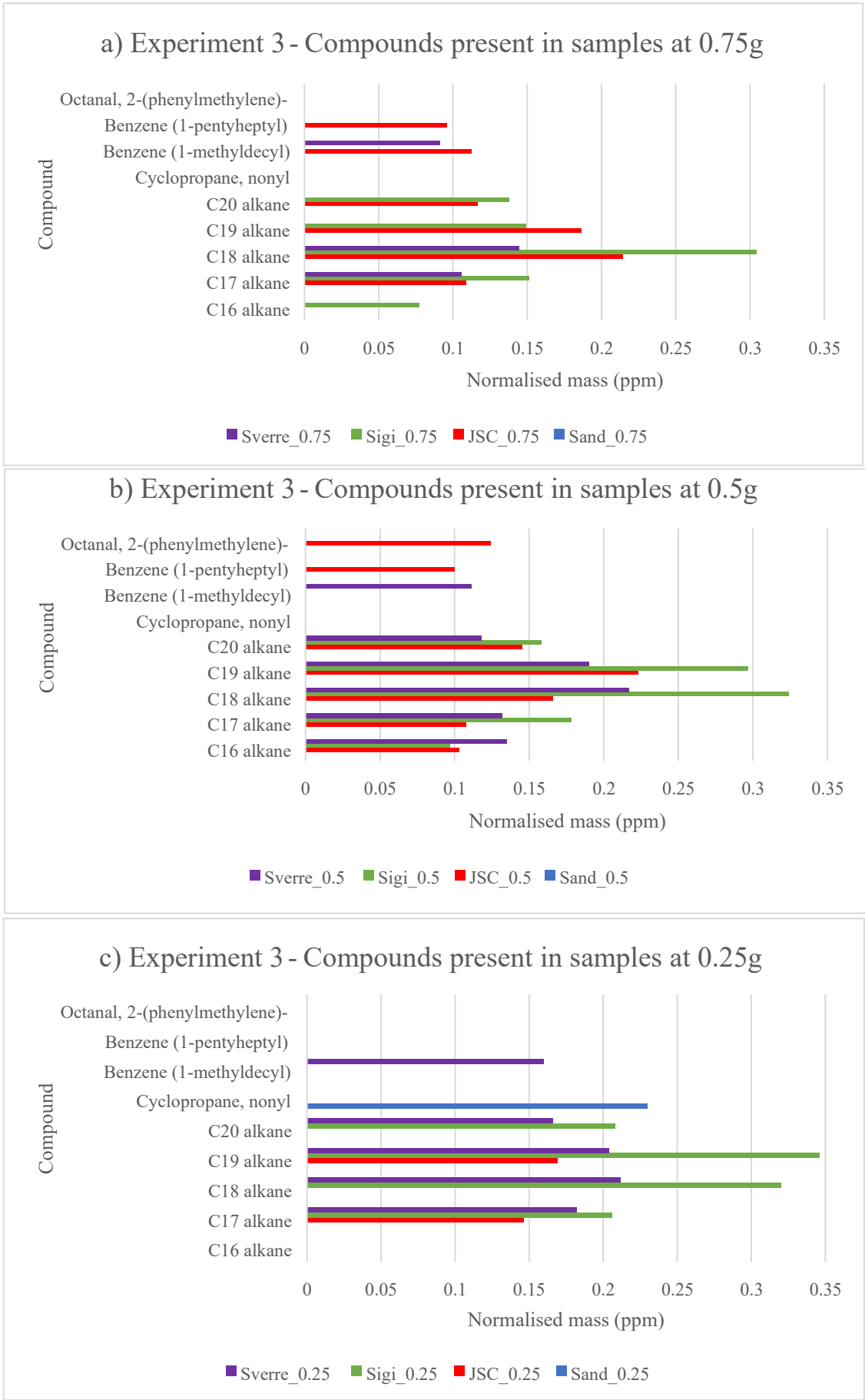

Figure 26 - Experiment 3 graphs showing the organic compounds detected in the a) 0.75g b) 0.5g and c) 0.25g sample batch

3.4.4 Summary

Experiment 3 attempted to understand the range of organics that could be detected at reduced sample masses.

- Alkanes were most abundant within the samples at 0.5g sample mass.
- Even when discounting all compounds detected in sample blanks and procedural blank, aromatic and aliphatic organic compounds were detected; C16-C20 alkanes, benzenes attached to alkyl groups and Octanal, 2-(phenylmethylene), an aldehyde with a phenyl group attached.
- Benzenes: detected in JSC at 0.1ppm within 0.75g and 0.5g samples. Detected in Sverre at 0.15ppm.
- Cyclopropane, nonyl is a cycloalkane which was only detected in the combusted sand at 0.25g sample mass.
- Although there were detections at these smaller masses, the normalised mass was low with no detection higher than 0.4ppm.
- Sigurdfjelle, overall, has the highest normalised mass (ppm) of alkanes C17-C20 of all the samples for each tested mass
- C16 was detected for the first and only time throughout the project. It was detected in all 3 samples at 0.5g. It was detected in Sigi at 0.75g but at 0.07ppm

Table 20 - Compounds detected within samples in Experiment 3 with their respective retention times (R.T). Compounds detected in any blanks were deemed contamination and are highlighted in red.

Experiment 3 Compounds	
Compound	**R.T (mins)**
Cyclopropane, nonyl	16.741
1-Decanol	16.824
2,2,4-Trimethyl- 1,3-pentanediol diisobutyrate	19.237
C16	19.561
Benzene (1-methyldecyl)	21.602
C17	21.699
Benzene (1-pentyheptyl)	22.147
Octanal, 2-(phenylmethylene)-	22.237
2-Propanol, 1-chloro-, phosphate (3:1)	22.871
C18	23.781
1,2-Benzenedicarboxylic acid, bis(2- methylpropyl) ester	24.402
Diphenyl Sulfone	25.298
C19	25.795
C20	27.732
Phenylmethanediol dibutanoate	28.105
9-Octadecenoic acid, methyl ester	29.242
1,3-Benzenedicarboxylic acid, bis(2-ethylhexyl) ester	39.696

3.5 Fractionating low-mass samples to improve detection sensitivity

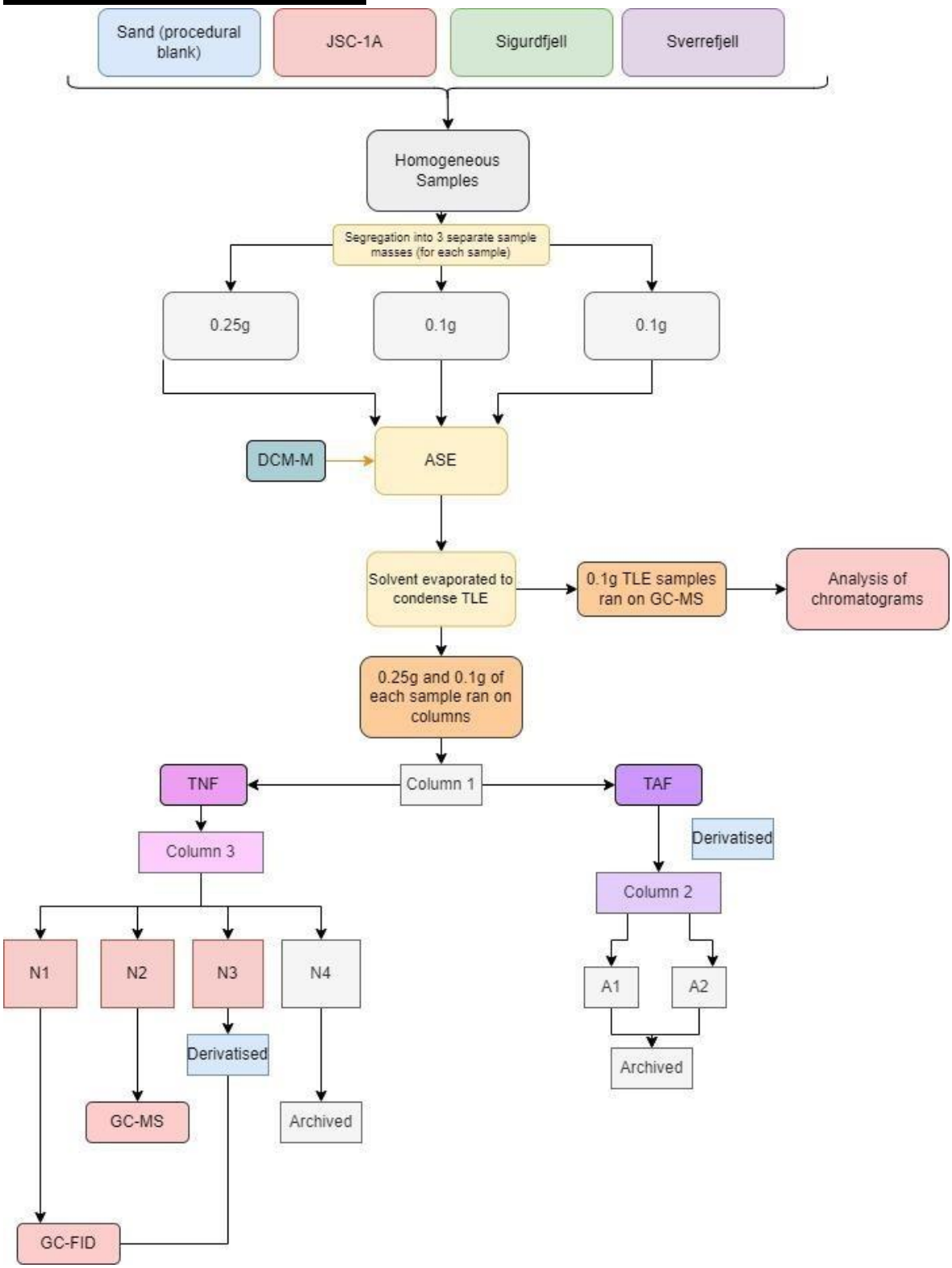

Figure 27- Flowchart outlining the process for Experiment 4

Experiment 4 took a different approach in terms of methodology. In order to simplify analysis, by splitting up organic compounds into their respective groups, we used column

chromatography. The column chromatography process is outlined within figure 27 showing the breakdown of separate fractions, further details of the column chromatography standard operation procedure are outlined in Appendix Section B.3.

0.1g of each sample was run for TLE using the same protocol as previous in order to complete the full sample mass suite. This would allow us to understand the detection limits of the GC-MS for organic compounds in basaltic material through various sample sizes.

0.1g and 0.25 of each sample went through column chromatography prior to GC-MS analysis. Samples were taken from the previously crushed sample batch.

3.5.1 Crushing

Sample which was previously crushed for experiment 3 (see section 3.4.1) was used for this experiment which had been stored within glass vials covered and capped and kept within an airtight sealed box.

3.5.2. Solvent Extraction

Solvent extractions were carried out on the ASE using DCM-M (9:1) with the same method as previously identified in Experiment 1, 2 and 3.

Table 21 - Experiment 4 Sum TLE and % of organics within each sample

Experiment 4 Sum TLE		
Sample	**Sum TLE (mg)**	**% organics**
BLK1	0.1	N/A
Sand_0.1_TLE	0.3	0.30000%
JSC_0.1_TLE	0.3	0.30000%
Sigi_0.1_TLE	0.2	0.20000%
Sverre_0.1_TLE	0.2	0.20000%
Sand_0.1_Columns	0.3	0.30000%
JSC_0.1_Columns	0	0.00000%
Sigi_0.1_Columns	0.5	0.50000%
Sverre_0.1_Columns	0.5	0.50000%
Sand_0.25_Columns	0.1	0.04000%
JSC__0.25_Columns	0.4	0.16000%
Sigi_0.25_Columns	0.2	0.08000%
Sverre_0.25_Columns	0.1	0.04000%
BLK2	0.1	N/A

0.1g of each sample was run for TLE on the GC-MS using the same method (Method 1) as used in previous experiments 1, 2 and 3.

The TNF fractions extracted from this experiment were condensed by running them on the GC-MS in 0.2µL rather than the previously used 0.5µL of solvent.

After solvent extraction using DCM-M on the ASE, 0.1g and 0.25g of each sample was then subjected to column chromatography. The method used for column chromatography is outlined in Appendix Section B.3.

3.5.3 GC-MS

For the 0.1g TLE fraction, alkanes C18 and C19 were present in relatively high concentrations (~2ppm) in JSC. These were the only compounds in this experiment which were not present in the sample blank.

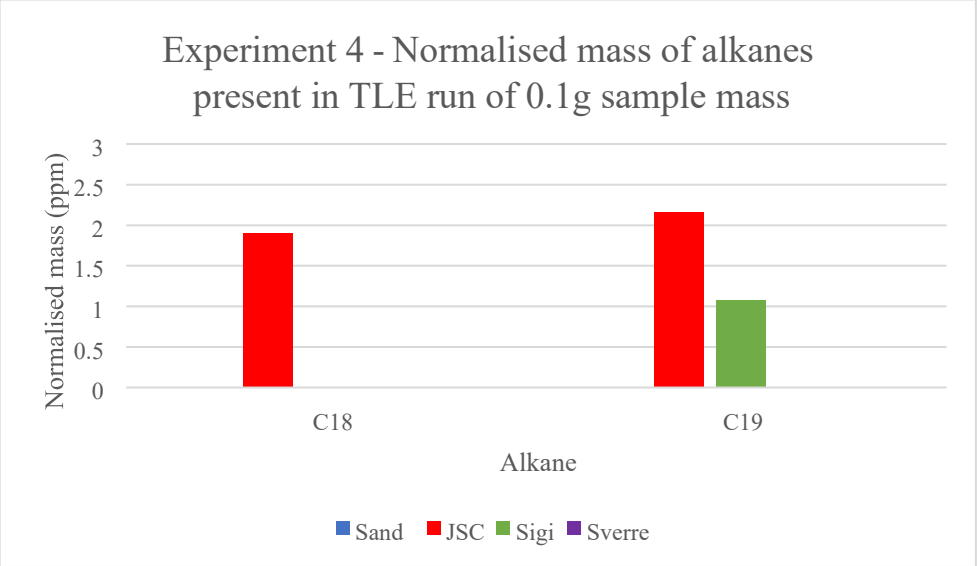

Figure 28- Graph from experiment 4 showing the alkanes present in samples

N1 fraction

The results of the N1 fraction for this experiment were unusable due to contamination of the hexane solvent.

N2 fraction

The compounds present for the N2 fractions could all be detected in the procedural blank implying contamination for both masses. The normalised mass for organic compounds detected was higher in the 0.1g mass compared to the 0.25g mass which may also imply contamination or an inaccurate result.

N3 fraction

The N3s were derivatised in this fraction. Diphenyl Sulfone, 1-Octadecanol, TMS derivative and Tris (2,4-di-tert-butyl phenyl) phosphate were detected dominantly in JSC. However, at 0.1g, Diphenyl Sulfone was detected at high concentrations (3.68ppm) in the procedural blank implying contamination.

1-Octadecanol is a long chain fatty alcohol with 18 carbon atoms. TMS derivative is a compound that reacted with TMS groups during derivatisation which improves its volatility for GC-MS. This was detected at relatively high concentrations within JSC; 0.25g-8.2ppm and 0.1g-3.2ppm.

Tris(2,4-di-tert-butylphenyl) phosphate was detected in JSC but was also detected in the sample blank. This compound has previously been detected in prior experiments in sample blanks and therefore can be confirmed as a contaminant.

TAFs and N4s were archived as the there was no access to the facilities required to run them at UofG.

3.5.4 Summary

- Need to re-run 0.1g for TLE again to confirm these alkane detections.
- GC-MS detected organic compounds in 0.1g of JSC. Alkanes C18 and C19 may only have been detected in JSC due to the relatively higher organic abundance. C19 alkane was also detected in Sigurdfjelle.
- The probability of the organic compound detected being C18 and C19 from the MS system was low (<20%) but the SNR was >5. Repetition of the experiments would help to confirm or deny this detection.

Table 22 - Compounds present within the Experiment 4 sample blank with their respective retention times (R.T) in minutes

Experiment 4 Sample Blank	
Compound	**RT (mins)**
Phthalate	24.347
Phthalate	25.905
Phthalate	26.16
11-Octadecenoic acid, methyl ester	29.194
1,4-Benzenedicarboxylic acid, bis(2-ethylhexyl) ester	39.64
Tris(2,4-di-tert-butylphenyl) phosphate	55.493

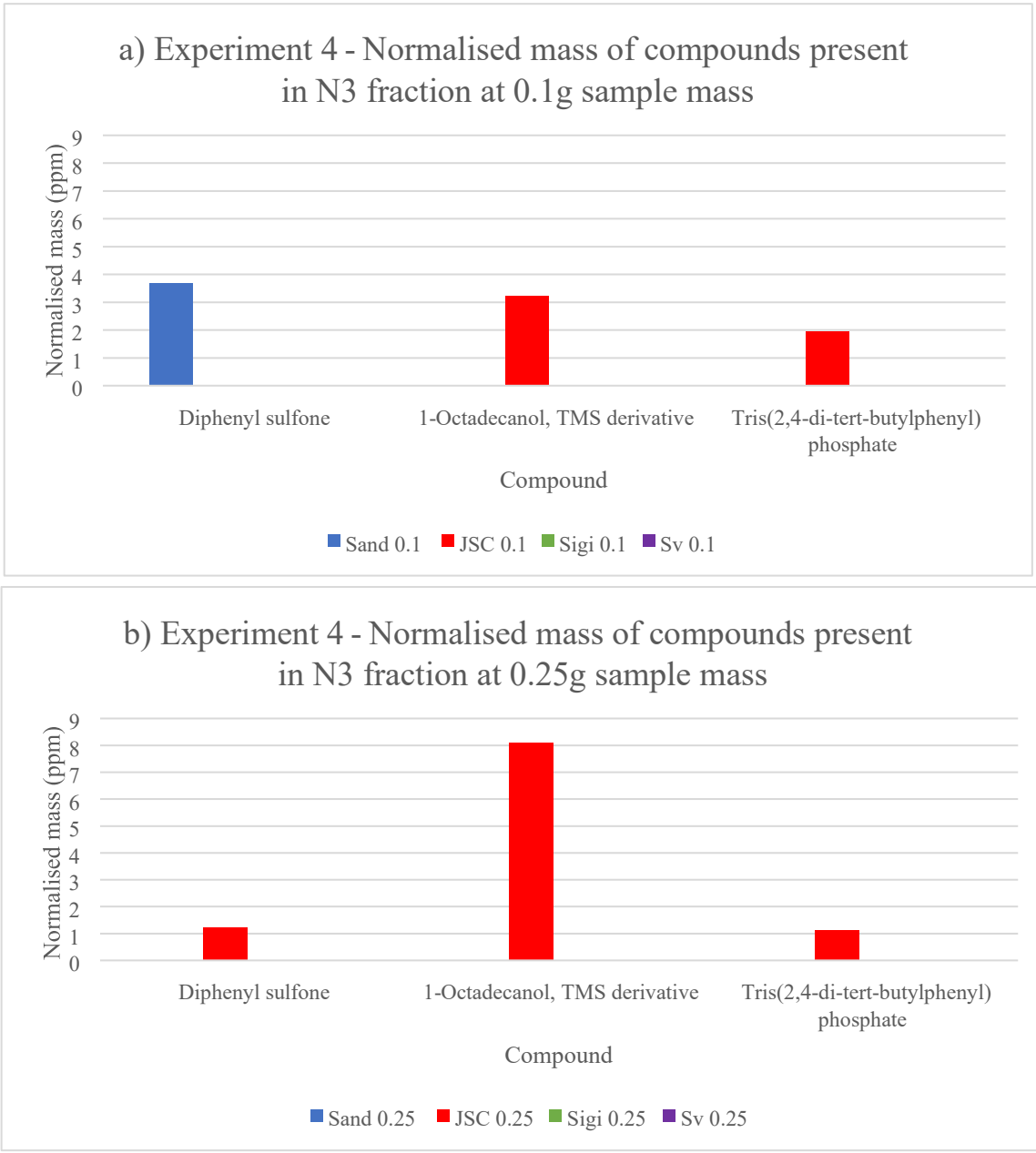

Figure 29- Graphs of compounds present in the N3 fraction of Experiment 4 at a) 0.1g and b) 0.25g sample mass

3.6 Verifying previous experiment results

This experiment was a rerun of Experiment 4 due to the contamination of the solvent standard preventing successful results from the N1 fraction. Enough sample remained from the bulk crushing procedure to avoid this step. The samples went through the exact same process for this experiment as they did experiment 4 except N1s and TAFs were run on the GC-FID as we knew the target compounds in regard to alkanes and FAMES. From the two sample blanks run for this experiment, it is clear that contamination was present throughout unfortunately prohibiting comprehensive analysis from this experiments results.

- Long chain alkanes not previously seen before were detected in 0.1g but not in 0.25g of any sample.
- Sample blank was contaminated so it was therefore difficult to conclude the validity of any of the compounds detected in the samples.
- Suspected lab contamination from improper cleaning procedure of ASE cells.
- Solvent blank run with the samples did not run properly and therefore difficult to establish a certain result from this experiment.
- Unable to successfully analyse results from GC-MS and GC-FID.

3.7 Experiments Summary

Table 23 - Experiment summary outlining the key findings from each experiment

Experiment	Lessons learned
1	Determined the most time efficient and effective crushing method (ball mill). Recognised that DCM-M (9:1) solvent extraction prior to GC-MS extracted a range of organic compounds which could be analysed readily on the GC-MS and therefore was a suitable method to continue with
2	Attempted to reduce sample loss from ball mill holders during sample extraction by using brushes but deduced that stainless steel material is more effective and ultimately introduces less contaminants into the sample batch.
3	Began reducing the sample mass to determine the smallest mass of sample that could be used and still provide a full organic suite. Organic compounds were detected down to 0.25g, but less than that found at 0.75g of sample mass.
4	1-2ppm of alkanes (C18, C19) detected at 0.1g. Column chromatography is a useful technique for the separation of compounds as it allows for a simpler analysis. However, it also introduces several steps prior to GC-MS analysis which could lead to an increase in contamination. N1 fraction was contaminated and therefore could not compare the alkane detection leading to a re-run of the experiment
5	Experiment 4 rerun. Ex5 was ultimately contaminated rendering the results unsuccessful. An important insight into the importance of proper cleaning protocol and laboratory contamination.

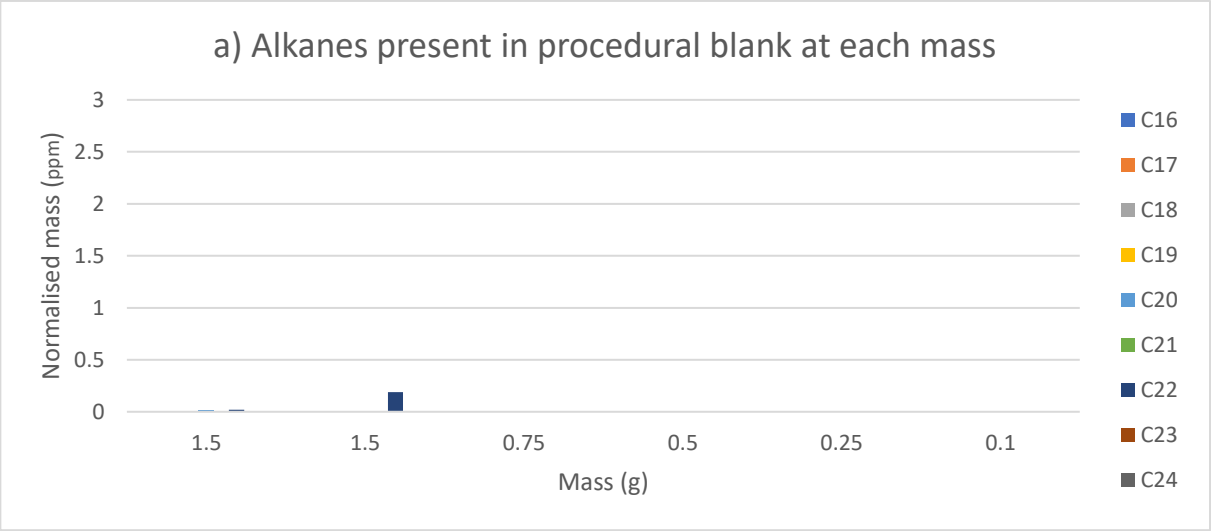

Procedural blank (sand)– Alkane concentration (µg/g) at various sample masses									
Alkane	C16	C17	C18	C19	C20	C21	C22	C23	C24
1.5g					0.017		0.021		
1.5g							0.188		
0.75g									
0.5g									
0.2g									
0.1g									

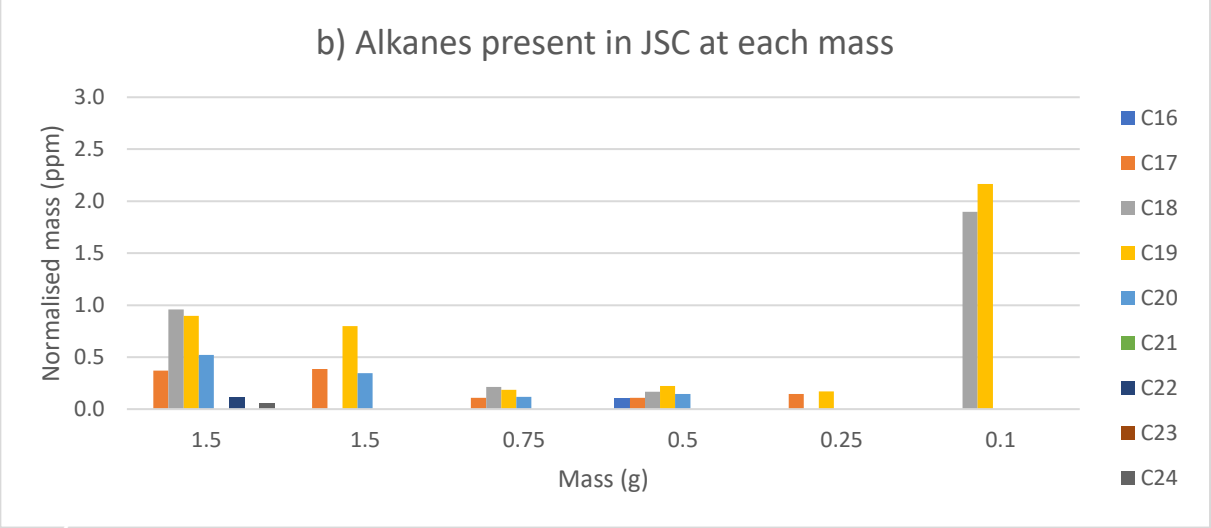

JSC – Alkane concentration (µg/g) at various sample masses									
Alkane	C16	C17	C18	C19	C20	C21	C22	C23	C24
1.5g		0.369	0.958	0.898	0.522		0.118		0.053
1.5g		0.384		0.798	0.347				
0.75g		0.109	0.214	0.186	0.116				
0.5g	0.103	0.108	0.166	0.223	0.145				
0.2g		0.146		0.169					
0.1g			1.899	2.165					

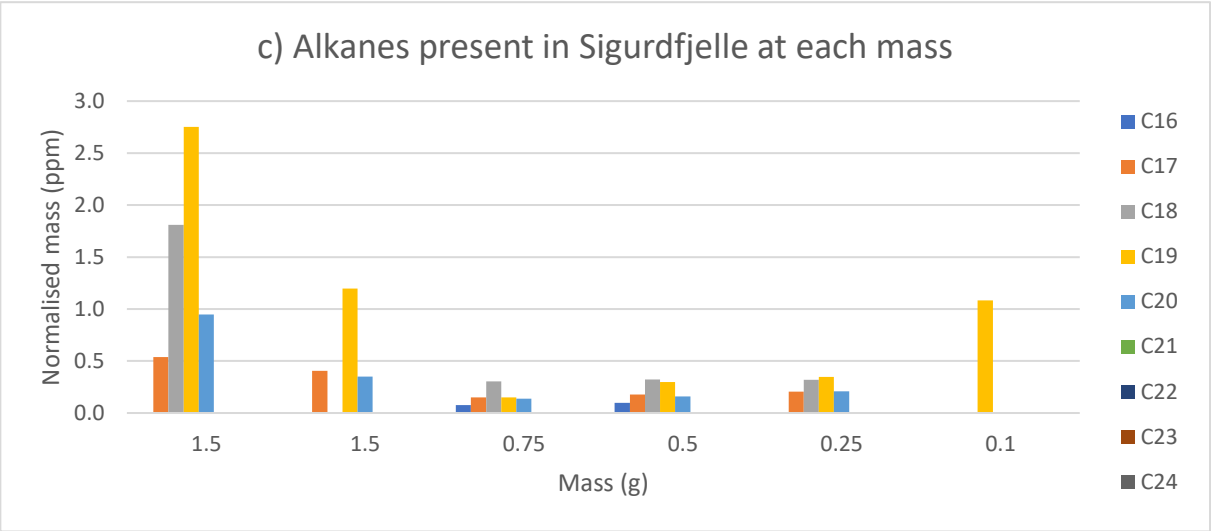

Sigurdfjelle – Alkane concentration (µg/g) at various sample masses									
Alkane	**C16**	**C17**	**C18**	**C19**	**C20**	**C21**	**C22**	**C23**	**C24**
1.5g		0.537	1.810	2.752	0.949				
1.5g		0.405		1.198	0.351				
0.75g	0.077	0.151	0.305	0.149	0.138				
0.5g	0.097	0.178	0.324	0.297	0.158				
0.2g		0.206	0.320	0.346	0.208				
0.1g				1.082					

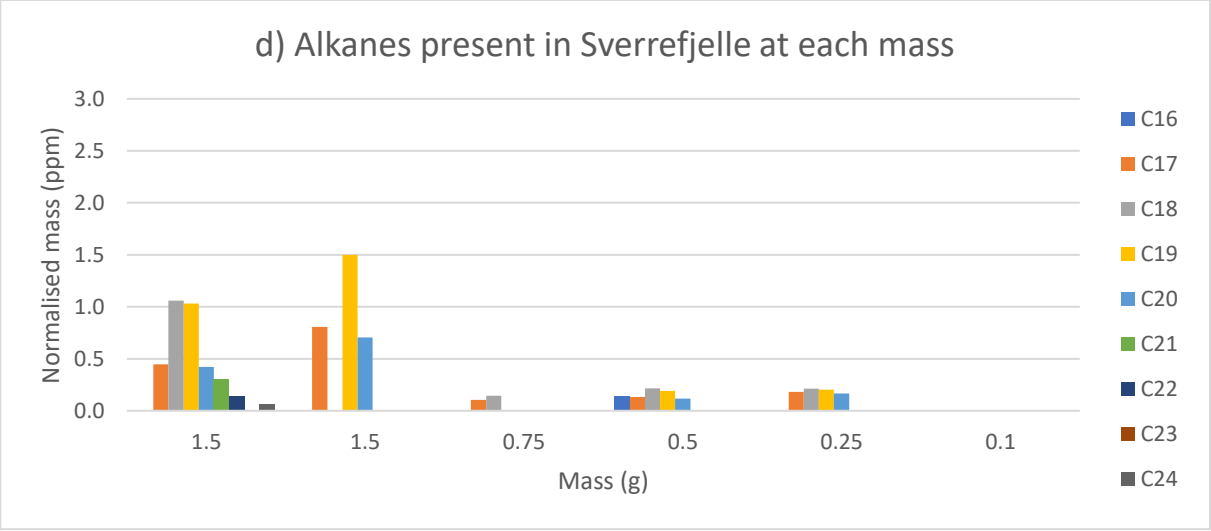

Sverrefjelle – Alkane concentration (µg/g) at various sample masses									
Alkane	**C16**	**C17**	**C18**	**C19**	**C20**	**C21**	**C22**	**C23**	**C24**
1.5g		0.445	1.058	1.032	0.421	0.302	0.137		0.061
1.5g		0.808		1.501	0.704				
0.75g		0.106	0.145						
0.5g	0.135	0.132	0.217	0.190	0.118				
0.2g		0.182	0.212	0.204	0.166				
0.1g									

Figure 30 –Summary graphs showing the normalised mass of alkanes present (µg/g or ppm) in each of the samples at different masses a) procedural blank, b) JSC c) Sigurdfjelle d) Sverrefjelle

4. Discussion

4.1 Summary of experiments

A series of experiments using Martian analogue materials aimed to optimise the GC-MS analytical protocol for the identification of Martian meteorite organics.

Table 24 - Aims and the outcomes of the laboratory experiments conducted for this project

Experiment	Aim	Outcome
1	Optimising sample preparation and solvent extraction	Ball mill crushing is the most efficient method of crushing basaltic samples. DCM-M (9:1) is a suitable solvent for organic extractions
2	Reducing sample loss during crushing	Brushes do not help reduce sample loss and may add an element of contamination
3	Determining GC-MS detection limits with decreasing sample mass	Organic compounds, including alkanes could be detected down to low masses (0.25g) despite a comparatively minor yield
4	Fractionating low-mass samples to improve detection sensitivity	0.1g of sample ran under previous method and detected alkanes in JSC and Sigi. Column chromatography results were uncertain for N1 and N2. N3 revealed a fatty alcohol in JSC
5	Verifying previous experiment results	Contamination of this experiment therefore disregarded

4.1.1 Results of methods

Comparing the data for the different methods used, there were very little variations between the solvent systems used. Notably, the ppm of the compounds within the samples which were crushing in the agate mortar and pestle is generally higher than that of the samples crushed by ball mill. This is also true when comparing method 3 and 4 which in turn would suggest that this is a result of the crushing method.

Alkanes were detected in Martian analogue material even at low sample masses 0.75g;0.5g;0.25g;0.1g. This detection has important implications for Mars Sample Return missions and for future meteorite analysis due to the low volume of material available for research and also the extraction of organics from basaltic rocks.

Overall, reducing the sample mass negatively correlates with the detection of alkanes, but with some exceptions. The average alkane normalised mass for Experiment 1 (method 1) within 1.5g samples mass is ~0.5ppm compared to Experiment 3 where the average is ~0.1ppm across sample masses 0.75 to 0.25g. However, within 0.1g of sample the average alkane detection was ~2ppm. This is an interesting discovery for analysing finite material; however, this was limited to only alkanes C18 and C19 within JSC and Sigurdfjelle and is not representative of a full sample suite.

From the graphs outlining the alkanes present for each sample at each mass, the concentration of the alkanes drops substantially, however, it also a positive result for these aliphatic compounds at low sample masses. The lack of consistency of the detection results, (i.e a detection of organic compounds in 1.5g and 0.5g but not 0.75g) especially within the BVC samples, could be due to the inhomogeneity of these Martian analogue samples, grain size variations, or contamination.

Other compounds that were detected throughout the experiments were dominantly contamination resulting from plasticisers. The detection and tracing of contamination has been an important learning outcome of this research. It emphasises the importance of appropriate sample storage and curation.

4.1.2 SEM

Carbonate globules were identified by the concentric rings similar to those found in ALH 84001 by Treiman et al., 2002. The globules present were surrounded by phyllosilicate and near grain boundaries which suggest a secondary formation such as hydrothermal alteration which is in agreement with Treiman, et al., 2002. The rings were concentrically and mineralogically zoned with the inner part of the globule dominantly magnesium carbonate and towards the outer was iron magnesium carbonate (Figure 30).

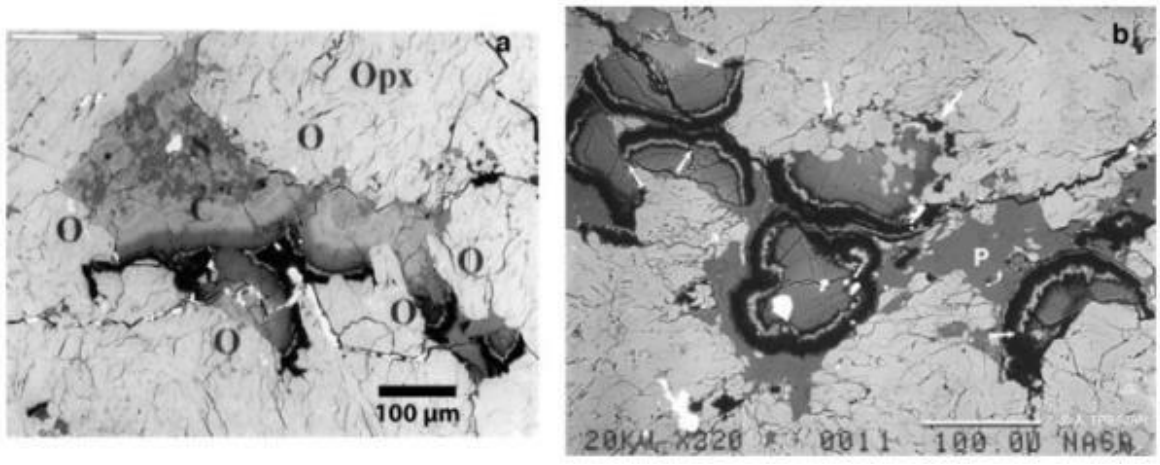

Figure 31- BSE images of the ALH 84001 carbonates from Treiman et al., 2021. A) Hemispherical carbonate surrounded by orthopyroxene and olivine. Concentric zoning amongst these globules and magnesite (black) outside and inside of globules. B) From Treiman 1995; Hemispherical carbonate globules appear broken within a plagioclase-glass surrounded by orthopyroxene. Carbonate rich core in upper left globule.

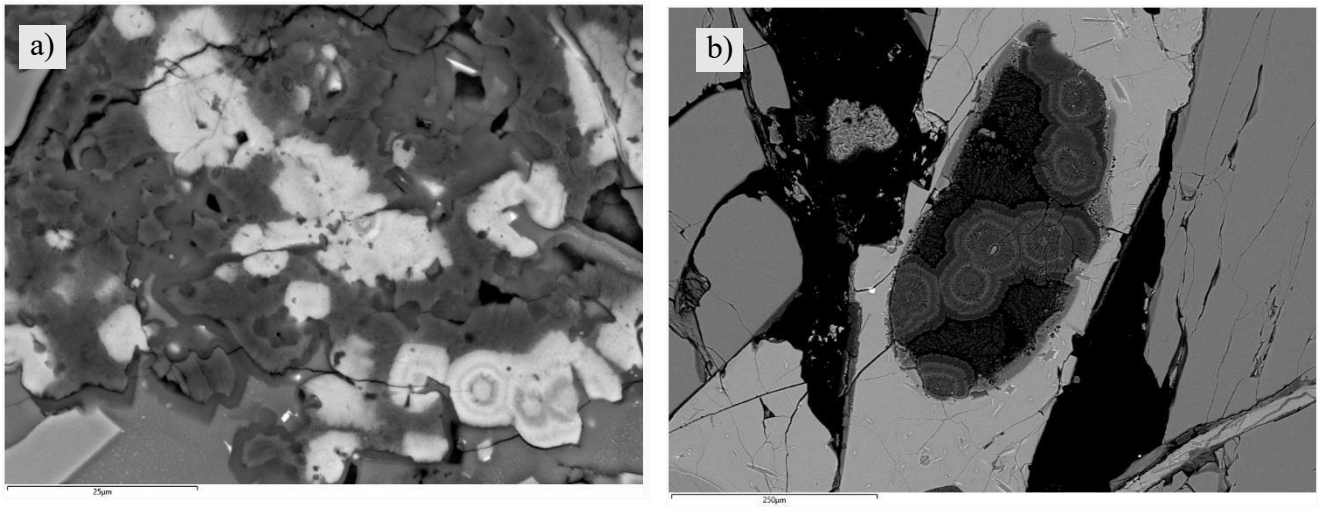

Figure 32- BSE images of a) Sverrefjelle and b) Sigurdfjelle. a) Displays evidence of dissolution of previous carbonate globules. b) shows intact carbonate globule within phyllosilicate

The SEM images of Sverrefjelle from the outset appeared relatively dull mineralogically and lacking in terms of carbonate rosettes. It appeared that in some areas as though dissolution had occurred where carbonate globules may have previously been. The shape of the group of concentric rings could be traced supporting this theory. As observed in Sigurdfjelle, there are areas which contain more carbonate globules (usually in association with specific mineral assemblages) than other areas. The carbonates in the BVC samples are believed to have formed as a result of hydrothermal activity associated with volcanism which by proxy can be inferred for the ALH 84001 carbonates (Treiman et al., 2002). The inhomogeneity of carbonates within the BVC basalts is also supported by the findings of Treiman et al., 2002.

4.1.3 Crushing technique

Mortar and pestle vs ball mill

When looking comparatively at the results (Table 11, Figure 20), the sample loss was higher using the mortar and pestle than when using the ball mill. The percentage loss of the mortar and pestle was at least 4 times higher for every sample apart from JSC. JSC was the only sample that had less sample loss using the mortar and pestle method than the ball mill method, but this is probably due to the nature of the sample being a fine-grained tephritic rock which was easily crushed in the mortar and pestle.

- Ball mill was more efficient in terms of time and sample loss.

  Time: Several hours were spent crushing samples Sigi and Sverre via mortar and pestle due to the hardness of the basaltic material and care taken to not lose any grains during the crushing process. The ball mill could be adjusted to shake the sample for a certain amount of time, the extraction process from the cell to vial was less time consuming than the mortar and pestle technique.

  Sample loss: Using the ball mill mitigates human error to a certain extent as it is a more contained procedure, however there may have been minute loss when weighing the material before transfer to the final vial storage. Sample loss from the mortar took place during crushing due to projectile fall out. Ball mill was overall the more effective method for the requirements of this project as time and frequency adjustments can be made for different materials.

- Using brushes to extract the fine material proved to increase sample loss (Table 25) and introduce contamination: Mobilisation of such fine grains by the nylon brushes resulted in sample being lost to the environment and also to the bristles of the brush. The difference was most noticeable in the finer grained sample of the procedural blank and JSC. Introduction of the brushes could have been partly responsible for the various benzene detections for this experiment as benzene is used in the manufacturing of nylon and synthetic fibres (ATSDR (2010))

Table 25 - Percentage loss of sample between Experiment 1 (without brushes) and Experiment 2 (with brushes)

Sample	Without brushes (% Loss)	With brushes (% Loss)	% Difference
Sand	0.857	1.2956	51.1785 increase
JSC	1.90	3.835	101.842 increase
Sigi	2.706	2.424	10.4% decrease
Sverre	1.889	2.778	47.0619 increase

Mortar and pestle and ball mill crushing are both common techniques for pulverising extra-terrestrial material (Sephton et al., 2004; Eigenbrode et al., 2018; Simkus et al., 2019 King et al., 2022; O'Brien, 2022; Peters et al., 2023), the significantly higher sample loss from the mortar and pestle method led to the ball mill being the preferential choice for this project.

4.1.4 Solvent Extraction

During sample preparation for the ASE, the vials of the samples were unloaded into the ASE cell by method of tapping the glass vial to enable a flow of sample out of the vial and into the funnel and subsequently the ASE cell. The technique of sample movement could have led to a discrepancy within the grain size where the larger grains come out first and therefore creating a bias in the distribution (Figure 34). Coarser material would be less effective than finer material during solvent extraction due to surface area variability (Figure 33).

For experiment 1 and 2, samples were crushed specifically for the respective experiment. The samples crushed for experiment 3 were used for experiments 3, 4 and 5. This could be reason as to why n-alkanes C18 and C19 were detected at such low sample masses (0.1g) in experiment 4. This theory proves the need for grain size analysis prior to solvent extraction to ensure a homogenous sample batch. Samples should also be crushed for each experiment however for the needs of this project, this method seemed suitable since the optimised crushing method, in terms of efficiency and sample loss, had already been established.

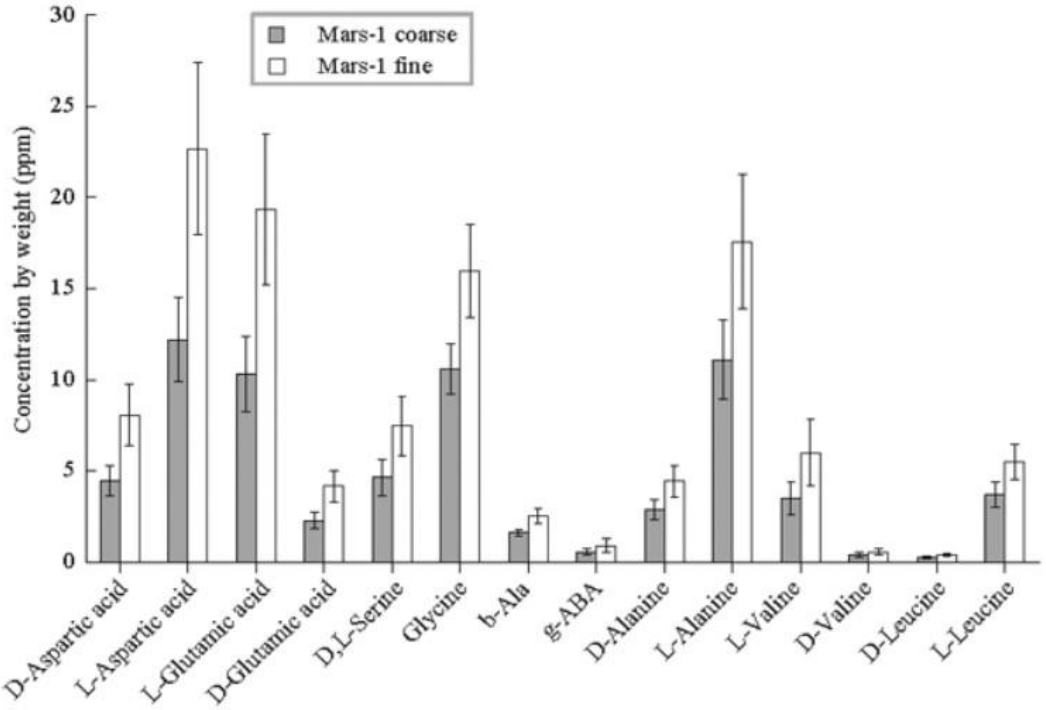

Figure 33 - Graph from Garry et al., 2006 highlighting the difference in the concentration of amino acids detected between coarse and fine samples of JSC-1

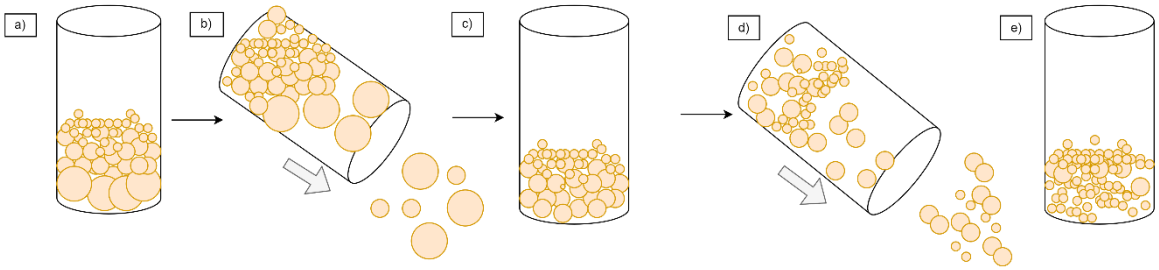

Figure 34 Sketch indicating the sample distribution which may lead to grain size discrepancies within the same batch. a) Sample after crushing stored in glass vial, not as homogenous a mix as expected. b) Pouring of the sample by carefully tapping the sides in order to stimulate controlled granular flow. c) The sample batch has smaller grains as a result of the larger ones exiting first. d) Pouring out more sample leads to an increase in small grains in the sample batch e) A more homogenous and finer grained sample as a result of granular segregation

The ASE is a good method for solvent extraction and worked well for the requirements of this project. Total Lipid Extract was successfully extracted from the samples despite being very minimal quantities - the low organic content was expected for this basaltic material and any detection, however minor, can be viewed a positive result. Considerations for the ASE used however could include the re-use of plastic caps which could be a source of phthalates within the sample.

Using the ASE to extract TLE for GC-MS analysis is the preferred method for solvent extraction and organic analysis. Column chromatography was a multi-step process that led

to contamination of the sample batch therefore this technique would not be recommended for future solvent extractions.

DCM-M vs Hex-Ace

DCM-M is a polar aprotic solvent which can dissolve polar and non-polar compounds. Relatively nonpolar organics are usually extracted using DCM (Simkus et al., 2019). The decision to use DCM-M over Hexane-Acetone comes as a result of numerous studies using the former solvent (Jenniskens et al., 2012; Simkus et al., 2019; Pizzarello et al., 2013). In addition, a wider range of organic material can be dissolved using DCM-M, as shown by the TLE results and as the focus was to extract as wide a range and as much organic material as possible, this solvent met the needs of this project.

4.1.5 GC-MS

For Experiment 1, 16 samples and 1 sample blank were run for TLE on the GC-MS, the 16 samples are made up of the 4 samples experiencing 4 different methods (Table 4). All 4 samples were run for TLE on the GC-MS at 50µL. The same compounds could be detected in the samples from all 4 methods. Any detection of a compound in the sample blank or procedural blank was treated as a contaminant. Table 26 outlines the compounds present in the sample blank and thus the contamination present.

Table 26 - Compounds within the sample blank which were also discovered in the samples (thus deemed contamination)

Experiment 1: Sample Blank	
Compound	R.T
1,2-Benzenedicarboxylic acid, bis(2-methylpropyl) ester	24.678
Diphenyl sulfone	25.57
Dibutyl phthalate	26.498
1,3-Benzenedicarboxylic acid, bis(2-ethylhexyl) ester	39.999

Table 27 - Compounds within Experiment 1 samples (not including alkanes)

Experiment 1 Compounds			
Compound	**Synonym**	**R.T**	**Formula**
2,2,4-Trimethyl-1,3-pentanediol diisobutyrate	TXIB ester	19.53	C16H30O4
Phenylmethanediol dibutanoate	n/a	28.4	C15H20O4
Hexanedioic acid, bis(2-ethylhexyl) ester	DOA ester	34.57	C22H42O4
1,4-Benzenedicarboxylic acid, bis(2-ethylhexyl) ester	Kodaflex dotp or WZ0883500	40.006	C24H38O4
Tris(2,4-di-tert-butylphenyl)phosphate	D16-834 Phosphate	56.548	C42H63O4P

GC-MS is an important and widely applied technique for the identification of organic compounds in extraterrestrial materials, including Martian meteorites and their respective analogues. Its ability to separate, identify and quantify complex mixtures of volatile and semi volatile organics has made it central to laboratory analysis and space missions such as Viking, Phoenix and Mars Science Laboratory (Curiosity) (Biemann et al., 1977; Ming et al., 2014; Freissinet et al., 2015). GC-MS has previously been used in the study of Martian meteorites ALH 84001, Tissint and NWA 7034, revealing diverse organic phases from PAHs to low molecular weight aliphatic hydrocarbons (Sephton, 2002; Steele et al., 2018; Schmitt-Kopplin et al., 2023).

The detection of alkanes within such samples is noteworthy; whilst these compounds can arrive from terrestrial contamination, their occurrence may also reflect abiotic synthesis pathways such as Fischer-Tropsch-type reactions or serpentinization-driven CO_2 reduction (McCollom & Seewald, 2007; Steele et al., 2022). Therefore, identifying alkanes in our samples is a significant finding as it demonstrates the analytical sensitivity of the GC-MS protocol. Refining protocols to aid in distinguishing indigenous hydrocarbons from terrestrial inputs enhances the interpretive robustness of GC-MS analyses for future Mars Sample Return investigations.

4.2 Organic content in BVC rocks

The BVC rocks from Spitsbergen, Svalbard discovered by the AMASE mission are carbonate-bearing mafic igneous rocks which host organic material associated with the mineral structure that was extracted using an optimised method of organic extraction through GC-MS. Long chain alkanes C10-C12 have been detected on the Martian near-surface at Gale Crater within the Cumberland drilled mudstone by the SAM suite onboard

Curiosity (Freissinet et al., 2025). These alkanes have been speculated to have originated from the saturation of long chain carboxylic acids and expands the suite of organics detected on Mars from aliphatic into aromatic (Freissinet et al., 2025). The detection of these organics on Mars shows that organics can be preserved in ancient sediments despite the highly oxidising environment and intense radiation (Freissinet et al., 2025) The detection of aliphatic hydrocarbons within our basaltic Martian analogue rocks is therefore an important steppingstone for future analysis of Martian rock samples.

Our SEM images show that the BVC samples used for this study contain carbonate globules similar to those found in ALH 84001 (Treiman et al., 2002; Steele et al., 2007). The rocks share further similarities (Table 2). The BVC carbonates are a proxy for the ALH 84001 carbonates (Treiman et al., 2002; Steele et al., 2007; Steele et al., 2022) and so identifying and subsequently extracting the organic matter from the Svalbard samples is important for deducing water-rock interactions during Early Mars.

Due to the similarity of the BVC carbonates and those within ALH 84001, we can infer a similar geological history alluding to a warmer and wetter Mars during the Noachian period ~3.9Ma when these carbonates precipitated. Although this may have been a local event, it cannot be ruled out that widespread aqueous, possibly hydrothermal, activity in occurred in Mars' early history (Halevy et al., 2011). A greater understanding of the organic matter associated with the carbonate globules in these rocks is vital for future analysis on abiotic organic matter in basaltic material from Mars.

4.2.1 Serpentinization for abiotic organic synthesis explored through an analogue

Serpentinization is an abiotic organic synthesis which involves olivine and orthopyroxene rich-rocks (ultramafic) reacting with aqueous fluid resulting in serpentinite, magnetite and hydrogen (Steele et al., 2022) creating a reducing chemical environment (Proskurowski et al., 2008). This hydrogen aids in creating a reducing chemical environment by reducing aqueous CO_2 to methane, CO and other organics including formic acid. CO and H can react via Fischer Tropsch reactions to produce alkanes and organics that include nitrogen (Steele et al., 2022).

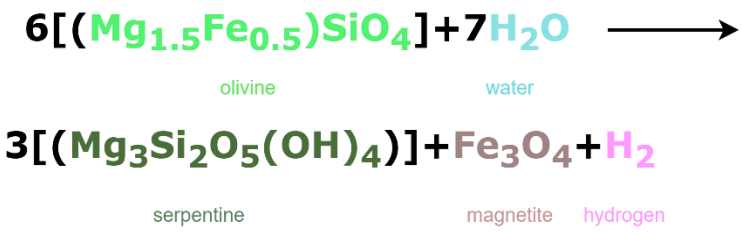

Figure 35- General reaction for serpentinization adapted from (Proskurowski et al., 2008)

There is evidence of this process occurring within ALH 84001, where magnetite can be found co-existing with a talc-like phase which would suggest that the serpentinization on Mars is responsible for the formation of the observed organics. However, this is not the case for all the magnetite within this meteorite. It can also be found in areas containing only amorphous silica, organic carbon and carbonate suggesting that Martian carbonation reactions are also a route for organic formation (Steele et al., 2022). The aqueous alteration of orthopyroxene produces carbonate globules, amorphous silicates, talc-like phases - this mineral assemblage is indicative of serpentinisation and mineral carbonation reactions on Early Mars which in turn would have influenced the Early Martian atmosphere and hydrosphere as it presents a source of atmospheric H_2 and a sink for liquid water (Schulte et al., 2006; Proskurowski et al., 2008; Steele et al., 2022; Tosca et al., 2025)

Fischer-Tropsch-type (FTT) synthesis is term to describe Fischer-Tropsch reactions but in relation to geologic processes, often underground, as the conditions during these processes are quite unique in terms of pressure, temperature, and carbon sources (Zhao et al., 2022). This reaction has important implications for how life on earth originated and also extra-terrestrially reduced carbon as it involves reducing inorganic source of carbon to form organic compounds regardless of the origin of the carbon, catalysts or the reductant (Zhao et al., 2022). Abiogenic long-chained hydrocarbons (up to n-C33) were detected by simulating FTT synthesis in ultradeep basin environments under hydrothermal conditions (Zhao et al., 2022). These findings are vital in looking for organics in current and future Martian missions as we continue to dig beneath the surface in search of organic material.

As well as the BVC rocks, there are other terrestrial analogues that can aid our understanding of sub-surface hydrothermal environments on Mars. The Lost City Hydrothermal Field (a.k.a Lost City) is located between the Mid-Atlantic Ridge and the Atlantis Transform fault within the Atlantic Ocean on the Atlantis Massif characterised by

ultramafic core complex hosting marine alkaline hydrothermal vents (Schulte et al., 2006). Lost City is an outstanding analogue for abiotic sources of organic carbon; carbon and hydrogen isotope data from this field indicate that methane found in the hydrothermal vents has an abiogenic origin. A high concentration of hydrogen is generated through serpentinization which drives the thermodynamic process for reducing CO^2 (Schulte et al., 2006; Russell et al., 2010). Therefore, methane, as well as higher chain hydrocarbons, could be formed abiotically in ultramafic hydrothermal systems via FFT processes (Summons et al., 2011). These findings which show that hydrocarbons may form abiotically in nature in the presence of ultramafic rocks, water and heat have important implications for abiotic organic synthesis on Mars (Schulte et al., 2006). Abiogenic hydrocarbon production is therefore a pathway for the alkane production in the BVC rocks which corresponds to the organic material found in the ALH 84001 ancient Martian meteorite. This analogue is discussed further in Appendix (Section A.1).

4.3 Mars Sample Return (MSR) and Analogues

Studying Martian analogues is crucial ahead of the Mars Sample Return mission. Analogues are a plentiful resource which hold a plethora of information which can help illuminate Mars' history. The search for organics within basaltic rocks with low organic content has been limited despite this being the dominant geology of Mars (as we know it). Using Earth-based proxies to explore abiotic organics within basaltic rock is an important step into understanding the formation, composition, and extraction of organic material (Beaty et al., 2019; Grady, 2020)

Martian meteorites are mainly igneous rocks which give insight into Mars' subsurface, therefore the presence of carbon based molecules within these rocks provides important perspective into the history of the red planet and in particular the environmental changes throughout the planets geological history (Mahaffy et al., 2007) Analysing analogues therefore provides further insight and context into an Mars' early history as it implies association with subglacial eruptions and hydrothermal alteration. As ALH 84001 has recorded some pf Mars' complex geologic history, it is beneficial to use analogues such as the BVC samples to help deduce a small part of the story to aid wider understanding. The sample collection rover for MSR will be fitted with a drill which will produce small cores (Grady, 2020), diving deeper into the Martian surface to unveil further information about Mars' geological and climatic history into a time where the planet was warmer, wetter and

potentially more habitable (Treiman, 2021; Farley et al., 2022; Hickman-Lewis et al., 2022).

The Martian analogue samples, Sigurdfjelle and Sverrefjelle, collected from the Bockfjorden Volcanic Complex in Svalbard, Norway were subject to SEM analysis in this project to ensure their suitability as Martian analogues. The data showed that our samples hosted carbonate globules akin both compositionally and texturally to those found in the ALH 84001 meteorite as previously discovered for BVC rocks by Steele et al., (2007) and Treiman (2003). Comparison of our SEM images from the BVC rocks and the SEM image of the ALH 84001 reveal striking similarities of the carbonate globules and show that there are the same mineral phases in association with the globules implying a similar origin of hydrothermal fluids (Steele et al., 2022).

The results from this study show that SOM could be extracted and analysed from our Martian analogues (BVC and JSC) using GC-MS. Investigating and extracting organic material from igneous rocks is important for Mars' sample return as the material being cached to be returned by this mission is dominantly igneous (Udry et al., 2020).

4.4 Contamination

Having multiple blanks (sample blanks and procedural blanks) was helpful in tracing the contamination throughout this project. Many of the compounds detected were synthetic and could have arisen from laboratory-based contamination. Tunney et al., 2020;2023 uses GC-MS to explore laboratory materials for contaminants and found a range of organics within nitrile gloves, aluminium foil and plastic boxes used for curation (Tunney et al., 2020, Tunney et al., 2023). 13-Docosenamide (Z), detected within the Sigurdfjelle sample, is used in many industrial settings including as a slip additive in the manufacturing of plastic and has recently been found associated with plastic zip lock bags (Tunney et al., 2020; Tunney et al., 2023) emphasising the importance of appropriate sample storage and curation**.** Table 27 outlines some of the organic compounds detected in the samples from experiment 1; TXIB ester is used mainly in the production of nylon and was therefore most likely a contaminant from poor curation practices. This can be supported by the detection of Kodaflex DOTP which is a primary plasticizer used in PVC plastics and cable materials.

Other compounds detected in the samples studied include Dodecanoic acid, 1-methylethyl ester which is a metabolite found in human saliva (de Lacy Costello et al., 2014) as well as Octanal, 2-(phenylmethylene) which can be found in the cosmetics industry as perfume and fragrances and also in the cleaning industry in products such as disinfectants and pest control items (ECHA, 2023). The detection of these types of compounds within our samples highlights the importance of always wearing appropriate PPE when handling extra-terrestrial materials to avoid terrestrial contamination.

The large number of benzenes attached to alkyl groups that were observed in Experiment 2 was a surprising observation and was quite clearly some variety of contamination as it was detected throughout the procedural and sample blanks. Further investigation into these structures revealed a possible origin of nitrile gloves; Tunney et al., 2020 performed swabs of nitrile gloves with DCM and ran them on the GC-MS to reveal an array of structures identical to those found in our experiment (Table 28). As the benzene-alkyls could be detected in the sample blank (introduced at the ASE cell preparation stage), the contamination could be attributed to the contact of the sample with the nitrile gloves used for PPE during sample preparation stages of the experiment. There may have also been some contribution from the introduction of the nylon brushes during the sample crushing stage. Phthalates can be traced throughout the project through the samples and the blanks. Phthalates are chemical compounds used to improve the durability of plastics. These compounds can leach from plastics over time. JSC, Sigurdfjelle and Sverrefjelle samples were all stored in plastic bags for years and so the phthalate contamination may be due to poor sample curation techniques raising a wider query as to how we transfer, store and curate MSR samples on their return to Earth.

The results of this project therefore highlight that contamination can be better tracked and traced throughout experiments by using procedural and sample blanks aiding in the mitigation of contamination and appropriate curation and storage methods for future work.

Table 28 -Organic compounds found in nitrile gloves during the Tunney et al. (2020) study that were also detected in Experiment 2 of this project

Compounds detected in nitrile gloves (Tunney et al., 2020) and present in Experiment 2 of this project
Benzene, (1-butylheptyl)-
Benzene, (1-propyloctyl)-
Benzene, (1-ethylnonyl)-
Benzene, (1-methyldecyl)-
Benzene, (1-pentylheptyl)-
Benzene, (1-butyloctyl)-
Benzene, (1-propylnonyl)-
Benzene, (1-ethyldecyl)-
Benzene, (1-methylundecyl)-
Benzene, (1-pentyloctyl)-
Benzene, (1-butylnonyl)-
Benzene, (1-propyldecyl)-
Benzene, (1-ethylundecyl)-
Benzene, (1-methyldodecyl)-
1,2-Benzenedicarboxylic acid, butyl octyl ester
1,3-Benzenedicarboxylic acid, bis(2-ethylhexyl) ester

4.5 Optimised method

Table 29 - Optimised method for GC-MS analytical protocol based on the findings of this project

Samples	BVC analogues with procedural blanks of combusted sand. Sample blanks at start and end of ASE cycle.
Crushing method	Stainless steel ball mill followed by extraction from the ball mill holders using a combination of stainless-steel equipment (tweezers and spatula). 1.5g of each sample. Sample and procedural blanks throughout.
Solvent Extraction	ASE 350 using DCM-M (9:1) as the solvent for extraction. Run samples for TLE at 50 μL.
Analysis	GC-MS analysis with 2 libraries for compound identification.

The optimised method set out by this project calls for a sample mass of 1.5g to extract a full suite of organic material from our samples. This sample mass is too large to be expected for research. Around 0.2g is an average amount that is given for research/processing (Hallis, in conversation) due to the limited, precious nature of the sample and therefore this method is not feasible. Continuation to optimise this method to reduce the sample mass required is important work ahead of the return due to the limited/finite quantities returned to Earth for further analysis (Grady, 2020). Understanding the optimum protocol for extracting organic from basaltic material on earth-based labs is of upmost importance prior to sample return and using Martian analogue material which is a plentiful resource is a useful aid to practice on and learn from.

5. Conclusions

The chapter will outline the main findings from this project and the future work that could be considered. The conclusions are separated into the following:

5.1.1 – Optimisation of sample preparation and crushing methods

5.1.2 – Textural and mineralogical observations

5.1.3 – Determination of optimal sample method

5.1.4 – Contamination tracing and mitigation

5.1.1 Optimisation of sample preparation and crushing methods

Our bulk rock crushing experiments demonstrated that ball milling is the most effective and efficient technique for producing a homogenous fine powder suitable for organic extraction. Compared to mortar and pestle, ball milling the samples generally generated a more consistent particle size, enhanced solvent-rock interaction and minimised sample loss leading to the conclusion that the most efficient method for crushing samples of this nature is by ball mill. This provides a key step towards improving reproducibility in the analysis of low carbon igneous planetary materials.

5.1.2 Textural and mineralogical observations

Scanning Electron Microscopy (SEM) analyses of the Bockfjorden Volcanic Complex (BVC) analogues, Sigurdfjelle and Sverrefjelle, revealed carbonate globules that bear a close textural and mineralogical resemblance to those in the Martian meteorite AL84001. The occurrence of concentric carbonate layers and microcrystalline textures imply secondary mineralisation under conditions consistent with *low temperature* aqueous alteration (Treiman, 2002). The similarities strengthen the analogical relevance of BVC basalts as terrestrial proxies for Martian material.

5.1.3 Optimal sample mass and method efficiency

Our GC-MS analytical protocol successfully identified solvent-soluble organic compounds in the Martian analogue samples. Experimental results showed that a basaltic sample mass of 1.5g produced optimal organic detection under BECS laboratory conditions. However, this is an unrealistically large mass to expect from finite Martian material as the distribution of meteoric material for scientific analysis is typically ~0.2g (Hallis, (in

discussion)). The findings therefore suggest that the established GC-MS protocol within the BECS facility is not optimal for the analysis of low-organic content in igneous rocks such as the BVC samples and Martian meteorites. The results highlight the challenges of detecting organics in low-carbon igneous materials and underscore the need for improved analytical sensitivity and protocols compatible with low sample masses. Various crushing and solvent extraction techniques were trialled. The optimised method for solvent extractions utilises the ASE to extract TLE for GC-MS analysis. The findings of this project thus contribute to the ongoing refinement of planetary organic geochemistry techniques and have direct implications for the analysis of materials returned by future Mars Sample Return missions.

5.1.4 Contamination and sample curation practices

The results from the GC-MS data show that phthalates and other plasticisers could be seen throughout the project and traced effectively through the use of sample and procedural blanks. Tunney et al., 2020 ran GC-MS analysis on DCM swabs of nitrile gloves to find a range of plasticisers which were also detected in this project (Table). This finding has important implications for future laboratory analyses of MSR material – the returned samples are expected to have experienced little to no contamination and so using appropriate PPE is extremely important as to not introduce avoidable terrestrial contamination. The results from Tunney et al., 2023 also demonstrate plasticisers leaching from zip-lock bags, a compound also detected in this study from the samples which have been stored in plastic bags which again emphasises the need for appropriate curation practices for extra-terrestrial material.

5.2 Future work

Based on the results, to develop this research, there are areas that I would expand upon and various techniques to test in order to continue in the optimisation of the protocol. There are also other methods that could be trailed for comparison and a number of analogues to sample.

5.2.1 Evaluation of other crushing methods

Planetary bill mills could be used to crush the samples to ensure they are pulverised down to the nanoscale. Grain size analysis prior to solvent extraction would confirm the homogeneity of the sample prior to solvent extraction on the ASE allowing for maximum

efficiency. Triplicate analysis during solvent extraction and GC-MS would allow for more accurate and reproducible results with more definitive errors. GC-IRMS on the carbonates within the basalt samples could aid in gaining a better understanding of their origin.

5.2.1 Grain size analysis

Grain size analysis post crushing and prior to solvent extraction would provide a greater insight into the sample and would benefit solvent extraction. A smaller grain size is preferable for solvent extraction as it would increase the efficiency of the extraction (ThermoFischer Scientific, 2013). Smaller grains also have an increased surface area in comparison to larger grains and thus increases the amount of solvent coming into contact with the sample in order to extract the maximum amount of organic matter from the sample batch.

Grain size analysis would also confirm the homogeneity of the sample. A smaller particle size can lead to a more homogenous mix and is therefore more representative of the entire solid sample during solvent extraction. Knowing more about the grain size prior to solvent extraction would also be beneficial for the reproducibility of the project.

There are several techniques that exist for grain size analysis including dry sieving, laser diffraction, optical image analysis and X-Ray Computed Tomography (XCT).

Optical imaging is a suitable approach for grain size analysis of crushed sample prior to total lipid extract (TLE) preparation and GC-MS analysis. This technique is entirely non-destructive, allowing grain size, shape, and textural information to be characterised without altering or contaminating the sample which is of upmost importance when working with low-mass, organic-sensitive material such as Martian rocks. Optical imaging also requires no dispersants, sonication or heating steps that could mobilise or degrade soluble organics, unlike techniques such as laser diffraction (Sephton & Botta, 2008). Image analysis software such as ImageJ, can quantify particle dimensions, aspect ratios and grain size distributions providing statistically robust data from small sample qualities.

X-Ray Computed tomography (XCT) is another non-destructive method for grain size analysis that uses X-ray transmission through a sample to produce a 3D computed tomographic image. XCT can be conducted on a loose powder or a solid sample and is useful in investigating the size and geometry of intraparticle porosity. It can also produce

measurements of 3D particle size, shape, and orientation (Houghton et al., 2024). Houghton et al., 2024 trialled four laboratory-based characterisation methods of particle size distribution (Laser particle size analysis, 2d automated image analysis, optical point counting and XCT) and concluded the most reliable method of measure particle size distribution with the smallest sorting values was XCT.

5.2.3 Pyrolysis

Pyrolysis is a sample preparation technique commonly carried out prior to GC-MS analysis. This process thermally decomposes the larger, high molecular weight molecules of a sample, the compounds then decompose into gases which can be readily analysed by GC-MS for structure information of the molecules or GC-IRMS for isotopic compositions of the specific molecules (Sephton, 2012). This separation procedure is especially valuable for macromolecular material within meteorites due to the wide array of isometric variations inherent to abiotic organics (Sephton, 2012). Many studies in the past have paired pyrolysis with GC-MS to investigate organics within meteoric material and with great success; Jaramillo et al., 2019 used this technique and found organic compound within Tissint that were similar to those previously found in Martian meteorites. By using pyrolysis paired with GC-MS, the SAM instrument suite was able to detect chlorinated compounds within material at the Martian surface despite the presence of oxychlorines which often destroy organic matter when exposed to thermal radiation (Freissinet et al., 2015).

5.2.4 GC-IRMS

GC-IRMS (gas chromatography- isotope ratio mass spectrometry) is a useful tool when analysing extra-terrestrial material as it aids in distinguishing between an indigenous compound and a terrestrial contaminant (Sephton et al., 2001). This method can provide the carbon isotope signature for specific compounds which would be indicative of the origin as Mars is enriched in D/H (Hallis, 2017). Thus, for future analyses on extraterrestrial materials, GC-IRMS would aid in defining organic material.

5.2.5 Context

Lack of exact context on our BVC samples in terms of collection site, storage etc. There is not a record of where the samples were taken from specifically, for example they may have

been from beach interacting with nearby water sources and there is also a long history of glaciation in the area which could have impacted our samples.

Another consideration regarding the context is curation; we are unable to determine how long our BVC samples were stored in the plastic bags that they were delivered to us. The contamination from plasticisers in our JSC and BVC samples could be attributed to the long-term effects of sample storage in plastic bags. The plastic contamination could also be from the plastic box they were stored in post-crushing or a separate laboratory contaminant. However, the detection of such compounds highlights the importance of suitable sample storage and curation from initial sample collection.

References

Alexiadis, A., Alberini, F., and Meyer, M.E., 2017, Geopolymers from lunar and Martian soil simulants: Advances in Space Research, v. 59, no. 1, p. 490–495, doi: 10.1016/j.asr.2016.10.003.

Allen, C.C., Jager, K.M., Morris, R.V., Lindstrom, D.J., Lindstrom, M.M., and Lockwood, J.P., 1998, JSC mars-1: A martian soil simulant: Space 98, doi: 10.1061/40339(206)54.

Amils, R., Fernández-Remolar, D., and the IPBSL Team, 2014, Río Tinto: A geochemical and mineralogical terrestrial analogue of Mars: Life, v. 4, no. 3, p. 511–534, doi: 10.3390/life4030511.

Amundsen, H.E.F., Griffin, W.L., and O'reilly, S.Y., 1987, The lower crust and upper mantle beneath Northwestern Spitsbergen: Evidence from xenoliths and geophysics: Tectonophysics, v. 139, no. 3–4, p. 169–185, doi: 10.1016/0040-1951(87)90095-3.

Anand, M., Russell, S.S., Blackhurst, R.L., and Grady, M.M., 2006, Searching for signatures of life on Mars: An fe-isotope perspective: Philosophical Transactions of the Royal Society B: Biological Sciences, v. 361, no. 1474, p. 1715–1720, doi: 10.1098/rstb.2006.1899.

Anders, E., 1996, Evaluating the evidence for past life on Mars: Science, v. 274, no. 5295, p. 2119–2121, doi: 10.1126/science.274.5295.2119-c.

Anderson, D.M., Biemann, K., Orgel, L.E., Oro, J., Owen, T., Shulman, G.P., Toulmin, P., and Urey, H.C., 1972, Mass spectrometric analysis of Organic Compounds, water and volatile constituents in the atmosphere and surface of Mars: The viking mars lander: Icarus, v. 16, no. 1, p. 111–138, doi: 10.1016/0019-1035(72)90140-6.

ATSDR (2021) Benzene, Centers for Disease Control and Prevention. Available at: https://wwwn.cdc.gov/TSP/substances/ToxSubstance.aspx?toxid=14 (Accessed: 28 June 2023).

Azua-Bustos, A., González-Silva, C., and Fairén, A.G., 2022, The Atacama Desert in northern Chile as an analog model of Mars: Frontiers in Astronomy and Space Sciences, v. 8, doi: 10.3389/fspas.2021.810426.

Bada, J.L., Glavin, D.P., McDonald, G.D., and Becker, L., 1998, A search for endogenous amino acids in martian meteorite ALH84001: Science, v. 279, no. 5349, p. 362–365, doi: 10.1126/science.279.5349.362.

Banks, D., Siewers, U., Sletten, R.S., Haldorsen, S., Dale, B., Heim, M., and Swensen, B., 1999, The thermal springs of Bockfjorden, Svalbard: II: Selected aspects of trace element hydrochemistry: Geothermics, v. 28, no. 6, p. 713–728, doi: 10.1016/s0375-6505(99)00019-x.

Baqué, M., Backhaus, T., Meeßen, J., Hanke, F., Böttger, U., Ramkissoon, N., Olsson-Francis, K., Baumgärtner, M., Billi, D., Cassaro, A., de la Torre Noetzel, R., Demets, R., Edwards, H., Ehrenfreund, P., et al., 2022, Biosignature stability in space enables their use for life detection on Mars: Science Advances, v. 8, no. 36, doi: 10.1126/sciadv.abn7412.

Barber, D.J., and Scott, E.R., 2002, Origin of supposedly biogenic magnetite in the martian meteorite Allan Hills 84001: Proceedings of the National Academy of Sciences, v. 99, no. 10, p. 6556–6561, doi: 10.1073/pnas.102045799.

Beard, B.L., Ludois, J.M., Lapen, T.J., and Johnson, C.M., 2013, Pre-4.0 billion year weathering on Mars constrained by Rb–SR geochronology on meteorite ALH84001: Earth and Planetary Science Letters, v. 361, p. 173–182, doi: 10.1016/j.epsl.2012.10.021.

Beaty, D.W., Grady, M.M., McSween, H.Y., Sefton-Nash, E., Carrier, B.L., Altieri, F., Amelin, Y., Ammannito, E., Anand, M., Benning, L.G., Bishop, J.L., Borg, L.E., Boucher, D., Brucato, J.R., et al., 2019, The potential science and engineering value of samples delivered to Earth by mars sample return: Meteoritics & Planetary Science, v. 54, no. S1, doi: 10.1111/maps.13242.

BECS Lab, 2013, Biomarkers for Environmental and Climate Science: University of Glasgow,.

Bell, J.F., Maki, J.N., Alwmark, S., Ehlmann, B.L., Fagents, S.A., Grotzinger, J.P., Gupta, S., Hayes, A., Herkenhoff, K.E., Horgan, B.H., Johnson, J.R., Kinch, K.B., Lemmon, M.T., Madsen, M.B., et al., 2022, Geological, multispectral, and meteorological imaging results from the Mars 2020 Perseverance Rover in jezero crater: Science Advances, v. 8, no. 47, doi: 10.1126/sciadv.abo4856.

Bibring, J.-P., Langevin, Y., Mustard, J.F., Poulet, F., Arvidson, R., Gendrin, A., Gondet, B., Mangold, N., Pinet, P., Forget, F., Berthé, M., Bibring, J.-P., Gendrin, A., Gomez, C., et al., 2006, Global Mineralogical and aqueous Mars history derived from Omega/Mars Express Data: Science, v. 312, no. 5772, p. 400–404, doi: 10.1126/science.1122659.

Biemann, K., 2007, On the ability of the Viking Gas Chromatograph–mass spectrometer to Detect Organic matter: Proceedings of the National Academy of Sciences, v. 104, no. 25, p. 10310–10313, doi: 10.1073/pnas.0703732104.

Bonin, B., 2012, Extra-terrestrial Igneous Granites and Related Rocks: A review of their occurrence and petrogenesis: Lithos, v. 153, p. 3–24, doi: 10.1016/j.lithos.2012.04.007.

Borg, L., and Drake, M.J., 2005, A review of meteorite evidence for the timing of magmatism and of surface or near-surface liquid water on Mars: Journal of Geophysical Research: Planets, v. 110, no. E12, doi: 10.1029/2005je002402.

Botta, O., and Bada, J.L., 2002, Extraterrestrial Organic Compounds in Meteorites: Surveys in Geophysics, v. 23, no. 5, p. 411–467, doi: 10.1023/a:1020139302770.

Bower, D.M., Yang, C.S.C., Hewagama, T., Nixon, C.A., Aslam, S., Whelley, P.L., Eigenbrode, J.L., Jin, F., Ruliffson, J., Kolasinski, J.R., and Samuels, A.C., 2021, Spectroscopic characterization of samples from different environments in a volcano-glacial region in Iceland: Implications for in situ planetary exploration: Spectrochimica Acta Part A: Molecular and Biomolecular Spectroscopy, v. 263, p. 120205, doi: 10.1016/j.saa.2021.120205.

Bridges, J.C., and Schwenzer, S.P., 2012a, The nakhlite hydrothermal brine on Mars: Earth and Planetary Science Letters, v. 359–360, p. 117–123, doi: 10.1016/j.epsl.2012.09.044.

Bridges, J.C., and Schwenzer, S.P., 2012b, The nakhlite hydrothermal brine on Mars: Earth and Planetary Science Letters, v. 359–360, p. 117–123, doi: 10.1016/j.epsl.2012.09.044.

Bridges, J.C., Hicks, L.J., and Treiman, A.H., 2019, Carbonates on Mars: Volatiles in the Martian Crust, p. 89–118, doi: 10.1016/b978-0-12-804191-8.00005-2.

Brown, A.J., Viviano, C.E., and Goudge, T.A., 2020, Olivine-carbonate mineralogy of the Jezero Crater Region: Journal of Geophysical Research: Planets, v. 125, no. 3, doi: 10.1029/2019je006011.

Cabane, M., Coll, P., Rodier, C., Israel, G., Raulin, F., Sternberg, R., Niemann, H., Mahaffy, P., Jambon, A., and Rannou, P., 2001a, In situ inorganic and Organic Analysis (PYR/CD-GC/MS) of the martian soil, on the Mars 2005 Mission: Planetary and Space Science, v. 49, no. 5, p. 523–531, doi: 10.1016/s0032-0633(00)00135-5.

Cabane, M., Coll, P., Rodier, C., Israel, G., Raulin, F., Sternberg, R., Niemann, H., Mahaffy, P., Jambon, A., and Rannou, P., 2001b, In situ inorganic and Organic Analysis (PYR/CD-GC/MS) of the martian soil, on the Mars 2005 Mission: Planetary and Space Science, v. 49, no. 5, p. 523–531, doi: 10.1016/s0032-0633(00)00135-5.

Callahan, M.P., Burton, A.S., Elsila, J.E., Baker, E.M., Smith, K.E., Glavin, D.P., and Dworkin, J.P., 2013, A search for amino acids and nucleobases in the martian meteorite Roberts Massif 04262 using liquid chromatography-mass spectrometry: Meteoritics & Planetary Science, v. 48, no. 5, p. 786–795, doi: 10.1111/maps.12103.

Carr, M.H., and Head, J.W., 2010, Geologic history of Mars: Earth and Planetary Science Letters, v. 294, no. 3–4, p. 185–203, doi: 10.1016/j.epsl.2009.06.042.

Chan, Q.H., Stroud, R., Martins, Z., and Yabuta, H., 2020, Concerns of organic contamination for sample return space missions: Space Science Reviews, v. 216, no. 4, doi: 10.1007/s11214-020-00678-7.

Chatzitheodoridis, E., Haigh, S., and Lyon, I., 2014, A conspicuous clay ovoid in Nakhla: Evidence for subsurface hydrothermal alteration on Mars with implications for astrobiology: Astrobiology, v. 14, no. 8, p. 651–693, doi: 10.1089/ast.2013.1069.

Chou, L., Mahaffy, P., Trainer, M., Eigenbrode, J., Arevalo, R., Brinckerhoff, W., Getty, S., Grefenstette, N., Da Poian, V., Fricke, G.M., Kempes, C.P., Marlow, J., Sherwood Lollar, B., Graham, H., et al., 2021, Planetary mass spectrometry for agnostic life detection in the solar system: Frontiers in Astronomy and Space Sciences, v. 8, doi: 10.3389/fspas.2021.755100.

Clark, J., Sutter, B., Archer, P.D., Ming, D., Rampe, E., McAdam, A., Navarro-González, R., Eigenbrode, J., Glavin, D., Zorzano, M.-P., Martin-Torres, J., Morris, R., Tu, V., Ralston, S.J., et al., 2021, A review of sample analysis at Mars-Evolved Gas Analysis Laboratory analog work supporting the presence of perchlorates and chlorates in Gale Crater, Mars: Minerals, v. 11, no. 5, p. 475, doi: 10.3390/min11050475.

Clemett, S.J., Dulay, M.T., Seb Gillette, J., Chillier, X.D., Mahajan, T.B., and Zare, R.N., 1998, Evidence for the extraterrestrial origin of polycyclic aromatic hydrocarbons in the martian meteorite ALH84001: Faraday Discussions, v. 109, p. 417–436, doi: 10.1039/a709130c.

Crawford, I., 2012, The scientific legacy of Apollo: Astronomy & Geophysics, v. 53, no. 6, doi: 10.1111/j.1468-4004.2012.53624.x.

De Gregorio, B.T., and Engrand, C., 2024, Diversity of complex organic matter in carbonaceous chondrites, idps, and ucamms: Elements, v. 20, no. 1, p. 24–30, doi: 10.2138/gselements.20.1.24.

D'Uston, C., 2011, MER, spirit and opportunity (Mars): Encyclopedia of Astrobiology, p. 1009–1014, doi: 10.1007/978-3-642-11274-4_1879.

ECHA (2023) Substance infocard; (E)-2-benzylideneoctanal, Substance information. Available at: https://echa.europa.eu/substance-information/-/substanceinfo/100.166.492 (Accessed: 16 May 2023)

Edwards, H., Vandenabeele, P., Jorge-Villar, S., Carter, E., Perez, F., and Hargreaves, M., 2007, The Rio Tinto Mars Analogue Site: An Extremophilic Raman Spectroscopic Study: Spectrochimica Acta Part A: Molecular and Biomolecular Spectroscopy, v. 68, no. 4, p. 1133–1137, doi: 10.1016/j.saa.2006.12.080.

Ehlmann, B.L., and Edwards, C.S., 2014, Mineralogy of the martian surface: Annual Review of Earth and Planetary Sciences, v. 42, no. 1, p. 291–315, doi: 10.1146/annurev-earth-060313-055024.

Ehlmann, B.L., Mustard, J.F., Murchie, S.L., Bibring, J.-P., Meunier, A., Fraeman, A.A., and Langevin, Y., 2011, Subsurface water and clay mineral formation during the early history of Mars: Nature, v. 479, no. 7371, p. 53–60, doi: 10.1038/nature10582.

Ehrenfreund, P., and Sephton, M.A., 2006, Carbon molecules in space: From astrochemistry to astrobiology: Faraday Discussions, v. 133, p. 277, doi: 10.1039/b517676j.

Eigenbrode, J., Benning, L.G., Maule, J., Wainwright, N., Steele, A., and Amundsen, H.E.F., 2009, A field-based cleaning protocol for sampling devices used in life-detection studies: Astrobiology, v. 9, no. 5, p. 455–465, doi: 10.1089/ast.2008.0275.

Eigenbrode, J.L., Summons, R.E., Steele, A., Freissinet, C., Millan, M., Navarro-González, R., Sutter, B., McAdam, A.C., Franz, H.B., Glavin, D.P., Archer, P.D., Mahaffy, P.R., Conrad, P.G., Hurowitz, J.A., et al., 2018, Organic matter preserved in 3-billion-year-old mudstones at Gale Crater, Mars: Science, v. 360, no. 6393, p. 1096–1101, doi: 10.1126/science.aas9185.

Elvevold, S., Blomeier, D., and Dallmann, W., 2007, Geology of Svalbard: Norsk polarinstitutt, Tromso, Norway.

Farley, K.A., Stack, K.M., Shuster, D.L., Horgan, B.H., Hurowitz, J.A., Tarnas, J.D., Simon, J.I., Sun, V.Z., Scheller, E.L., Moore, K.R., McLennan, S.M., Vasconcelos, P.M., Wiens, R.C., Treiman, A.H., et al., 2022, Aqueously altered igneous rocks sampled on the floor of Jezero crater, Mars: Science, v. 377, no. 6614, doi: 10.1126/science.abo2196.

Franz, H.B., Mahaffy, P.R., Webster, C.R., Flesch, G.J., Raaen, E., Freissinet, C., Atreya, S.K., House, C.H., McAdam, A.C., Knudson, C.A., Archer, P.D., Stern, J.C., Steele, A., Sutter, B., et al., 2020, Indigenous and exogenous organics and surface–atmosphere cycling inferred from carbon and oxygen isotopes at Gale Crater: Nature Astronomy, v. 4, no. 5, p. 526–532, doi: 10.1038/s41550-019-0990-x.

Franz, H.B., McAdam, A.C., Ming, D.W., Freissinet, C., Mahaffy, P.R., Eldridge, D.L., Fischer, W.W., Grotzinger, J.P., House, C.H., Hurowitz, J.A., McLennan, S.M., Schwenzer, S.P., Vaniman, D.T., Archer Jr, P.D., et al., 2017, Large sulfur isotope fractionations in martian sediments at Gale Crater: Nature Geoscience, v. 10, no. 9, p. 658–662, doi: 10.1038/ngeo3002.

Freissinet, C., Glavin, D.P., Mahaffy, P.R., Miller, K.E., Eigenbrode, J.L., Summons, R.E., Brunner, A.E., Buch, A., Szopa, C., Archer, P.D., Franz, H.B., Atreya, S.K., Brinckerhoff, W.B., Cabane, M., et al., 2015, Organic molecules in the sheepbed mudstone, Gale Crater, Mars: Journal of Geophysical Research: Planets, v. 120, no. 3, p. 495–514, doi: 10.1002/2014je004737.

Freissinet, C., Glavin, D.P., Archer, P.D., Teinturier, S., Buch, A., Szopa, C., Lewis, J.M., Williams, A.J., Navarro-Gonzalez, R., Dworkin, J.P., Franz, Heather.B., Millan, M., Eigenbrode, J.L., Summons, R.E., et al., 2025, Long-chain alkanes preserved in a Martian mudstone: Proceedings of the National Academy of Sciences, v. 122, no. 13, doi: 10.1073/pnas.2420580122.

Garry, J.R., ten Kate, I.L., Martins, Z., Nørnberg, P., and Ehrenfreund, P., 2006, Analysis and survival of amino acids in martian regolith analogs: Meteoritics & Planetary Science, v. 41, no. 3, p. 391–405, doi: 10.1111/j.1945-5100.2006.tb00470.x.

Georgiou, C.D., and Deamer, D.W., 2014, Lipids as universal biomarkers of extraterrestrial life: Astrobiology, v. 14, no. 6, p. 541–549, doi: 10.1089/ast.2013.1134.

Gibson, E.K., McKay, D.S., Thomas-Keprta, K.L., Wentworth, S.J., Westall, F., Steele, A., Romanek, C.S., Bell, M.S., and Toporski, J., 2001, Life on mars: Evaluation of the evidence within Martian meteorites ALH84001, Nakhla, and Shergotty: Precambrian Research, v. 106, no. 1–2, p. 15–34, doi: 10.1016/s0301-9268(00)00122-4.

Gibson, Jr., E.K., McKay, D.S., Clemett, S.J., Thomas-Keprta, K.L., Wentworth, S.J., Robert, F., Verchovsky, A.B., Wright, I.P., Pillinger, C.T., Rice, T., Van Leer, B., Meibom, A., Mostefaoui, S.M., and Le, L., 2006, Identification and analysis of carbon-bearing phases in the martian meteorite nakhla: SPIE Proceedings, doi: 10.1117/12.690503.

Gil-Lozano, C., Baron, F., Gaudin, A., Lorand, J.-P., Fernandez, V., Hamon, J., and Mangold, N., 2021, Understanding the formation of carbonates on Mars: Experimental approach: Goldschmidt2021 abstracts, doi: 10.7185/gold2021.4414.

Glavin, D.P., Aubrey, A.D., Callahan, M.P., Dworkin, J.P., Elsila, J.E., Parker, E.T., Bada, J.L., Jenniskens, P., and Shaddad, M.H., 2010, Extraterrestrial amino acids in the almahata Sitta meteorite: Meteoritics & Planetary Science, v. 45, no. 10–11, p. 1695–1709, doi: 10.1111/j.1945-5100.2010.01094.x.

Glavin, D.P., Bada, J.L., Brinton, K.L., and McDonald, G.D., 1999, Amino acids in the martian meteorite Nakhla: Proceedings of the National Academy of Sciences, v. 96, no. 16, p. 8835–8838, doi: 10.1073/pnas.96.16.8835.

Glavin, D.P., Dworkin, J.P., Aubrey, A., Botta, O., Doty, J.H., Martins, Z., and Bada, J.L., 2006, Amino acid analyses of Antarctic CM2 meteorites using liquid chromatography-time of flight-mass spectrometry: Meteoritics & Planetary Science, v. 41, no. 6, p. 889–902, doi: 10.1111/j.1945-5100.2006.tb00493.x.

Glavin, D.P., Freissinet, C., Miller, K.E., Eigenbrode, J.L., Brunner, A.E., Buch, A., Sutter, B., Archer, P.D., Atreya, S.K., Brinckerhoff, W.B., Cabane, M., Coll, P., Conrad, P.G., Coscia, D., et al., 2013, Evidence for perchlorates and the origin of chlorinated

hydrocarbons detected by Sam at the Rocknest Aeolian deposit in Gale Crater: Journal of Geophysical Research: Planets, v. 118, no. 10, p. 1955–1973, doi: 10.1002/jgre.20144.

Goesmann, F., Brinckerhoff, W.B., Raulin, F., Goetz, W., Danell, R.M., Getty, S.A., Siljeström, S., Mißbach, H., Steininger, H., Arevalo, R.D., Buch, A., Freissinet, C., Grubisic, A., Meierhenrich, U.J., et al., 2017, The Mars Organic Molecule Analyzer (moma) instrument: Characterization of organic material in martian sediments: Astrobiology, v. 17, no. 6–7, p. 655–685, doi: 10.1089/ast.2016.1551.

Goncharov, A.G., Nikitina, L.P., Borovkov, N.V., Babushkina, M.S., and Sirotkin, A.N., 2015, Thermal and redox equilibrium conditions of the upper-mantle xenoliths from the quaternary volcanoes of NW Spitsbergen, Svalbard archipelago: Russian Geology and Geophysics, v. 56, no. 11, p. 1578–1602, doi: 10.1016/j.rgg.2015.10.006.

Goodwin, A., Schröder, C., Bonsall, E., Garwood, R.J., and Tartèse, R., 2024, Abiotic origin of organics in the Martian regolith: Earth and Planetary Science Letters, v. 647, p. 119055, doi: 10.1016/j.epsl.2024.119055.

Goudge, T.A., Mustard, J.F., Head, J.W., Fassett, C.I., and Wiseman, S.M., 2015, Assessing the mineralogy of the watershed and fan deposits of the Jezero crater paleolake system, Mars: Journal of Geophysical Research: Planets, v. 120, no. 4, p. 775–808, doi: 10.1002/2014je004782.

Goulas, A., Binner, J.G.P., Harris, R.A., and Friel, R.J., 2017, Assessing extraterrestrial regolith material simulants for in-situ resource utilisation based 3D printing: Applied Materials Today, v. 6, p. 54–61, doi: 10.1016/j.apmt.2016.11.004.

Grady, M.M., 2020, Exploring Mars with returned samples: Space Science Reviews, v. 216, no. 4, doi: 10.1007/s11214-020-00676-9.

Grotzinger, J.P., Crisp, J., Vasavada, A.R., Anderson, R.C., Baker, C.J., Barry, R., Blake, D.F., Conrad, P., Edgett, K.S., Ferdowski, B., Gellert, R., Gilbert, J.B., Golombek, M., Gómez-

Elvira, J., et al., 2012, Mars Science Laboratory Mission and Science Investigation: Space Science Reviews, v. 170, no. 1–4, p. 5–56, doi: 10.1007/s11214-012-9892-2.

Gupta, S., Mangold, N., Dromart, G., Gasnault, O., Le Mouelic, S., and Bell, J., 2021, Evidence for a delta-lake system and ancient flood deposits at Jezero Crater, Mars, from the perseverance rover: Geological Society of America Abstracts with Programs, doi: 10.1130/abs/2021am-370714.

Guzman, M., McKay, C.P., Quinn, R.C., Szopa, C., Davila, A.F., Navarro-González, R., and Freissinet, C., 2018, Identification of chlorobenzene in the viking gas chromatograph-mass spectrometer data sets: Reanalysis of viking mission data consistent with aromatic organic compounds on Mars: Journal of Geophysical Research: Planets, v. 123, no. 7, p. 1674–1683, doi: 10.1029/2018je005544.

Halevy, I., Fischer, W.W., and Eiler, J.M., 2011, Carbonates in the martian meteorite Allan Hills 84001 formed at 18 ± 4 °C in a near-surface aqueous environment: Proceedings of the National Academy of Sciences, v. 108, no. 41, p. 16895–16899, doi: 10.1073/pnas.1109444108.

Hallis, L.J., 2017, D/H ratios of the inner Solar System: Philosophical Transactions of the Royal Society A: Mathematical, Physical and Engineering Sciences, v. 375, no. 2094, p. 20150390, doi: 10.1098/rsta.2015.0390.

Hausrath, E.M., Treiman, A.H., Vicenzi, E., Bish, D.L., Blake, D., Sarrazin, P., Hoehler, T., Midtkandal, I., Steele, A., and Brantley, S.L., 2008, Short- and long-term olivine weathering in Svalbard: Implications for Mars: Astrobiology, v. 8, no. 6, p. 1079–1092, doi: 10.1089/ast.2007.0195.

Hays, L.E., Graham, H.V., Des Marais, D.J., Hausrath, E.M., Horgan, B., McCollom, T.M., Parenteau, M.N., Potter-McIntyre, S.L., Williams, A.J., and Lynch, K.L., 2017, Biosignature preservation and detection in Mars Analog Environments: Astrobiology, v. 17, no. 4, p. 363–400, doi: 10.1089/ast.2016.1627.

He, D., Wang, X., Yang, Y., He, R., Zhong, H., Wang, Y., Han, B., and Jin, F., 2021, Hydrothermal synthesis of long-chain hydrocarbons up to C24 with NaHCO3-assisted stabilizing cobalt : Proceedings of the National Academy of Sciences, v. 118, no. 51, doi: 10.1073/pnas.2115059118.

Head, J.W., Mustard, J.F., Kreslavsky, M.A., Milliken, R.E., and Marchant, D.R., 2003, Recent ice ages on Mars: Nature, v. 426, no. 6968, p. 797–802, doi: 10.1038/nature02114.

Hecht, M.H., Kounaves, S.P., Quinn, R.C., West, S.J., Young, S.M., Ming, D.W., Catling, D.C., Clark, B.C., Boynton, W.V., Hoffman, J., DeFlores, L.P., Gospodinova, K., Kapit, J., and Smith, P.H., 2009, Detection of perchlorate and the soluble chemistry of martian soil at the Phoenix Lander Site: Science, v. 325, no. 5936, p. 64–67, doi: 10.1126/science.1172466.

Heinz, J., and Schulze-Makuch, D., 2020, Thiophenes on Mars: Biotic or abiotic origin? Astrobiology, v. 20, no. 4, p. 552–561, doi: 10.1089/ast.2019.2139.

Hickman-Lewis, K., Moore, K.R., Hollis, J.J., Tuite, M.L., Beegle, L.W., Bhartia, R., Grotzinger, J.P., Brown, A.J., Shkolyar, S., Cavalazzi, B., and Smith, C.L., 2022, In situ identification of Paleoarchean biosignatures using colocated perseverance rover analyses: Perspectives for *in situ* mars science and sample return: Astrobiology, v. 22, no. 9, p. 1143–1163, doi: 10.1089/ast.2022.0018.

Hicks, L.J., Bridges, J.C., and Gurman, S.J., 2014, Ferric saponite and Serpentine in the nakhlite martian meteorites: Geochimica et Cosmochimica Acta, v. 136, p. 194–210, doi: 10.1016/j.gca.2014.04.010.

Horgan, B.H.N., Anderson, R.B., Dromart, G., Amador, E.S., and Rice, M.S., 2020, The mineral diversity of Jezero crater: Evidence for possible lacustrine carbonates on Mars: Icarus, v. 339, p. 113526, doi: 10.1016/j.icarus.2019.113526.

Houghton, J.E., Behnsen, J., Duller, R.A., Nichols, T.E., and Worden, R.H., 2024, Particle size analysis: A comparison of laboratory-based techniques and their application to geoscience: Sedimentary Geology, v. 464, p. 106607, doi: 10.1016/j.sedgeo.2024.106607.

Hynek, B.M., and Di Achille, G., 2017, Geologic map of Meridiani Planum, Mars: Scientific Investigations Map, doi: 10.3133/sim3356.

Jaramillo, E.A., Royle, S.H., Claire, M.W., Kounaves, S.P., and Sephton, M.A., 2019, Indigenous organic-oxidized fluid interactions in the TISSINT mars meteorite: Geophysical Research Letters, v. 46, no. 6, p. 3090–3098, doi: 10.1029/2018gl081335.

Jenniskens, P., Fries, M.D., Yin, Q.-Z., Zolensky, M., Krot, A.N., Sandford, S.A., Sears, D., Beauford, R., Ebel, D.S., Friedrich, J.M., Nagashima, K., Wimpenny, J., Yamakawa, A., Nishiizumi, K., et al., 2012, Radar-enabled recovery of the Sutter's mill meteorite, a carbonaceous chondrite regolith breccia: Science, v. 338, no. 6114, p. 1583–1587, doi: 10.1126/science.1227163.

Johansson, A., Gee, D.G., Larionov, A.N., Ohta, Y., and Tebenkov, A.M., 2005, Grenvillian and Caledonian evolution of eastern svalbard - A tale of two Orogenies: Terra Nova, v. 17, no. 4, p. 317–325, doi: 10.1111/j.1365-3121.2005.00616.x.

Jones, E.G., 2018, Shallow transient liquid water environments on present-day Mars, and their implications for life: Acta Astronautica, v. 146, p. 144–150, doi: 10.1016/j.actaastro.2018.02.027.

Jorge-Villar, S.E., Edwards, H.G., and Benning, L.G., 2011, Raman spectroscopic analysis of Arctic nodules: Relevance to the Astrobiological Exploration of Mars: Analytical and Bioanalytical Chemistry, v. 401, no. 9, p. 2927–2933, doi: 10.1007/s00216-011-5385-5.

JUNGCLAUS, G., CRONIN, J.R., MOORE, C.B., and YUEN, G.U., 1976, Aliphatic amines in the Murchison meteorite: Nature, v. 261, no. 5556, p. 126–128, doi: 10.1038/261126a0.

King, A.J., Daly, L., Rowe, J., Joy, K.H., Greenwood, R.C., Devillepoix, H.A.R., Suttle, M.D., Chan, Q.H.S., Russell, S.S., Bates, H.C., Bryson, J.F.J., Clay, P.L., Vida, D., Lee, M.R., et al., 2022, The Winchcombe Meteorite, a unique and pristine witness from the outer solar system: Science Advances, v. 8, no. 46, doi: 10.1126/sciadv.abq3925.

KMINEK, G., and BADA, J., 2006, The effect of ionizing radiation on the preservation of amino acids on Mars: Earth and Planetary Science Letters, v. 245, no. 1–2, p. 1–5, doi: 10.1016/j.epsl.2006.03.008.

Koike, M., Nakada, R., Kajitani, I., Usui, T., Tamenori, Y., Sugahara, H., and Kobayashi, A., 2020, In-situ preservation of nitrogen-bearing organics in Noachian Martian carbonates: Nature Communications, v. 11, no. 1, doi: 10.1038/s41467-020-15931-4.

Kring, DavidA., Swindle, TimothyD., Gleason, JamesD., and Grier, JenniferA., 1998, Formation and relative ages of maskelynite and carbonate in ALH84001: Geochimica et Cosmochimica Acta, v. 62, no. 12, p. 2155–2166, doi: 10.1016/s0016-7037(98)00133-1.

Kumar, P., Pattanaik, J.K., Khare, N., and Balakrishnan, S., 2018, Geochemistry and provenance study of sediments from Krossfjorden and Kongsfjorden, Svalbard (Arctic Ocean): Polar Science, v. 18, p. 72–82, doi: 10.1016/j.polar.2018.06.001.

Lapen, T.J., Righter, M., Brandon, A.D., Debaille, V., Beard, B.L., Shafer, J.T., and Peslier, A.H., 2010, A younger age for ALH84001 and its geochemical link to shergottite sources in Mars: Science, v. 328, no. 5976, p. 347–351, doi: 10.1126/science.1185395.

Lawless, J.G., Zeitman, B., Pereira, W.E., Summons, R.E., and Duffield, A.M., 1974, Dicarboxylic acids in the Murchison meteorite: Nature, v. 251, no. 5470, p. 40–42, doi: 10.1038/251040a0.

Lewis, J.M.T., Najorka, J., Watson, J.S., and Sephton, M.A., 2018, The search for Hesperian Organic matter on Mars: Pyrolysis studies of sediments rich in sulfur and Iron: Astrobiology, v. 18, no. 4, p. 454–464, doi: 10.1089/ast.2017.1717.

Lin, Y., El Goresy, A., Hu, S., Zhang, J., Gillet, P., Xu, Y., Hao, J., Miyahara, M., Ouyang, Z., Ohtani, E., Xu, L., Yang, W., Feng, L., Zhao, X., et al., 2014a, NanoSIMS analysis of organic carbon from the TISSINT martian meteorite: Evidence for the past existence of subsurface organic-bearing fluids on Mars: Meteoritics & Planetary Science, v. 49, no. 12, p. 2201–2218, doi: 10.1111/maps.12389.

Lin, Y., El Goresy, A., Hu, S., Zhang, J., Gillet, P., Xu, Y., Hao, J., Miyahara, M., Ouyang, Z., Ohtani, E., Xu, L., Yang, W., Feng, L., Zhao, X., et al., 2014b, NanoSIMS analysis of organic carbon from the TISSINT martian meteorite: Evidence for the past existence of subsurface organic-bearing fluids on Mars: Meteoritics & Planetary Science, v. 49, no. 12, p. 2201–2218, doi: 10.1111/maps.12389.

Liu, Y., Baziotis, I.P., Asimow, P.D., Bodnar, R.J., and Taylor, L.A., 2016, Mineral Chemistry of the TISSINT meteorite: Indications of two-stage crystallization in a closed system: Meteoritics & Planetary Science, v. 51, no. 12, p. 2293–2315, doi: 10.1111/maps.12726.

Mahaffy, P., 2007, Exploration of the habitability of mars: Development of analytical protocols for measurement of organic carbon on the 2009 Mars science laboratory: Space Science Reviews, v. 135, no. 1–4, p. 255–268, doi: 10.1007/s11214-007-9223-1.

Mahaffy, P.R., Webster, C.R., Cabane, M., Conrad, P.G., Coll, P., Atreya, S.K., Arvey, R., Barciniak, M., Benna, M., Bleacher, L., Brinckerhoff, W.B., Eigenbrode, J.L., Carignan, D., Cascia, M., et al., 2012, The sample analysis at Mars Investigation and Instrument Suite: Space Science Reviews, v. 170, no. 1–4, p. 401–478, doi: 10.1007/s11214-012-9879-z.

Martins, Z., Botta, O., Fogel, M.L., Sephton, M.A., Glavin, D.P., Watson, J.S., Dworkin, J.P., Schwartz, A.W., and Ehrenfreund, P., 2008, Extraterrestrial nucleobases in the Murchison meteorite: Earth and Planetary Science Letters, v. 270, no. 1–2, p. 130–136, doi: 10.1016/j.epsl.2008.03.026.

Martins, Z., Modica, P., Zanda, B., and d'Hendecourt, L.L., 2015, The amino acid and hydrocarbon contents of the Paris meteorite: Insights into the most primitive CM chondrite: Meteoritics & Planetary Science, v. 50, no. 5, p. 926–943, doi: 10.1111/maps.12442.

McCollom, T.M., and Seewald, J.S., 2007, Abiotic synthesis of organic compounds in deep-sea hydrothermal environments: ChemInform, v. 38, no. 20, doi: 10.1002/chin.200720264.

McKay, D.S., Gibson, E.K., Thomas-Keprta, K.L., Vali, H., Romanek, C.S., Clemett, S.J., Chillier, X.D., Maechling, C.R., and Zare, R.N., 1996, Search for past life on Mars: Possible relic biogenic activity in martian meteorite ALH84001: Science, v. 273, no. 5277, p. 924–930, doi: 10.1126/science.273.5277.924.

McSween, H.Y., 2018, The search for biosignatures in martian meteorite Allan Hills 84001: Biosignatures for Astrobiology, p. 167–182, doi: 10.1007/978-3-319-96175-0_8.

Melwani Daswani, M., Schwenzer, S.P., Reed, M.H., Wright, I.P., and Grady, M.M., 2016, Alteration minerals, fluids, and gases on early Mars: Predictions from 1-d flow geochemical modeling of mineral assemblages in meteorite ALH 84001: Meteoritics & Planetary Science, v. 51, no. 11, p. 2154–2174, doi: 10.1111/maps.12713.

Millan, M., Williams, A.J., McAdam, A.C., Eigenbrode, J.L., Steele, A., Freissinet, C., Glavin, D.P., Szopa, C., Buch, A., Summons, R.E., Lewis, J.M., Wong, G.M., House, C.H., Sutter, B., et al., 2022, Sedimentary Organics in Glen Torridon, Gale Crater, Mars: Results from the Sam Instrument Suite and supporting laboratory analyses: Journal of Geophysical Research: Planets, v. 127, no. 11, doi: 10.1029/2021je007107.

Mittlefehldt, D.W., 1994, ALH84001, a cumulate orthopyroxenite member of the martian meteorite clan: Meteoritics, v. 29, no. 2, p. 214–221, doi: 10.1111/j.1945-5100.1994.tb00673.x.

Morris, R.V., Ruff, S.W., Gellert, R., Ming, D.W., Arvidson, R.E., Clark, B.C., Golden, D.C., Siebach, K., Klingelhöfer, G., Schröder, C., Fleischer, I., Yen, A.S., and Squyres, S.W., 2010, Identification of carbonate-rich outcrops on Mars by the spirit rover: Science, v. 329, no. 5990, p. 421–424, doi: 10.1126/science.1189667.

Nakada, R., Tanabe, G., Kajitani, I., Usui, T., Shidare, M., and Yokoyama, T., 2021, Exafs determination of clay minerals in martian meteorite Allan Hills 84001 and its implication

for the noachian aqueous environment: Minerals, v. 11, no. 2, p. 176, doi: 10.3390/min11020176.

Navarro-González, R., Vargas, E., de la Rosa, J., Raga, A.C., and McKay, C.P., 2010, Reanalysis of the viking results suggests perchlorate and organics at Midlatitudes on Mars: Journal of Geophysical Research, v. 115, no. E12, doi: 10.1029/2010je003599.

Nyquist, L.E., Bogard, D.D., Shih, C.-Y., Greshake, A., Stöffler, D., and Eugster, O., 2001, Ages and geologic histories of martian meteorites: Space Sciences Series of ISSI, p. 105–164, doi: 10.1007/978-94-017-1035-0_5.

Orata, F., 2012, Derivatization reactions and reagents for gas chromatography analysis: Advanced Gas Chromatography - Progress in Agricultural, Biomedical and Industrial Applications, doi: 10.5772/33098.

Osinski, G.R., Cockell, C.S., Pontefract, A., and Sapers, H.M., 2020, The role of meteorite impacts in the origin of life: Astrobiology, v. 20, no. 9, p. 1121–1149, doi: 10.1089/ast.2019.2203.

O'Brien, Á., 2022, Extra-terrestrial organics: organic matter in meteorites and martian analogues [thesis]: University of Glasgow.

O'Brien, Á.C., Hallis, L.J., Regnault, C., Morrison, D., Blackburn, G., Steele, A., Daly, L., Tait, A., Tremblay, M.M., Telenko, D.E.P., Gunn, J., McKay, E., Mari, N., Salik, M.A., et al., 2022, Using organic contaminants to constrain the terrestrial journey of the Martian Meteorite Lafayette: Astrobiology, v. 22, no. 11, p. 1351–1362, doi: 10.1089/ast.2021.0180.

Peters, C.A., and George, S.C., 2018, Hydrocarbon biomarkers preserved in carbonate veins of potentially Paleoproterozoic age, and implications for the early biosphere: Geobiology, v. 16, no. 6, p. 577–596, doi: 10.1111/gbi.12305.

Peters, S., Semenov, D.A., Hochleitner, R., and Trapp, O., 2023, Synthesis of prebiotic organics from CO2 by catalysis with meteoritic and volcanic particles: Scientific Reports, v. 13, no. 1, doi: 10.1038/s41598-023-33741-8.

Phillips, R.J., Zuber, M.T., Solomon, S.C., Golombek, M.P., Jakosky, B.M., Banerdt, W.B., Smith, D.E., Williams, R.M., Hynek, B.M., Aharonson, O., and Hauck II, S.A., 2001, Ancient geodynamics and Global-Scale Hydrology on Mars: Science, v. 291, no. 5513, p. 2587–2591, doi: 10.1126/science.1058701.

Pizzarello, S., Davidowski, S.K., Holland, G.P., and Williams, L.B., 2013, Processing of meteoritic organic materials as a possible analog of early molecular evolution in planetary environments: Proceedings of the National Academy of Sciences, v. 110, no. 39, p. 15614–15619, doi: 10.1073/pnas.1309113110.

Proskurowski, G., Lilley, M.D., Seewald, J.S., Früh-Green, G.L., Olson, E.J., Lupton, J.E., Sylva, S.P., and Kelley, D.S., 2008, Abiogenic hydrocarbon production at Lost City Hydrothermal Field: Science, v. 319, no. 5863, p. 604–607, doi: 10.1126/science.1151194.

Rech, J.A., Quade, J., and Hart, W.S., 2003, Isotopic evidence for the source of Ca and s in soil gypsum, anhydrite and calcite in the Atacama Desert, Chile: Geochimica et Cosmochimica Acta, v. 67, no. 4, p. 575–586, doi: 10.1016/s0016-7037(02)01175-4.

ROCHETTE, P., GATTACCECA, J., CHEVRIER, V., HOFFMANN, V., LORAND, J.-P., FUNAKI, M., and HOCHLEITNER, R., 2005, Matching martian crustal magnetization and magnetic properties of Martian meteorites: Meteoritics & Planetary Science, v. 40, no. 4, p. 529–540, doi: 10.1111/j.1945-5100.2005.tb00961.x.

Ruff, S.W., and Farmer, J.D., 2016, Silica deposits on Mars with features resembling hot spring biosignatures at El Tatio in Chile: Nature Communications, v. 7, no. 1, doi: 10.1038/ncomms13554.

Rull, F., Veneranda, M., Manrique-Martinez, J.A., Sanz-Arranz, A., Saiz, J., Medina, J., Moral, A., Perez, C., Seoane, L., Lalla, E., Charro, E., Lopez, J.M., Nieto, L.M., and Lopez-

Reyes, G., 2022, Spectroscopic study of terrestrial analogues to support rover missions to Mars – A raman-centred review: Analytica Chimica Acta, v. 1209, p. 339003, doi: 10.1016/j.aca.2021.339003.

Russell, M.J., Hall, A.J., and Martin, W., 2010, Serpentinization as a source of energy at the origin of life: Geobiology, v. 8, no. 5, p. 355–371, doi: 10.1111/j.1472-4669.2010.00249.x.

Santos, A.R., Agee, C.B., McCubbin, F.M., Shearer, C.K., Burger, P.V., Tartèse, R., and Anand, M., 2015, Petrology of igneous clasts in northwest Africa 7034: Implications for the petrologic diversity of the Martian crust: Geochimica et Cosmochimica Acta, v. 157, p. 56–85, doi: 10.1016/j.gca.2015.02.023.

Schmitt-Kopplin, P., Gabelica, Z., Gougeon, R.D., Fekete, A., Kanawati, B., Harir, M., Gebefuegi, I., Eckel, G., and Hertkorn, N., 2010, High molecular diversity of extraterrestrial organic matter in Murchison meteorite revealed 40 years after its fall: Proceedings of the National Academy of Sciences, v. 107, no. 7, p. 2763–2768, doi: 10.1073/pnas.0912157107.

Schulte, M., Blake, D., Hoehler, T., and McCollom, T., 2006, Serpentinization and its implications for life on the early Earth and Mars: Astrobiology, v. 6, no. 2, p. 364–376, doi: 10.1089/ast.2006.6.364.

Semprich, J., Filiberto, J., Treiman, A.H., and Schwenzer, S.P., 2021, Constraints on the formation of carbonates and low-grade metamorphic phases in the Martian crust as a function of H2O-CO2 fluids : Meteoritics & Planetary Science, v. 57, no. 1, p. 77–104, doi: 10.1111/maps.13775.

Sephton, M.A., 2004, Organic matter in ancient meteorites: Astronomy and Geophysics, v. 45, no. 2, doi: 10.1046/j.1468-4004.2003.45208.x.

Sephton, M.A., 2012, Pyrolysis and mass spectrometry studies of Meteoritic Organic matter: Mass Spectrometry Reviews, v. 31, no. 5, p. 560–569, doi: 10.1002/mas.20354.

Sephton, M.A., 2013, Aromatic units from the macromolecular material in meteorites: Molecular probes of Cosmic Environments: Geochimica et Cosmochimica Acta, v. 107, p. 231–241, doi: 10.1016/j.gca.2012.12.042.

Sephton, M.A., and Botta, O., 2008, Extraterrestrial organic matter and the detection of life: Space Sciences Series of ISSI, p. 25–35, doi: 10.1007/978-0-387-77516-6_4.

Sephton, M.A., Bland, P.A., Pillinger, C.T., and Gilmour, I., 2004, The preservation state of organic matter in meteorites from Antarctica: Meteoritics & Planetary Science, v. 39, no. 5, p. 747–754, doi: 10.1111/j.1945-5100.2004.tb00116.x.

Sephton, M.A., Chan, Q.H., Watson, J.S., Burchell, M.J., Spathis, V., Grady, M.M., Verchovsky, A.B., Abernethy, F.A., and Franchi, I.A., 2023, Insoluble macromolecular organic matter in the Winchcombe Meteorite: Meteoritics & Planetary Science, doi: 10.1111/maps.13952.

Sephton, M.A., Pillinger, C.T., and Gilmour, I., 1998, Δ13C of free and macromolecular aromatic structures in the Murchison meteorite: Geochimica et Cosmochimica Acta, v. 62, no. 10, p. 1821–1828, doi: 10.1016/s0016-7037(98)00108-2.

Sephton, M.A., Pillinger, C.T., and Gilmour, I., 2000, Aromatic moieties in meteoritic macromolecular materials: Analyses by hydrous pyrolysis and Δ13C of individual compounds: Geochimica et Cosmochimica Acta, v. 64, no. 2, p. 321–328, doi: 10.1016/s0016-7037(99)00282-3.

Sephton, M.A., Wright, I.P., Gilmour, I., de Leeuw, J.W., Grady, M.M., and Pillinger, C.T., 2002, High molecular weight organic matter in Martian meteorites: Planetary and Space Science, v. 50, no. 7–8, p. 711–716, doi: 10.1016/s0032-0633(02)00053-3.

Shaheen, R., Niles, P.B., Chong, K., Corrigan, C.M., and Thiemens, M.H., 2014, Carbonate formation events in ALH 84001 trace the evolution of the martian atmosphere: Proceedings of the National Academy of Sciences, v. 112, no. 2, p. 336–341, doi: 10.1073/pnas.1315615112.

Siljeström, S., Freissinet, C., Goesmann, F., Steininger, H., Goetz, W., Steele, A., Amundsen, H., and AMASE11 team, 2014, Comparison of prototype and laboratory experiments on moma GCMS: Results from the amase11 campaign: Astrobiology, v. 14, no. 9, p. 780–797, doi: 10.1089/ast.2014.1197.

Simkus, D.N., Aponte, J.C., Elsila, J.E., Parker, E.T., Glavin, D.P., and Dworkin, J.P., 2019, Methodologies for analyzing soluble organic compounds in extraterrestrial samples: Amino acids, amines, monocarboxylic acids, aldehydes, and ketones: Life, v. 9, no. 2, p. 47, doi: 10.3390/life9020047.

Skjelkvåle, B.-L., Amundsen, H.E.F., O'Reilly, S.Y., Griffin, W.L., and Gjelsvik, T., 1989, A primitive alkali basaltic stratovolcano and associated eruptive centres, northwestern Spitsbergen: Volcanology and tectonic significance: Journal of Volcanology and Geothermal Research, v. 37, no. 1, p. 1–19, doi: 10.1016/0377-0273(89)90110-8.

Smyrak-Sikora, A., Nicolaisen, J.B., Braathen, A., Johannessen, E.P., Olaussen, S., and Stemmerik, L., 2021, Impact of growth faults on mixed siliciclastic-carbonate-evaporite deposits during rift climax and reorganisation—Billefjorden Trough, Svalbard, Norway: Basin Research, v. 33, no. 5, p. 2643–2674, doi: 10.1111/bre.12578.

Snyder, C.W., and Evans, N., 1981, The final phases of the Viking Mission to Mars: Icarus, v. 45, no. 1, p. 2–24, doi: 10.1016/0019-1035(81)90003-8.

Soffen, G.A., and Snyder, C.W., 1976, The first viking mission to Mars: Science, v. 193, no. 4255, p. 759–766, doi: 10.1126/science.193.4255.759.

Squyres, S.W., Arvidson, R.E., Bollen, D., Bell, J.F., Brückner, J., Cabrol, N.A., Calvin, W.M., Carr, M.H., Christensen, P.R., Clark, B.C., Crumpler, L., Des Marais, D.J., d'Uston, C., Economou, T., et al., 2006, Overview of the opportunity mars exploration rover mission to Meridiani Planum: Eagle Crater to purgatory ripple: Journal of Geophysical Research: Planets, v. 111, no. E12, doi: 10.1029/2006je002771.

Steele, A., Benning, L.G., Wirth, R., Schreiber, A., Araki, T., McCubbin, F.M., Fries, M.D., Nittler, L.R., Wang, J., Hallis, L.J., Conrad, P.G., Conley, C., Vitale, S., O'Brien, A.C., et al., 2022, Organic synthesis associated with serpentinization and carbonation on early Mars: Science, v. 375, no. 6577, p. 172–177, doi: 10.1126/science.abg7905.

Steele, A., Fries, M.D., Amundsen, H.E., Mysen, B.O., Fogel, M.L., Schweizer, M., and Boctor, N.Z., 2007, Comprehensive Imaging and Raman spectroscopy of carbonate globules from martian meteorite ALH 84001 and a terrestrial analogue from Svalbard: Meteoritics & Planetary Science, v. 42, no. 9, p. 1549–1566, doi: 10.1111/j.1945-5100.2007.tb00590.x.

Steele, A., McCubbin, F.M., and Fries, M.D., 2016, The provenance, formation, and implications of reduced carbon phases in Martian meteorites: Meteoritics & Planetary Science, v. 51, no. 11, p. 2203–2225, doi: 10.1111/maps.12670.

Steele, A., McCubbin, F.M., Fries, M., Kater, L., Boctor, N.Z., Fogel, M.L., Conrad, P.G., Glamoclija, M., Spencer, M., Morrow, A.L., Hammond, M.R., Zare, R.N., Vicenzi, E.P., Siljeström, S., et al., 2012, A reduced organic carbon component in martian basalts: Science, v. 337, no. 6091, p. 212–215, doi: 10.1126/science.1220715.

Steininger, H., Goesmann, F., and Goetz, W., 2012, Influence of magnesium perchlorate on the pyrolysis of organic compounds in Mars analogue soils: Planetary and Space Science, v. 71, no. 1, p. 9–17, doi: 10.1016/j.pss.2012.06.015.

Stern, J.C., McAdam, A.C., Ten Kate, I.L., Bish, D.L., Blake, D.F., Morris, R.V., Bowden, R., Fogel, M.L., Glamoclija, M., Mahaffy, P.R., Steele, A., and Amundsen, H.E.F., 2013, Isotopic and geochemical investigation of two distinct Mars analog environments using evolved gas techniques in Svalbard, Norway: Icarus, v. 224, no. 2, p. 297–308, doi: 10.1016/j.icarus.2012.07.010.

Summons, R.E., Amend, J.P., Bish, D., Buick, R., Cody, G.D., Des Marais, D.J., Dromart, G., Eigenbrode, J.L., Knoll, A.H., and Sumner, D.Y., 2011, Preservation of martian organic

and environmental records: Final report of the Mars Biosignature Working Group: Astrobiology, v. 11, no. 2, p. 157–181, doi: 10.1089/ast.2010.0506.

Sushchevskaya, N.M., Evdokimov, A.N., Belyatsky, B.V., Maslov, V.A., and Kuz'min, D.V., 2008a, Conditions of quaternary magmatism at Spitsbergen Island: Geochemistry International, v. 46, no. 1, p. 1–16, doi: 10.1134/s0016702908010011.

Sushchevskaya, N.M., Evdokimov, A.N., Belyatsky, B.V., Maslov, V.A., and Kuz'min, D.V., 2008b, Conditions of quaternary magmatism at Spitsbergen Island: Geochemistry International, v. 46, no. 1, p. 1–16, doi: 10.1134/s0016702908010011.

Sánchez-García, L., Aeppli, C., Parro, V., Fernández-Remolar, D., García-Villadangos, M., Chong-Diaz, G., Blanco, Y., and Carrizo, D., 2018, Molecular biomarkers in the subsurface of the Salar Grande (Atacama, Chile) evaporitic deposits: Biogeochemistry, v. 140, no. 1, p. 31–52, doi: 10.1007/s10533-018-0477-3.

Sánchez-García, L., Fernández-Martínez, M.A., Moreno-Paz, M., Carrizo, D., García-Villadangos, M., Manchado, J.M., Stoker, C.R., Glass, B., and Parro, V., 2020, Simulating Mars Drilling Mission for searching for life: Ground-truthing lipids and other complex microbial biomarkers in the iron-sulfur rich Río Tinto Analog: Astrobiology, v. 20, no. 9, p. 1029–1047, doi: 10.1089/ast.2019.2101.

Tarnas, J.D., Stack, K.M., Parente, M., Koeppel, A.H., Mustard, J.F., Moore, K.R., Horgan, B.H., Seelos, F.P., Cloutis, E.A., Kelemen, P.B., Flannery, D., Brown, A.J., Frizzell, K.R., and Pinet, P., 2021, Characteristics, origins, and biosignature preservation potential of carbonate-bearing rocks within and outside of jezero crater: Journal of Geophysical Research: Planets, v. 126, no. 11, doi: 10.1029/2021je006898.

ten Kate, I.L., 2010, Organics on Mars? Astrobiology, v. 10, no. 6, p. 589–603, doi: 10.1089/ast.2010.0498.

ThermoFischer Scientific, 2013, Methods Optimization in Accelerated Solvent Extraction,.

ThermoFischer Scientific, 2016, Unsurpassed Extraction Technology Accelerated Solvent Extraction,.

Trainer, M.G., Wong, M.H., McConnochie, T.H., Franz, H.B., Atreya, S.K., Conrad, P.G., Lefèvre, F., Mahaffy, P.R., Malespin, C.A., Manning, H.L.K., Martín-Torres, J., Martínez, G.M., McKay, C.P., Navarro-González, R., et al., 2019, Seasonal variations in atmospheric composition as measured in Gale Crater, Mars: Journal of Geophysical Research: Planets, v. 124, no. 11, p. 3000–3024, doi: 10.1029/2019je006175.

Treiman, A.H., 1998, The history of Allan Hills 84001 revised: Multiple shock events: Meteoritics & Planetary Science, v. 33, no. 4, p. 753–764, doi: 10.1111/j.1945-5100.1998.tb01681.x.

Treiman, A.H., 2003, Submicron magnetite grains and carbon compounds in martian meteorite ALH84001: Inorganic, abiotic formation by shock and thermal metamorphism: Astrobiology, v. 3, no. 2, p. 369–392, doi: 10.1089/153110703769016451.

Treiman, A.H., 2005, The nakhlite meteorites: Augite-rich igneous rocks from Mars: Geochemistry, v. 65, no. 3, p. 203–270, doi: 10.1016/j.chemer.2005.01.004.

Treiman, A.H., 2012, Eruption age of the Sverrefjellet Volcano, Spitsbergen Island, Norway: Polar Research, v. 31, no. 1, p. 17320, doi: 10.3402/polar.v31i0.17320.

Treiman, A.H., 2021, Uninhabitable and potentially habitable environments on Mars: Evidence from meteorite ALH 84001: Astrobiology, v. 21, no. 8, p. 940–953, doi: 10.1089/ast.2020.2306.

Treiman, A.H., Amundsen, H.E.F., Blake, D.F., and Bunch, T., 2002, Hydrothermal origin for carbonate globules in martian meteorite ALH84001: A terrestrial analogue from Spitsbergen (Norway): Earth and Planetary Science Letters, v. 204, no. 3–4, p. 323–332, doi: 10.1016/s0012-821x(02)00998-6.

Tunney, L.D., Herd, C.D., and Hilts, R.W., 2020, Organic contamination on the surface of meteorites as a function of space and time: A case study of the buzzard coulee h4 chondrite: Meteoritics & Planetary Science, v. 55, no. 8, doi: 10.1111/maps.13551.

Tunney, L.D., Hill, P.J., Herd, C.D., and Hilts, R.W., 2023, Testing materials to mitigate terrestrial organic contamination of meteorites: Implications for collection, curation, and handling of astromaterials: Meteoritics & Planetary Science, v. 58, no. 2, p. 207–217, doi: 10.1111/maps.13948.

Tutolo, B.M., Hausrath, E.M., Kite, E.S., Rampe, E.B., Bristow, T.F., Downs, R.T., Treiman, A., Peretyazhko, T.S., Thorpe, M.T., Grotzinger, J.P., Roberts, A.L., Archer, P.D., Des Marais, D.J., Blake, D.F., et al., 2025, Carbonates identified by the curiosity rover indicate a carbon cycle operated on ancient Mars: Science, v. 388, no. 6744, p. 292–297, doi: 10.1126/science.ado9966.

Udry, A., Howarth, G.H., Herd, C.D., Day, J.M., Lapen, T.J., and Filiberto, J., 2020, What martian meteorites reveal about the interior and surface of Mars: Journal of Geophysical Research: Planets, v. 125, no. 12, doi: 10.1029/2020je006523.

University of Glasgow, 2013, BECS: Instruments: University of Glasgow, Available at: https://www.gla.ac.uk/schools/ges/research/researchfacilities/biomarkers%20for%20environmental%20and%20climate%20science/#agilentgcms(5977amsd%2F7890bgcsystem) (Accessed: 28 June 2025). .

Vago, J.L., Westall, F., Pasteur Instrument Teams, Landing S, Coates, A.J., Jaumann, R., Korablev, O., Ciarletti, V., Mitrofanov, I., Josset, J.-L., De Sanctis, M.C., Bibring, J.-P., Rull, F., Goesmann, F., Steininger, H., et al., 2017, Habitability on early Mars and the search for biosignatures with the ExoMars Rover: Astrobiology, v. 17, no. 6–7, p. 471–510, doi: 10.1089/ast.2016.1533.

Wang, Z., and Jocelyn Paré, J.R., 1997, Chapter 3 Gas Chromatography (GC): Principles and applications: Techniques and Instrumentation in Analytical Chemistry, p. 61–91, doi: 10.1016/s0167-9244(97)80012-1.

Williams, A.J., Eigenbrode, J., Floyd, M., Wilhelm, M.B., O'Reilly, S., Johnson, S.S., Craft, K.L., Knudson, C.A., Andrejkovičová, S., Lewis, J.M.T., Buch, A., Glavin, D.P., Freissinet, C., Williams, R.H., et al., 2019, Recovery of fatty acids from mineralogic Mars analogs by TMAH thermochemolysis for the sample analysis at Mars Wet Chemistry Experiment on the curiosity rover: Astrobiology, v. 19, no. 4, p. 522–546, doi: 10.1089/ast.2018.1819.

Wordsworth, R., Knoll, A.H., Hurowitz, J., Baum, M., Ehlmann, B.L., Head, J.W., and Steakley, K., 2021, A coupled model of episodic warming, oxidation and geochemical transitions on early Mars: Nature Geoscience, v. 14, no. 3, p. 127–132, doi: 10.1038/s41561-021-00701-8.

Wordsworth, R.D., 2016, The climate of early Mars: Annual Review of Earth and Planetary Sciences, v. 44, no. 1, p. 381–408, doi: 10.1146/annurev-earth-060115-012355.

Wray, J.J., 2012, Gale crater: The mars science laboratory/curiosity rover landing site: International Journal of Astrobiology, v. 12, no. 1, p. 25–38, doi: 10.1017/s1473550412000328.

Zhao, Z., LIU, X., LU, H., and Peng, P., 2022, Abiotic hydrocarbons generation simulated by Fischer-Tropsch synthesis under hydrothermal conditions in ultra-deep basins: Acta Geologica Sinica - English Edition, v. 96, no. 4, p. 1331–1341, doi: 10.1111/1755-6724.14977.

Zolotov, M.Yu., and Shock, E.L., 2000, An abiotic origin for hydrocarbons in the Allan Hills 84001 Martian meteorite through cooling of magmatic and impact-generated gases: Meteoritics & Planetary Science, v. 35, no. 3, p. 629–638, doi: 10.1111/j.1945-5100.2000.tb01443.x.

Appendix

Abbreviations

AMASE: Arctic Mars Analog Svalbard Expedition

ASE: Accelerated Solvent Extraction

BECS: Biomarkers for Environmental and Climate Science

BSE: Backscatter Electron Microscopy

BVC: Bockfjorden Volcanic Complex

D/H: deuterium/hydrogen

DCM-M: Dichloromethane-methanol

EDS: Energy dispersive x-ray spectroscopy

EI: Electron Ionisation

ESA: European Space Agency

FTT: Fischer–Tropsch-type

GC-FID: Gas chromatography – flame ionization detector

GC-IRMS: Gas chromatography – isotope ratio mass spectrometry

GC-MS: Gas chromatography – mass spectrometry

GEMS: Geoanalytical electron microscopy and spectroscopy

Hex-Ace: Hexane-Acetone

HP-LC: High-performance liquid chromatography

HyPy: Hydropyrolysis

INCA: Integrated Calibration and Application Tool

JSC(-1A): Johnston Space Centre, Martian soil simulant sample

LC-MS: Liquid chromatography – mass spectrometry

M/Z: Mass to charge ratio

MSR: Mars Sample Return

NASA – National Aeronautics and Space Administration

NIST: National Institute of Standards and Technology

Py: Pyrolysis

R.T: Retention Time

SE: Secondary Electrons

SEM: Scanning electron microscopy

Sigi: Sigurdfjelle sample from BVC, Svalbard

SNR: Signal to noise ratio

SOP: Standard Operating Procedure

Sverre or Sv: Sverrefjelle(t) sample from BVC, Svalbard

TIC: Total Ion Count

TLE: Total lipid extract

TOF-SIMS - Time-of-Flight Secondary Ion Mass Spectrometry

UKAS: United Kingdom Accreditation Service

UofG – University of Glasgow

Section A

A.1 Further information on Martian analogues

A1.1 Atacama Desert

The Atacama Desert in Chile has been explored as a Martian analogue for the past 20 years due to its similarity of extreme environmental features such as aridity, salinity and high UV (Rech et al., 2003). The Atacama desert is renowned for being the driest place on Earth with the highest UV radiation levels and yet is host to extremophiles making it an important proxy for life on Mars (Azua-Bustos et al., 2022). New equipment constructed for Martian rovers has been tested on this site to understand the distribution of microbial life and to test the detection limits of the instrumentation (Azua-Bustos et al., 2022). A hypersaline halite unit dating back ~9Ma was investigated in this region to find a range of preserved biosignatures, this detection has important implications regarding the search for life in evaporitic deposits on Mars (Sánchez-García et al., 2018). A1.2 Rio Tinto Basin Rio Tinto (Red River) is a 100km-long river in southwestern Spain which is characterised by its blood-red colour. The river is located on one of the largest sulfidic deposits in the world and is extremely acidic (pH <2.5) with a high concentration of heavy metals such as Fe, Cu, As, An (Rull et al., 2022). As a result, mineral deposits are common along the water edge and are dominantly sulphates such as gypsum, copiapite and jarosite as well as more complex Mg and Ca sulphates (Amils et al., 2014). Despite this area having unhospitable qualities, chemolithotrophic acidophilic microorganisms thrive in this environment and are responsible for the iron and sulphur cycles (Amils et al., 2014). The Rio Tinto basin hosts minerals and properties akin to Meridiani Planum on Mars discovered by MER missions such as hematite, sulphates, jarosite, goethite and salts which questions the ideology of hospitable environment and has implications for life on Mars making this site an interesting Martian analogue (Amils et al., 2007). This basin lies within the Jaroso Hydrothermal System which is an analogue for the hydrothermal processes that may have taken place early in Mars' history (Rull et al., 2022). This hydrothermal system is rich in iron and sulphur and produces extensive mineral deposits along the edge of the water (Edwards et al., 2007). Precipitation of these minerals was a result of hydrothermal acidic solutions abundant in heavy metals (Rull et al., 2022). The appearance of jarosite in this location has important connotations for astrobiology on Mars since NASA rover Opportunity discovered jarosite at Meridiani Planum indicating that perhaps Mars had a similar hydrothermal system in which microbes survived.

A.2 Alternative techniques for organic extraction in meteorites

A.2.1 HPLC: Nakhla

Nakhla fell in Egypt in 1911 and is the founder of the Nakhlite type meteorite. High performance liquid chromatography identified amino acids in the Martian meteorite Nakhla (Glavin et al., 1999). However, it is still uncertain as to whether these are terrestrial or extra-terrestrial in origin. The nature of the fall of this meteorite is key reason for this debate. It landed in agricultural farmland near the Nile River Delta, where the rock broke up into fragments, some ~1.5kg which were buried up to 30cm deep and also found in a Lake shore area. When nearby sediment was tested, it also contained the same amino acids present in Nakhla (Glavin et al., 1999). Indigenous reduced carbon was observed in Nakhla within iddingsite-rich phases using Stepped-Combustion Isotopic Mass Spectrometry (Gibson et al., 2006). The structure of the carbon phase indicates a nonterritorial origin and an association with iddingsite could be indicative of early Martian history with evidence of aqueous alteration (Gibson et al., 2006). Further study into an oval structure within this meteorite using a variety of techniques including time-of-flight secondary ion mass spectrometry (TOF-SIMS) analysis reveal an abiotic structure akin to organic matter within the sedimentary rocks at Gale crater (Chatzitheodoridis et al., 2013). This emphasises the importance of understanding terrestrial and extra-terrestrial signatures in order to address terrestrial contamination in future analysis.

Section B

B.1 Equipment used for sample concentration

B.1.1 Sample Concentrators

Figure 36 - Turbovap LV Concentration Workstation within fumehood

The first sample concentrator is the TurboVap LV Concentration Workstation. The 60mL vials are placed here to begin the process of TLE condensing by evaporating the solvent. The water bath gives a steady temperature and vortex of nitrogen flow can be time controlled. When there is a small volume of solvent left in the vials, this is transferred into the pre-weighed and pre-labelled 8mL vials using pastuer pipettes for each sample.

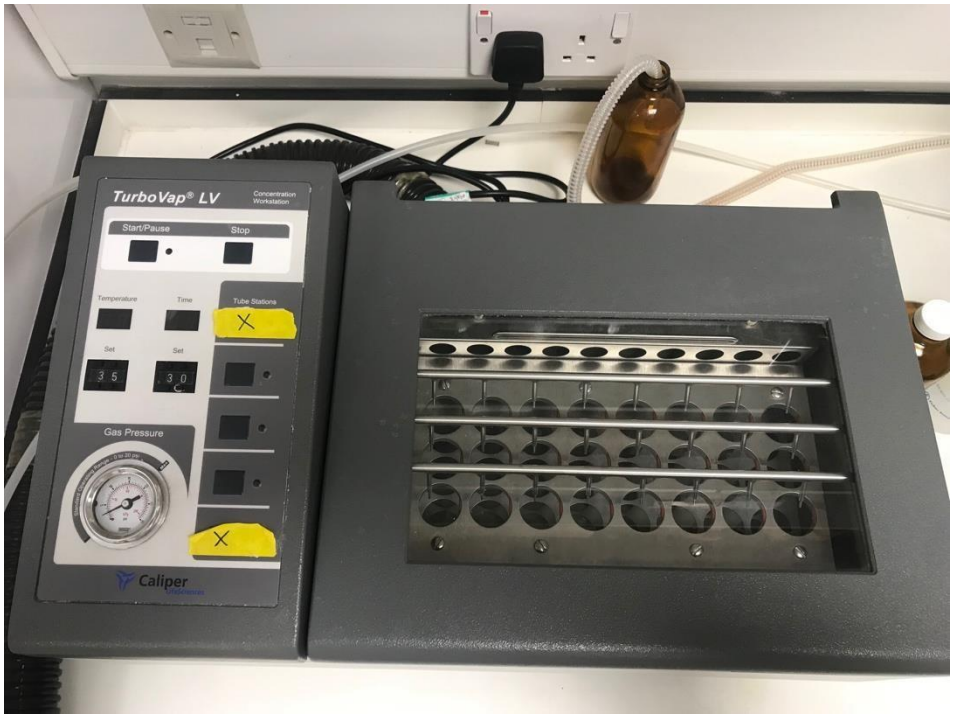

Figure 37 - Techne Sample Concentrator within the laminar flow hood

Once the sample is transferred into the 8mL vials, it is evaporated further using the Techne Sample Concentrator (Figure 37) stored in the fume hood. The block is heated to approximately 40 degrees and nitrogen is pumped in through the top as a steady stream. Constant monitoring is required as volatile elements can be lost if over evaporation occurs. Once condensed, the samples are prepared appropriately for the GC.

B.2 Further information regarding the ASE

B.2.1 Benefits of ASE

The ASE 350 is an efficient, flexible and reliable method for automated solvent extraction for sample preparation (ThermoFischer, 2016) compared to previous techniques such as Soxhlet. Soxhlet (or the reflux technique) was traditionally the standard technique used for solvent extractions and would often take over 24 hours per sample. This method would consume a larger volume of solvent (between 300-1000mL) per sample (between 1-100g). The ASE, however, can process 24 samples in a single set up, processing 1 sample every ~30 minutes and with substantially less solvent at between 5-150mL per sample between 1-100g therefore making it more cost and time effective.

B.2.2 ASE Cell Preparation

The ASE cells are prepared by inserting a combusted filter into each end cap with sterilized tweezers on a surface of aluminium to mitigate contamination. Body is then screwed onto one end cap and lined with one spatula of combusted sand to prevent sample being trapped or lost to the end cap.

Before filling the cell with homogenised sample, each cell (attached to end cap) was placed on the balance and subsequently 0'd to monitor the weight of the sample. Each sample was added slowly and incrementally to reach the desired sample size. A stainlesssteel funnel sterilised was used to reduce sample loss from vial to cell. Each cell was filled with homogenised sample, topped with combusted sand, and labelled with a corresponding BECS ID number i.e 4119 – Sand_BM_DCM (Sample_Crushing Method_ Solvent) to keep track of samples. 8ml glass vials were pre-labelled with permanent marker and weighed before and after TLE extraction to gain the sum TLE (ug).

B.3 Set up and standard operating procedures (SOP)

The standard operating procedures were conducted in accordance with the SOP created for the BECS Lab by Professor Jamie L Toney and carried out with Ali Salik.

B.3.1 Column Chromatography set up

1. Area is lined with aluminium foil and all required equipment is collected; Column holder, glass wool, silica, aminopropyl, combusted sand, sterilised tweezers and spatula, combusted Pasteur pipettes and scratch pen.
2. The pastuer pipettes are initially cut using the glass pen leaving approximately 6cm capillary tube at the bottom.
3. Using the tweezers, insert the glass wool into the bottom of the pipette, using another pipette to push it down to the end of the wider part (before the start of the thinner section).
4. Insert the silica into the column using the spatula and the funnel. ~4cm of silica into the column levelled by gentle taps on the side.
5. Combusted sand is added on top of the silica using the spatula and funnel. ~ ¼ of a spatula of sand to finish the column preparation procedure to ensure that the sample was trapped in the cell and not the end cap during solvent extraction.
6. Store prepared columns in a clean beaker and cover with aluminium foil to avoid contamination.

Acid/Neutral Separation Procedure

The first step of column chromatography is the acid/neutral separation of the TLE through aminopropyl-silica gel (LC-NH2 SPE Si-gel) chromatography. Two different solvent systems are utilised to extract the TNF (total neutral fraction) and TAF (total acid fraction) from the TLE for each sample. The first solvent system collects what is dissolvable in that system (TNF) and then the second collects what is dissolvable in this system (TAF).

TNF

The first solvent system is DCM-Isopropyl alcohol (1:1) which collects the TNF which is the non-ionic compounds from the mixture which do not hold an electric charge. The solvent system is flushed through the column 3 times in order to create a uniform solvent system before adding the sample and collected in a vial labelled ‘rinse’. Solvent is pushed through the column until just above the sand layer using a pump. It is important to ensure

that the column does not dry up when pushing the solvent through so the uniform flow is not disrupted. The TNF is then dried via evaporation to condense organics.

TAF

The second solvent system is Ether w/4% Acetic Acid which collects the TAF in which the target compounds are acidic in nature. There is no wash in between solvent systems but remember to swap vials into labelled TAF fraction vials.

Method:

Keep 2 pasteur pipettes on the side; one for cleaning and one for moving solvent.

1. Have the TLE sample ready
2. Rinse DCM-ISO round TLE vial and then add to the column
3. Discard of this pipette (New pipette for each sample)
4. Swap 8ml vials from rinse to wash to collect the first fraction (TNF) and push it through
5. Before the sample reaches the top of the sand, add the solvent system – This is the first wash
6. Do 3 'washes' total for each sample
7. After 3rd wash move straight to adding the next solvent system (Ether w/4% Acetic Acid) - *remember to swap vials*
8. After all samples are collected, they are dried with N_2 in the Sample Concentrator

Derivitisation of the TAF

The TAF must be methylated prior to GC-MS or GC-FID analysis. Ensure TAF vials are completely dry before adding 100ml of BF_3 using syringe, capping with Teflon lined caps and storing in oven for 1 hour at 70 degrees. Cool for 5 minutes after oven and cleanse the caps in a decon bath. Dry the derivatised samples with N_2 using the concentrator then they are ready for the 'clean up' through silica columns.

The Si-gel columns are used to extract two fractions (A1 and A2). Load sample with hexane into the column to extract the A1 fraction, do 3 rinses of hexane and collect in corresponding vial (Hexane fraction is not required for further analysis). After this, wash the sample vials with DCM and do 3 rinses in the columns to extract the A2 fractions into the corresponding 8ml vials. Dry with N_2 and store in cryoboxes until analysis.

TNF Separation (N1, N2, N3, N4)

The TNF is further separated using 230-400 mesh/35-70 micron silica powder to elute 4 different fractions for separate organic content (Table 30)

Table 30 - Separation of the TNF into 4 fractions; solvent required, volume and the organic content targeted for each fraction

Fraction	Solvent	Volume ml (solvent)	Organic Content
N1	Hexane	4	Aliphatic hydrocarbons
N2	DCM	4	Ketone/Ester/Aromatics
N3	Ethyl acetate:hexane (25:75)	4	Alcohols
N4	Methanol	4	Polar

1. Rinse hexane through column twice to create uniform solvent system and collect this in the rinse vial.
2. Add hexane to TNF vial and use Pasteur pipette to rinse it around a few times in vial
3. Load sample into column (uptake ~1.5ml) and switch to N1 vial
4. Rinse hexane through 3 times to collect in N1 vial (use pump to push everything through)
5. Add DCM into TNF vial and rinse around to collect everything
6. Load sample into column (uptake ~1.5ml) and switch to N2 vial (use pump to push everything through)
7. Rinse DCM through the column 3 times and collect in corresponding vial
8. Next fraction is N3 – switch straight to Etac-Hex using Pasteur pipette to transfer solvent into column and switch into N3 vial.
9. Rinse Etac-Hex through the column 3 times to elute N3 fraction (collect in vial).
10. Final solvent system is Methanol. Add methanol and rinse through twice to collect in N4 vial. Rinse through once and on the second rinse dry out the column.
11. Store fractions in back of the fumehood under foil and wash TNF vials.

The N3 fraction requires BSTFA derivatisation no more than 48 hours prior to running them on the GC. The N4 fraction collected was archived as this requires LC-MS analysis.

N3 Derivatization

Derivitisation increases the volatility of the analyte and also decreases its polarity which is beneficial for the chromatography characteristics and allows for improved sample analysis (Sephton, 2001). The N3 fraction is derivatised by bis (trimethylsilyl) trifluoroacetamide (BSTFA). Ensure the vials are completely dry prior to the process. The N3 vials each get 20 µl of pyridine and 15 µl of hexane. The syringe used for this process is rinsed with hexane 3 times and then DCM 3 times between pyridine and hexane and after to prevent cross contamination. Pyridine is added to all vials, rinsed and then hexane added to all vials. The vials are then capped and stored in the oven at 80 degrees Celsius for 2 hours in order to have a complete reaction.

B.3.2 GC-FID

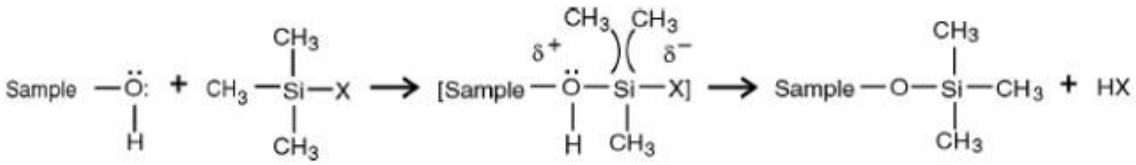

N1 and A1 preparation for GC-FID is slightly different to the other fractions.

1. Rinse the syringe in the 'wash' hexane vial 3 times
2. Uptake 30ul of clean hexane at bottom of TAF vial
3. Wash vial sides ½ way up
4. Draw up the hexane once it's down to 20µl
5. Insert into the insert and cap immediately.

Repeat this step for all TAFs and transfer into fridge when done. Get fresh hexane and fresh wash hexane and repeat process for N1s. Repeat these steps. N1's and TAFs (A1s) are run on the GC-FID. N1's N2's and N3s are dried up.

Figure 38 - Specifications for the GC-FID

B.3.3 Standard Operating Procedures from Professor Jamie Toney

Automatic Solvent Extraction (ASE) Operation Procedure (SOP)

Below is the SOP for the use of the ASE in BECS, as created by Professor Jaime Toney.

Operating Procedures for ASE 350

Loading the ASE cells for a run:

1. We have 24 10ml cells. On average, a 10ml cell can hold ~3g of sediment (depending on its properties). Make sure you extract a sufficient amount of sample for your analyses.
2. Use 60ml collection vials for 10ml cells.
3. In general, end-caps of cells should remain assembled during the wash process, unless particularly dirty samples were extracted
4. Put a glass fiber filter onto the top of the cell body. Make sure the filter does not overlap the ridge at the edge of the cell; this will prevent the end-cap from making an appropriate seal.
5. Place the cell on the balance and zero it. Load freeze-dried sample into the cell using the specialized funnel. Weigh the samples directly in the cell. Keep the threads on the cell body and cap free of dust particles to prevent thread fouling and extend the life of the cell.
6. Fill any void volume in the cell with combusted sand; this reduces the amount of solvent used during the extraction.

7. Place a filter on the top of the cell body and screw the end-cap onto the top of the cell body. Hand-tighten only – do not use excessive force. Do not attach any labels to the cell. For sample identification, write on the top cap with a marking pen.
8. Place the loaded cells into the tray slots on ASE 350 in numerical order. Hang the cells vertically in the tray slots. Make sure the marked side is on top. Load the labelled collection vials in the corresponding vial tray slots. The vials should be capped with the open-hole-screw-thread caps with either Teflon septa or aluminium foil.
9. Make sure that a 250ml collection bottle is in the R1 rinse slot. Empty rinse vials and the waste vial after each run.

Operating the ASE 350:

10. Check the level of N2 gas in the cylinder in the cage outside. Make sure that the residual pressure is above 200psi before starting a new sequence. Check the air pressure to make sure it ~100psi.
11. Turn the flow 'on' in the lab with the valve on the wall.
12. Make sure the clear protective shield on the ASE's lower carousel is closed.
13. Perform the "rinse" function on the ASE, at least three times prior to extracting your samples
14. Check that the amount of solvent in the solvent bottles. Add more solvent if needed, then hand-tighten the cap. Press the trays button on the keypad to engage or disengage the tray.
15. Use Method Control to run all extractions. Press menu to display the MENU OF SCREENS, and press Enter (or 1) to display the LOAD METHOD OR SEQUENCE screen. If you are extracting traditional lake, bog, or sediment samples - input METHOD 1 and press the ENTER again.

    a. The LOAD METHOD OR SEQUENCE screen closes and the CURRENT STATUS screen displays, showing the method number loaded and the status of the ASE 350 with various operating parameters.

    b. The oven will begin heating from room temperature to 120°C. Each sample takes about 60min and consumes about 30ml solvent.

    16. Most runs will not need this!! [Compress the cells (if needed). Get to the main menu, press 7 (Diagnostic menu), press ". . ." (3 dots). Then put in 9137 and press enter. Press 8 (Manual control). Make sure the ASE has control of the trays (you won't be able to turn the trays, if you can, press trays button once). Go to the right hand column, and put in cell 1. Press ASE arm (out). Press ASE arm (up). Press ASE arm (in). Press Oven compression

(yes). After 10 seconds, press oven compression (no). After 5 seconds. Press ASE arm (out). Press ASE arm (down). Move onto cell 2, and repeat.]

17. Press START to run a sequence of samples. There are seven main steps in the extraction process: (1) Loading the cell; (2) Filling the cell; (3) Heating the cell

a. (equilibration); (4) Static extraction; (5) Flushing with fresh solvent; (6) Purging solvent from the system; (7) Unloading the cell.

18. After the extraction, uncap the cells. Residual sample can be discarded or stored in corresponding labelled whirlpak bags. Disassemble the cell bodies from the end-caps.

a. Note: end-caps should not be taken apart unless particularly dirty samples were extracted.

19. Clean all the parts according to the Cleanup Procedure. This should be done immediately after use to make the instrument ready for the next person to use.

20. The composition of the extracts generated by the ASE 350 is similar to that generated by Soxhlet or other liquid extraction techniques using the same solvent system.

Evaporation of the samples by Techne Evaporation or Turbovap:

1. Remove the solvent with Nitrogen using the Techne evaporator if you are using 60ml vials. Simply select the correct aluminium block, place them in the heating block and blow down with nitrogen. (If quick turn around time is important samples can be transferred to combusted 40ml vials and evaporated by following step #2.)
2. Remove the solvent with Nitrogen using the Turbo Evaporator. Use a water bath temperature of 35°C for ca. 30min. Monitor the solvent evaporation progress. Do not let the samples remain without solvent – volatile compounds can be lost. Carry out further chromatographic clean-up procedures before GC-FID analysis.

Cleanup Procedures for ASE Cells:

Note: careful cleaning of the cells is very important to avoid contamination of your samples and to prolong the lifetime of the static valves, which are expensive. Follow the steps carefully. GC grade and HPLC grade solvents are expensive. Initial cleaning should use the general grade solvents available from chemistry department.

1. Disassemble the ASE bodies from the end-caps. If you have run particularly dirty samples, then completely disassemble the end-caps (removing the retaining rings with the ring tool).

2. Put any sand in a beaker labeled “dirty ASE sand” and discard in the trash or save your sediments in whirlpak bags. If disassembling the end-caps, separate the small parts
a. (filters, o-rings, retaining rings) from the big parts (cell caps, bodies, and inner rings).
3. Rinse and scrub all parts with water to remove any sediment, sand, and hydrophilic compounds. Let the parts dry in the oven for a few hours before proceeding.
4. We have one small Teflon jar and two big Teflon jars. The small stainless steel filters should be cleaned in the small jar, while all other cell parts should be cleaned in big jars. It is very important that the filters are cleaned very well, otherwise small sample particles in the filter will block the static valve (£400 each).
5. Put half of the end-caps into a Teflon jar #1 and fill the remaining space with cell bodies. (Note: small parts should go in the small Teflon jar.) Fill with ‘Rinse 2 Acetone’ and sonicate for 30 minutes – this is Rinse 1*.
a. *Note that ‘Rinse 1 Acetone’ should be ‘Rinse 2 Acetone’ from previous cleaning process. 2
6. Move the parts into Teflon jar #2 and fill with fresh acetone – this is Rinse 2. (For the small parts, strain the old acetone out and fill with fresh acetone.) Dispose of the acetone used as Rinse 1 and load the remaining half of the big parts into that jar. Fill with fresh acetone. Sonicate all 3 jars for 30 minutes. Note that you have now staggered the cleaning procedure such that half of the big parts are one step behind the other half.
7. Move the big parts that have undergone Rinse 2 into the empty Teflon jar. Fill with
a. DCM:MeOH 2:1. This is Rinse 3. (For the small parts, strain out the acetone and fill with DCM:MeOH 2:1, as well.) Dispose of the acetone in the big jar, and then move the other half of the big parts into it. Fill with fresh acetone. Sonicate everything for another 30 minutes.
8. Line a steel tray that the cells are stored in with a fresh piece of aluminum foil. Remove the small parts and big parts (keeping the cell bodies and end-caps in separate trays) that have gone through all three rinses and let the parts dry in the tray in the fume hood loosely covered in foil. Do not dump out the DCM:MeOH in the big jar – instead, move the last half of the big parts into it and return this jar to the sonicator for Rinse 3.
a. You can reuse the DCM:MeOH Rinse 3 up to three times. When the last jar is done, remove the parts and let them dry in the tray.
9. When the cells are dry, cover the tray more tightly with aluminum foil and place the tray on the shelf above the ASE cell prep area. Label the foil with your name, the date, and “clean.”

Further GC-MS Sample Preparation

Acid/Neutral Separation Procedure:

1. Use the column stand to hold six short, glass pipettes
2. Using tweezers pull a small, fluffy wad of glass wool out and twist into a ball. Push the quartz wool into the top of the short pipette.
3. Use the long pipette to gently push the wool into the tip of the short pipette. The wool should fit snuggly enough to prevent Si-gel beads from passing, but should not be so tight that it restricts the flow of solvent.
4. Use the modified funnel to put ~4cm of dry, LC-NH2 SPE Si-gel into the short pipette.
5. Tap on the side of the pipette gently until the Si-gel settles.
6. Add a small amount of combusted sand to the top of the column to help prevent drying of the upper layer of silica gel.
7. Clean the LC-NH2 SPE column with 3 bed-volumes (5 to 10 ml) of 1:1 DCM:isopropyl alcohol (ISO).
8. Re-dissolve and transfer the aliquot of TLE with a small amount of 1:1 DCM:ISO (x3) onto the LC-NH2 SPE column. Allow the sample to seep into the silica gel.
9. Elute the Total Neutral Fraction (TNF) with 4ml of 1:1 DCM:ISO and collect the TNF into an 8ml sample vial.
10. Elute the Total Acid Fraction (TAF) with 4ml of ether with 4% acetic acid. Collect the TAF into an 8ml sample vial.
11. Dry the TNF and TAF gently under N2.
12. The TAF needs methylation, while the TNF needs further separation through Si-gel.

Clean up and further Separation of the Total Neutral Fraction (TNF)

1. The mass of TNF that is added to a silica gel column should not exceed 10mg, because the ratio of the weight of the TLE to the weight of the silica in the column should not exceed 1:100. (e.g., we use ~1g (1000mg) of silica so the maximum TNF weight is 10mg.)

2. Prepare 230-400 mesh/35-70 micron silica powder (stored under the hood. Note: this is different from the specialized LC-NH2 Si-gel used in the Acid:Neutral separations).

3. Use the column stand to hold six short, glass pipettes

4. Using tweezers pull a small, fluffy wad of glass wool out and twist into a ball. Push the quartz wool into the top of the short pipette.

5. Use the long pipette to gently push the wool into the tip of the short pipette. The wool should fit snuggly enough to prevent Si-gel beads from passing, but should not be so tight that it restricts the flow of solvent.
6. Use the modified funnel to put ~5cm of dry, Si-gel into the short pipette.
7. Tap on the side of the pipette gently until the Si-gel settles.
8. Add a small amount of combusted sand to the top of the column to help prevent drying of the upper layer of silica gel.
9. Prepare your workstation. Make sure your 8ml vials are labelled and you have enough of the solvent mixtures shown in Table 14
10. In this section you will separate the TNF into the four fractions (N1, N2, N3 & N4) by eluting with the volume of solvents listed in Table 1. The solvents will be loaded onto the column using a syringe. The individual fractions will be collected into 8ml vials.
11. Clean the Si-gel by eluting with 4ml of hexane. (Note: it is important to use the full 4ml of hexane)
12. Re-dissolve the TNF in as little hexane as possible (~200ul, x3) with sonication, if necessary, and load onto the column using a pipette.
13. Collect the N1 to N4 fractions in 8ml vials using solvents as shown in Table 1.
    The solvents and solvent volumes used in Si-gel chromatography for separation of the TNF into four fractions (Table 2a)
14. Blow down the solvent in all four fractions under N2. Both the aliphatic and aromatic fractions are ready for GC-FID analysis. All four fractions can be transferred to a GC-vial (2-ml) using DCM (x3).
15. The N1 & N2 fractions can be dried down under N2 and store in labeled cryoboxes until they are ready to run.
16. The ethyl acetate:hexane and methanol fractions need BSTFA derivitisation before GC analysis. (Note: If you plan to measure GDGTs, weigh the N4 GC vials before transfer and record the N4 mass after the transfer and drying.)

Preparing to run samples on the GC-FID and GC-MS

First, do a pilot run:

1. All samples should be dry and in GC vials.
2. Before running a full set of samples from a batch/project, run a few pilot samples to get an idea of concentration.
3. Dilute and only use an aliquot of the sample. This applies to TNF and TAF.

4. Dissolve your sample in 500µl of n-Hexane, take an appropriate aliquot (i.e. 100 ul) and transfer that into a vial with an insert. You can then dilute/concentrate in the insert without messing about with the original sample.
5. Run on the GC-FID. Use the BECS standard mix as an external standard to quantify the concentration of your samples. (If you are running three pilots, run the standard before and after the three samples.)
6. Once you work out the amount of sample aliquot and concentration to run on the GCFID from the pilot samples, prepare the rest of your samples for a GCFID.
7. An internal standard should be used to quantify your compounds. If the concentration of your pilot samples is consistent, you can use Section 10 to determine the amount of internal standard to add. If your pilot samples are highly variable in concentration, then you will have to run all samples once before determining the correct amount of standard to add.

Adding GC Standards to Determine Concentration

1. Add standards to fractions that you are analyzing. (Make sure that you are certain about
your calculations before adding anything to your samples!!)
2. Use the results from the pilot samples in Section 9 to see which standards and how much should be added.
3. The sample should not have a concentration higher than 10000 ng/ l (10 µg/ml). (If your
sample is strongly colored, use caution with analysis. First dilute it until coloration is weak. Organic/pigment-rich samples can contaminate the injector and destroy the column.)
4. As above, you will dissolve your sample in 500µl of n-hexane, take an appropriate aliquot and transfer that into an insert. You can then dilute or concentrate in the insert without messing about with the original sample.
5. Prepare a GC standard that will be ~10µg of standard per 1mg of your compound. This will be dependent on the concentration of your pilot samples. For example, if you plan to dissolve your sample in 50µl of solvent for the GC-FID run, then your GC standard should be 10µg/ml in 50µl. This way, you can transfer your sample, dry it under N2, then add 50µl of your GC standard mixture to the sample, cap and are ready to run. (See notes below on creating a ‘mother solution’)

6. Note: Trial run your prepared GC standard on the GC-FID before adding it to your samples… be sure that you have calculated the correct concentration!! After your trial runs, check:

a. That the standard is not co-eluting with any of the natural compounds in your sample.

b. If needed adjust your GC-standard concentration, so that in your GC runs the standard peak height is about twice that of your compounds of interest.

7. Typically, BAME (C23 FAME) is a good GC standard for the neutral fractions. An alkane or ketone is good for the TAF

Section C

C.1 Supplementary Data

Raw data, calibration curves and further processed graphs and tables can be found at the following link:

SUPPLEMENTARYDATA_JodieDouglas.xlsx